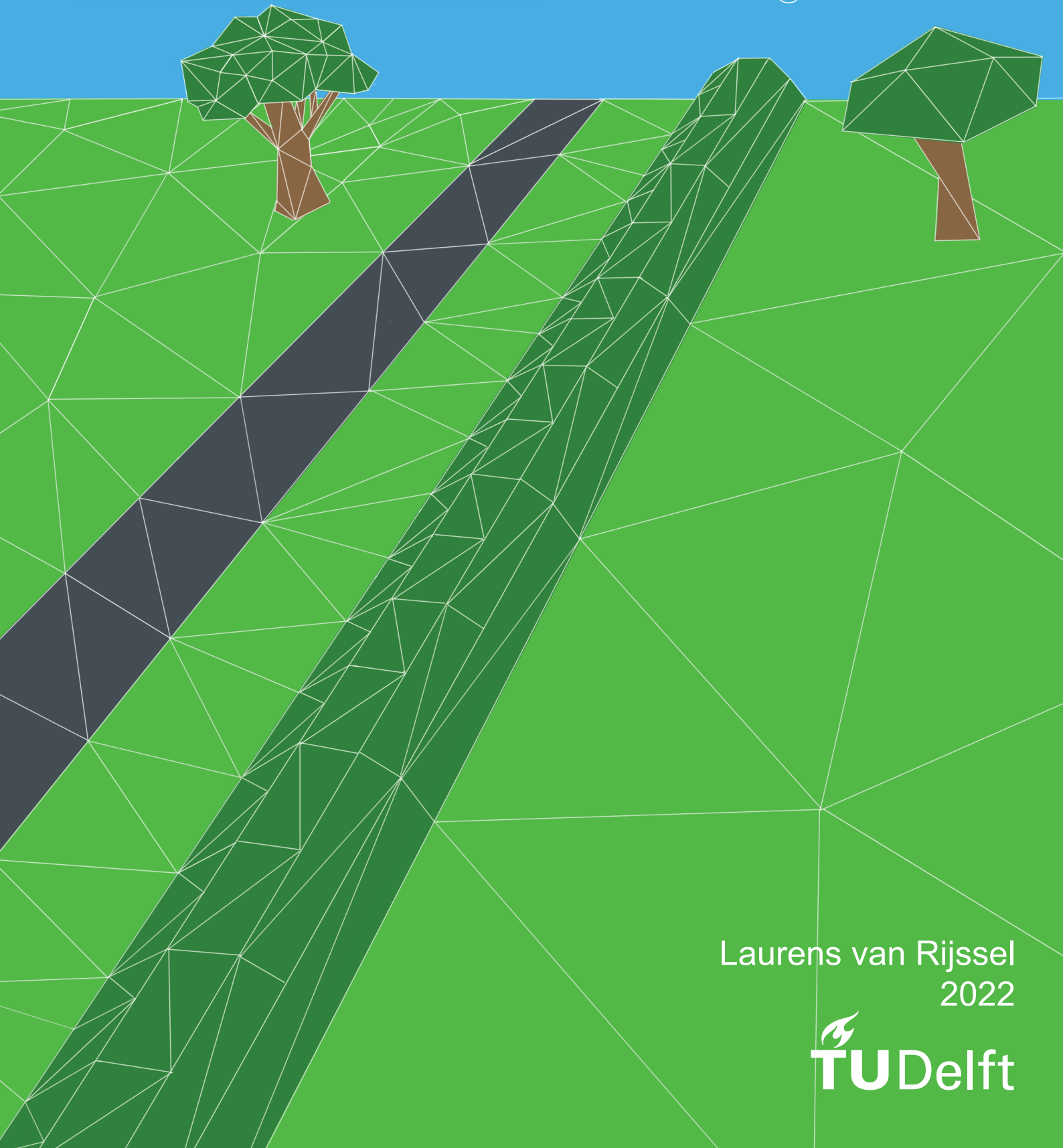MSc thesis in Geomatics

Generating consistent triangular terrain elevation data for noise modelling

Laurens van Rijssel
2022

TUDelft

MSc thesis in Geomatics

Generating consistent triangular terrain elevation data for noise modelling

Laurens van Rijssel

January 2022

A thesis submitted to the Delft University of Technology in partial fulfillment of the requirements for the degree of Master of Science in Geomatics

Abstract

In 2016, a collaboration between the TU Delft, RIVM and a few other companies started to automate the generation of environmental input data for noise modelling. As a part of that cooperation a promising triangle based data structure is researched to represent terrain elevation. Due to the properties of its generation it can provide certainty over the presence of objects while the format allows for efficient cross sections extraction. Yet a persistent challenge remains, the large file size makes exchange and processing of terrain data troublesome. This research aims to optimize the terrain elevation data to decrease the file size while ensuring accurate noise calculations.

Using an in-depth analysis of the usage of terrain elevation in noise modelling in a Dutch and European context, a environmental based approach for a triangulated terrain generation is developed. This approach is conceptually implemented to facilitate the calculation of noise values using terrain generated with the provided approach. Empirical tests have been conducted to measure the influence of different terrain elevation settings over a variety of terrains.

The study concludes by providing an advice on an approach for elevation model generation. Several insights are discovered regarding the impact of terrain elevation accuracy on noise propagation calculations. Compared to a currently publicly available terrain data set a size reduction of 50 to 90% can be obtained without quality reduction.

Acknowledgements

Contents

Contents

List of Figures

List of Tables

List of Tables

Acronyms

1 Introduction

Noise pollution (i.e. environmental noise) is a major health problem in Europe, especially in urban areas. The majority of the environmental noise comes from roads and railways, causing continual noise in work and living environments. This exposure to noise over 55 dB affects an estimated 135 million people in Europe (European Environmental Agency, 2020). Long term exposure to noise causes psychological and physiological stress leading to several adverse health effects. It can cause annoyance, cardiovascular diseases, reduced cognitive performance (mainly among children) and sleep disturbance. These effects in term can cause displeasure, higher stress levels, reduced learning performance and reduced energy levels respectively (Basner et al., 2014). The World Health Organization and Joint Research Committee (2017) estimated that each year, between 1.0 and 1.6 million DALYs (Disability-Adjusted Life-Years) are lost in the EU due to environmental noise, in 2020 this was estimated at roughly one million, noting that this was limited by the amount of data and expected to be higher. (European Environmental Agency, 2020). The WHO Regional Office for Europe (2018) strongly advices to reduce both the emitted noise itself and on the route between the source and the affected population. In order to reduce the noise pollution, i.e. reduce number of people exposed to harmful levels of environmental noise, this noise should be monitored.

The European parliament and European Union (2002) adopted a directive which requires EU member states to produce noise maps every five years. A noise map is the representation of noise indicators, either modelled or measured, in a given scenario. Measuring noise using sensors is both cost- and time-expensive, especially for larger areas. Modelling noise using prediction software is, compared to measuring, relatively cheap, fast and scalable. It is therefore most common to model noise and use measurements as verification (Murphy and King, 2014). Modelling noise consists of two steps in common noise prediction software;

1. Determine the noise sources around a point of interest and extract the relevant environmental information between the noise sources and the point of interest (i.e. retrieve a terrain cross section with semantic data) from a digital model of the environment.

2. Compute the noise level at the point of interest, given the noise source and the course of the terrain and any other object between the point of interest and the noise source.

The Environment and Planning Act (Dutch law)[1], to be active from 2022, will increase the amount and complexity of noise computations. Provincial roads and industrial sites will be included in a monitoring mechanism which is now only used for state roads and major railways. In addition, a new monitoring mechanism for city roads will be adopted. The provincial roads will be added to the sources used for the country wide noise mapping round.

While modelling noise is relatively fast and scalable, large scale computations remain time intensive. This is due to the high number of sources and receivers as well as the complex interaction of noise with its environment. The environment is represented in a digital representation of the terrain, called the environmental model. To continuously reduce the health effects of noise pollution (i.e. reduce the human exposure to harmful noise levels), the amount and detail of noise studies is continuously increased, as mentioned in the upcoming law. While computer performance also increases, there remains a balance between the amount of computations and the complexity of individual computations. One can conduct more computations if the individual computations become less complex (i.e. time consuming). The complexity is caused by the calculation method and the amount of detail in the environmental model.

The current balance is to automatically generate a simple and small environmental model, which contains many relevant objects. However, there certainty that no relevant objects are omitted cannot be

---

[1] https://www.government.nl/documents/reports/2017/02/28/environment-and-planning-act

guaranteed. Therefore, the model is manually inspected and adjusted by a noise expert to provide the certainty. This allows to make large scale computations within a reasonable time. However, the manual inspection may introduce a human error and may cause varying results for the same area when inspected several times.

Another approach is to fully automate the generation of an environmental model which can provide the certainty to omit the manual inspection, while keeping the computation time reasonable. The majority of the complexity in the environmental model originates from the terrain elevation information. Therefore optimising this information would simplify the model. However, a simpler terrain should not lead to less accuracy and precision of predictions. In other words, the terrain should be optimised, not simplified. A method to provide a higher certainty is to use a Triangular Irregular Network (TIN) data structure (this is further explained in chapter 2). During this research the generation of such an efficient terrain model is studied where a balance between accurate noise output and a reasonable computational performance is sought.

An overview of recent work and the current state of noise modelling, terrains and terrain generation is provided in chapter 2. The methodology in chapter 3 explains the approach of the research. In chapter 4 a model is proposed on how to generate an optimized terrain. In order to verify the model, the model is further elaborated and an implementation is presented in chapter 5. The implementation of the model is then verified and tuned in chapter 6.

1.1 Research questions

This research aims to study how a triangular mesh based elevation model can be created such that it is optimised for noise modelling. A terrain is optimised when the predicted noise levels are sufficient while the data size and processing speed are minimal. The main research question therefore is stated as;

What is the local minimal accuracy for a triangular irregular network to produce accurate noise predictions according to Dutch and European noise methods?

The minimal accuracy is sought as this provides the optimal balance between minimising the computation time and sufficient quality for accurate noise predictions. It is local as a TIN does not require a constant accuracy. The triangular irregular network (TIN) contains the elevation information and is part of the environmental model. The environment model will be used as input for noise modelling according to the Dutch RMG 2012 and the European CNOSSOS. The process of developing the environment model consists of three phases in which the following questions will be answered;

1. Which parameters influence the required elevation accuracy of the triangular irregular network?

2. How can a triangular irregular network (TIN) be generated according to the local accuracy based on the parameters?

3. Which parameter settings provide a balance between quality of the output and performance?

2 Background and related literature

In this research two fields of study are combined, predicting the propagation of noise in an environment and the digital representation and generation of a height field. First an introduction in noise modelling standards and how they predict noise propagation in an environment is provided by discussing the related works. The effect of terrain elevation on the noise level is further analysed by means of a theoretical analysis. This is followed by an overview of different approaches to represent a height field and its functionality for noise predictions. Given the analysis and the suitability of a triangular mesh based terrain model an analysis is given on how such a terrain can and should be generated. In section 2.2.6 an overview is provided of possible software applications that allow the requested triangulation. As the software has a large influence on the data preparation, an application is already selected at this stage of the report. At last the scope and the boundaries of the study are provided to provide focus within the topic.

2.1 Noise modelling: predicting noise behaviour in an environment

There are many interactions between noise, the medium in which it propagates and physical objects. The medium defines the speed at which the sound waves propagate and how much of the acoustic energy is absorbed by the medium. Solid physical objects cause reflections which increase the noise level in some areas, where softer objects absorb more energy than they reflect and therefore reduce the noise level. These effects are incorporated in noise modelling methods which predict the amount of noise given a noise source and a environment.

Modelling noise generally consists of two steps, extracting all source paths for each point of interest (also called receiver point) and computing the noise level for each receiver based on all the related sources. The path consists of a 2D vertical cross section of the environmental model with information about the source and receiver (e.g. height, emitted noise, direction). The environmental model consists of the acoustic properties of the ground, elevation data and building data sets. Regarding this model, there is no standard or law that prescribes the characteristics of the data sets used, resulting in a variety of approaches and methods. Generally the following data is included; (also depicted in Figure 2.1);

- Immission (receiver) points; points where the noise levels are to be determined.

- Noise sources; these are mostly roads and railways, but may include industry noise sources (aircraft noise is modelled separately). All sources either include emission levels on a dB scale directly, or it is derived from provided information like amount and type of traffic.

- Buildings; buildings with a certain Level of Detail (LoD), commonly 1.2 or 1.3 as described by Biljecki et al. (2016)).

- Elevation data; information about elevation of the natural terrain, excluding buildings and bridges.

- Noise barriers; information about barriers placed next to roads to reduce the noise level behind the barrier.

- Ground type data; the acoustical property of the ground surface which causes noise to get reflected or absorbed.
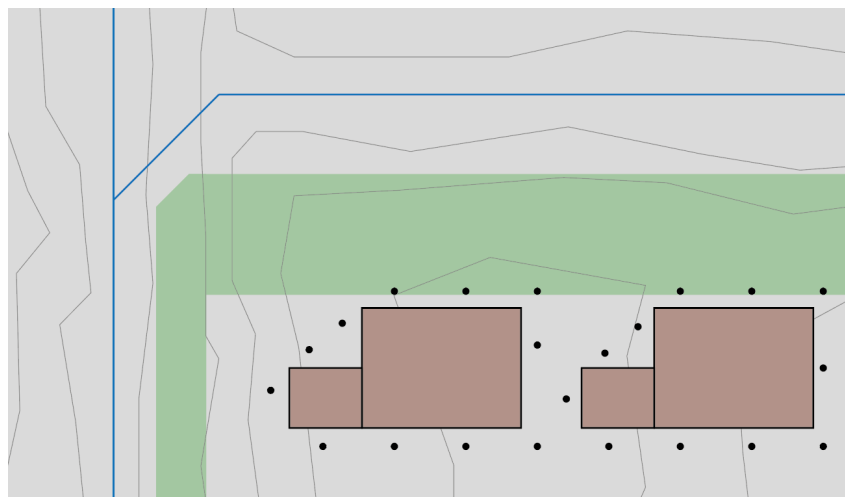
Figure 2.1: Schematic representation of typical noise modelling input data. Blue; roads, Grey/green; absorption factor 0 or 1, pink; buildings (including height), dots; immission points, grey lines; height lines.
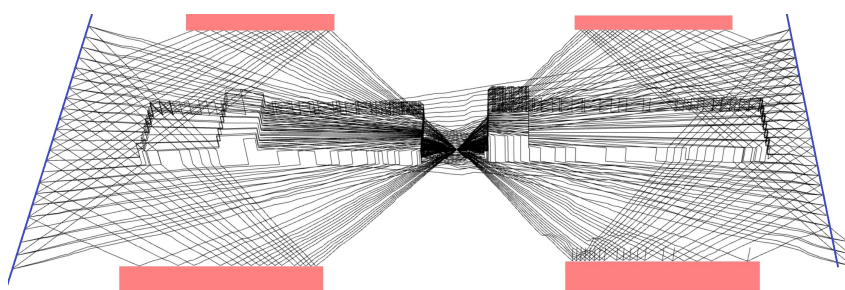
Figure 2.2: Schematic representation of step 1 of noise modelling; extracting propagation paths, a single receiver is located in the center with roads on both sides. Representation includes several buildings in pink (and in the middle, which are included in the paths), direct and reflected paths (source: van Rijssel et al. (2020)).

In **step 1** all propagation paths for the receivers are extracted (see Figure 2.2). Some EU member states prescribe methods on how to extract the paths, but this may not cover all aspects (e.g. the dutch method (RMG) provides some approaches for noise source allocation and valid reflections, but leaves room for interpretation in other situations as shown in van Rijssel et al. (2020)). This reduces both the transparency of determination and cross comparison of noise maps produced with different methods. To account for this the ISO standard 17534[1] was developed which allows to compare results with sample data sets and methods. Peters et al. (2018) noted that the environment data is partially generated per project and thus overlapping projects result in duplicate work and may cause a different output.

In **step 2** the noise levels are computed for each source - receiver path (see Figure 2.3). For this several methods are, all publicly, available. In the Netherlands this is the RMG 2012[2]. More information about these standards in a European context is provided in Section 2.1.1.

In the Netherlands two commercial companies provide software applications to compute noise levels according to the RMG, namely DGMR (GeoMilieu)[3] and dirActivity (WinHavik)[4]. DGMR has a countrywide environment model with ground type, building and elevation data in separate layers. This

---

[1] https://www.iso.org/standard/59974.html
[2] https://wetten.overheid.nl/BWBR0031722/2021-04-01
[3] https://dgmrsoftware.nl/producten/geluid-en-luchtkwaliteit/geomilieu/
[4] https://www.diractivity.nl/
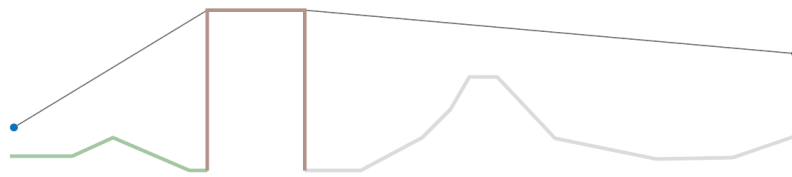
Figure 2.3: Schematic representation of the data in step 2 of noise modelling; a vertical cross section of the terrain to compute receiver noise level based on emission noise and terrain: blue dot; emission point, green line; absorbing ground, brown line; building, grey line; reflective ground, black line; shortest propagation path (diffracted) and black dot; receiver point.

information is used in their software. To include elevation data these applications use height lines representing relevant height profiles in the terrain. In the software the elevation profile of the propagation path is extracted from the height lines and used to test for a line of sight and computation of mean height planes.

The noise levels that are predicted in the noise software are long-term yearly averaged noise indicators for specified time periods. As noise pollution during the night causes more harm, the WHO Regional Office for Europe (2018) recommended to use different maximum noise values for night emitted noise, namely 44 (rail) and 45 (road) dB. During the day this is 54 (rail) and 53 (road) dB. To include this difference in a single representing value, separate noise level indicators are described, namely; L_{den} (day-evening-night level) (24h), which weighs the night levels heavier then day noise levels and L_{night} (night level) (23.00-7.00h). Upon reading this report, the term (predicted) noise level refers to these noise indicators.

2.1.1 A European standard for noise modelling

When different computational methods are used, comparing noise maps is difficult. Therefore the Environmental Noise Directive (END) prescribes that a common noise assessment method is to be used by all EU member states, after it is developed (European parliament and European Union, 2002, Article 6.2). Such a method describes three main topics; placement of immission points on the terrain for usable results. Secondly, prediction of the noise level emitted from a source given the amount of traffic and characteristics of the source. Thirdly, prediction of generated noise levels at the immission point based on road, rail, industrial and aircraft sources.

In 2012 the CNOSSOS was introduced (Kephalopoulos et al., 2012). The method was further developed and implemented in a new annex II of the 2002/49/EC directive (END) (European parliament and European Union, 2015). This directive states that the CNOSSOS method was to be used from December 31st 2018. In earlier mapping rounds, member states could use a method common to the other member states to produce noise maps every five years, e.g. 2007, 2012, 2017 (European parliament and European Union, 2002, Article 1.1a). Therefore, the method will be used in the mapping round of 2022. After initial implementation tests by the Netherlands it could be concluded that the CNOSSOS method provided reasonably accurate results in most scenarios, but also contained some flaws (Vergoed and van Leeuwen, 2018). This led to an amendment for the CNOSSOS method (Kok and van Beek, 2019) that was accepted in December 2020 (European parliament and European Union, 2020).

While the incorporation of CNOSSOS will improve the comparability across noise maps from different EU member states with standardisation of noise sources and prediction of noise levels, it does not prescribe the input model (in terms of format, quality etc.). Secondly, it does not prescribe how to extract propagation paths, i.e. what paths are valid or how to convert noise source line segments into point sources. Acknowledging the important progress CNOSSOS has brought, it still allows for variation between output noise maps when different input models are used.

2.1.2 Collaboration on automated generation of input data

In 2017, RIVM, TU Delft, and several other institutions started a collaboration to automate the generation of noise input data from country wide openly available data (Peters et al., 2018). The collaboration aimed to automatically generate noise modelling input data for existing software, which required the input elevation data to be a collection of height lines. It is likely that these lines are extracted from a TIN, as is done by Stoter et al. (2020).

Both publications mention that in noise modelling software these height lines are converted back into a TIN, implicating the propagation paths and terrain cross section can be directly extracted from a TIN. Arguably it requires duplicate work to extract lines from a TIN and then create a TIN from these lines. In addition, it first highly simplifies the terrain, followed by interpolating again and therefore adding estimated information back to it, evidently leading to loss of information and loss of certainty. For this reason Stoter et al. (2020) recommended to create a TIN and develop noise modelling software that can directly read and process a TIN, thus omitting the height lines.

Given the input data (point cloud) is accurate and correct, an algorithm to produce a TIN directly should allow to satisfy all conditions of the elevation model. It allows to have a variable level of detail, aiming to keep terrain details where needed, and omitting details where the impact is insignificant leading to both a model with minimal information, while allowing quality assurance and efficient cross section extraction. This recommendation was followed by publishing sample data on the TU Delft website[5] and a project to develop noise modelling software based on a TIN (van Rijssel et al., 2020). The project was a proof of concept which developed noise modelling software with results comparable with GeoMilieu. Later the sample data was expanded to a country wide model[6]. This model creates a TIN directly from the Algemeen Hoogtebestand Nederland (Dutch general elevation model) (AHN) point cloud and allows for efficient and accurate terrain simplifications.

2.1.3 General principle of noise calculations in RMG and CNOSSOS

In this paragraph a short introduction is provided in how the RMG and CNOSSOS compute the noise level at a receiver point, given a single noise source and the terrain in between. These methods can be used for road, railway, industry and airborne traffic. As this research only covers road and railway sources, only these are considered in this analysis. Both RMG and CNOSSOS prescribe how the compute the source noise level based on type of source, amount of traffic, road material and other factors. From this a noise level in dB is given for eight octave bands (63, 125, 250, 500, 1000, 2000, 4000 and 8000 Hz).

To compute the total attenuation during a direct (line of sight) propagation, both methods provide several sources of energy loss, as shown in table 2.1. Note that the variable 'distance' is the shortest distance through air between source and receiver, which, in the case of diffraction, lays over the terrain like an elastic band, as the line S-O-R depicted in Figure 2.5.

Note that while both methods have numerous overlaps in attenuation types and dependent variables, the formulas, and therefore the outcomes, are different. The overview aims to indicate the types of attenuation and which variables influence it.

2.1.4 Use of elevation data in noise modelling methods

In this section the use of height information for both noise methods is analysed. Table 2.2 shows how both the RMG and CNOSSOS use height information in their model.

RMG uses only the elevation in the first 70 meter around the source and receiver points to estimate the mean height of the terrain. The CNOSSOS method uses a different approach where a straight line is fitted over the line segments by means of a root mean square error (RMSE) approach, this line is called

---

[5]https://3d.bk.tudelft.nl/opendata/noise3d/en.html
[6]https://3d.kadaster.nl/3d-geluid/

Table 2.1: Overview of sound energy losses along a direct propagation path for both CNOSSOS and RMG 2012 method. Distance; shortest distance between source and receiver, Ground absorption factor; absorbent fraction of the path as value from 0 to 1.

CNOSSOS		RMG 2012	
Type of energy loss	**Dependent variables**	**Type of energy loss**	**Dependent variables**
Divergence	Distance	Divergence	Distance
Atmospheric absorption	Distance Atmospheric coefficient	Atmospheric absorption	Distance
Ground effect	Equivalent source height Equivalent receiver height Ground absorption factor Distance	Ground effect	Equivalent source height Equivalent receiver height Ground absorption factor Distance
		Meteorological effect	Distance Equivalent source height Equivalent receiver height

Table 2.2: Comparison of how height is used in both the RMG and CNOSSOS

RMG	**CNOSSOS**
Determine whether there is a direct (i.e. line of sight) or diffracted path and identify diffraction points.	Determine whether there is a direct (i.e. line of sight) or diffracted path and identify diffraction points.
The mean height of the first 70 meters (source area) and last 70 meters (receiver area) (they may overlap) are used in the ground effect. If the path is less than 70 meters both source and receiver use the total path length.	Fitting of a mean height plane by means of a linear least-squares-adjustment on the elevation points.
Representative height is computed as source / receiver height minus the average height (0 if negative).	Representative height is computed as the orthogonal distance between source / receiver and the mean plane (0 if negative) (See distance z_s and z_r in Figure 2.4).
	In the case of vertical diffraction (Figure 2.5) the total propagation is subdivided in sections per diffraction point, where a separate mean plane is computed.

the mean plane (see Figure 2.4 and 2.5). Together with the absolute height of the source / receiver and the fraction of absorbing ground, the ground effect is computed.

While both methods have similarities in the approach, mainly their way to determine the ground height differs. Where the RMG method is used for building and infrastructure permits in the Netherlands, CNOSSOS is used for the country wide noise map (Geluidskartering) according to the Environmental Noise Directive.

2.1.5 Influence of noise propagation height

In this section the role of any type of object is analysed in RMG and CNOSSOS and the relevance of the amount of accuracy based on the distance to such an object is determined.

The objects used in noise modelling are the different noise sources (e.g. roads, railways and industry), noise barriers and buildings, therefore these will be considered in this section. Noise prediction methods, like RMG and CNOSSOS provide information about what noise is emitted from a source and at what height. Under normal circumstances noise is predicted to travel in a straight line. When obstacles are in

1: Actual relief
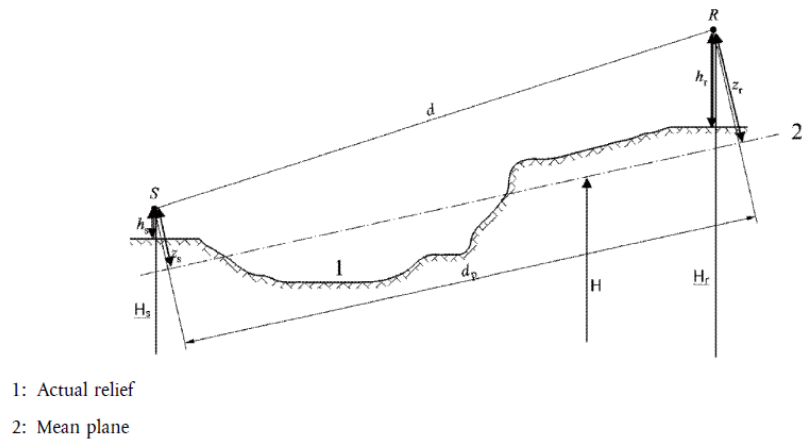
2: Mean plane

Figure 2.4: Mean elevation plane for direct path and relative height (European parliament and European Union, 2015, L 168/27)

1: Source side

2: Receiver side
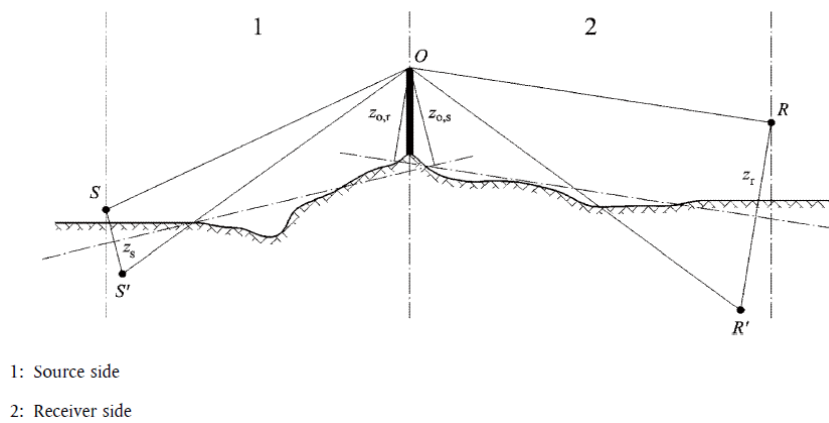
Figure 2.5: Mean elevation plane for a diffracted path and relative height (European parliament and European Union, 2015, L 168/36)

Table 2.3: Ground attenuation effect (damping) over distance with a source height of 0.05 m (CNOSSOS road) and a receiver height of 4 meter (in line with the Noise directive) where the ground is fully absorbing and frequency of emitted noise is 500 Hz. CNOSSOS favourable (downwind) condition left and homogeneous condition right, the blue lines are drawn according to ISO standard 9613, comparable to the ground attenuation in the RMG. The ISO9613-CM line represents the inclusion of the meteo effect of the RMG.
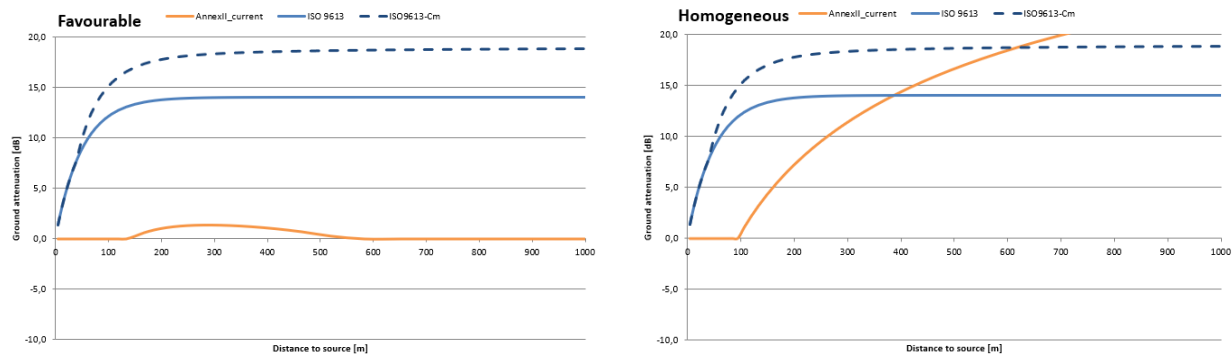
line between the source and receiver, diffraction will occur where the noise level will reduce as it needs to diffract (bend) over the obstacle. These are called homogeneous conditions. However, due to wind, varying air pressure and temperature, sound does not always propagate in a straight line. Most of the noise traveling down wind will propagate in a curve, leading to less noise reduction and allowing it to travel higher distances (one can observe this when listening for a road that is upwind compared to no- or down-wind). These circumstances are called favourable conditions as they cause noise to travel further. In the RMG the homogeneous (line of sight) condition is implemented as a noise correction for unfavourable circumstances. This is called the meteorological effect. The noise level at an immission point is computed using both conditions.

Based on the geographical location, a weight for both conditions is provided to define how often this condition is met. In the RMG this weight is included in the meteo effect. In the Netherlands generally homogeneous conditions occur 70% of the time, where favourable conditions occur 30% of the time. While homogeneous is clearly dominant in terms of weight, this condition causes exponentially increasing absorption as the path length gets longer (see table 2.3), not to mention the increasing chances of diffraction. The attenuation in favourable conditions even reduces back to zero over larger distances in flat areas as the noise propagates higher over the terrain. Note that this is only the ground effect, the other effects still increase with distance. Therefore it can be said favourable conditions play a dominant role in noise that propagates more than 400 meters where homogeneous conditions fade out.

The figures in table 2.7 illustrate the sound propagation in homogeneous and favourable conditions for both RMG and CNOSSOS for different path lengths. Note that the homogeneous conditions are only shown for distances up to 300 meters, as sound does not propagate much further in homogeneous conditions and therefore only the favourable condition matter over longer distances. In this representation the ground underneath noise sources and receivers are assumed to be flat. While the Dutch landscape is generally flat, high- and rail-ways are generally elevated above the terrain. When road and railways are constructed a foundation is placed on which the asphalt and rails are placed. Therefore, in practice the source heights are some what elevated above the terrain. For railroads this is generally higher with a 0.3 m rock bedding and 0.2 m to the top of the rail, which is the reference height upon which the source heights are placed. Short paths, below 150 meter, are not included in the overview. The difference between favourable and homogeneous difference fades out, while the noise height above terrain in homogeneous conditions are higher than those for larger distances (150 and 300 meter) as the receiver is higher than the terrain. The curvature in favourable conditions is computed according to the formulas of each method, for the RMG formula 2.1 and 2.2 are used to determine the height at a certain position along the path;
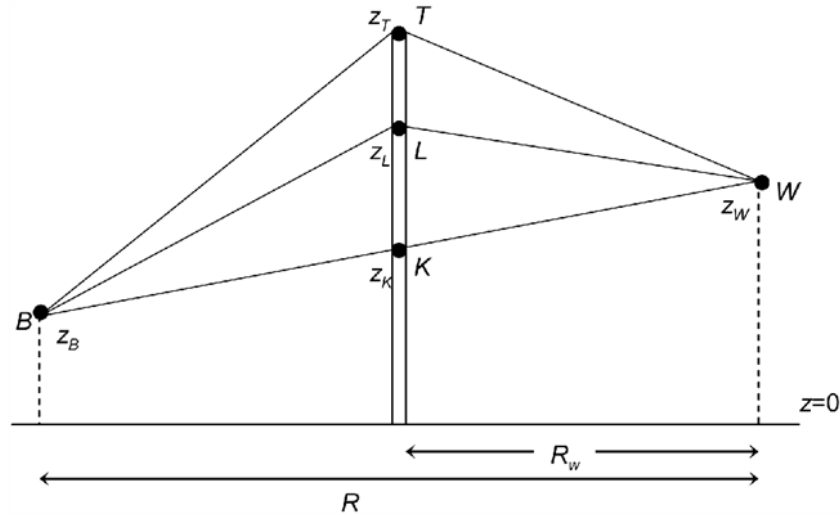
Figure 2.6: Schematic representation of a noise barrier in the RMG where B: source, W: immission point, T: top of the barrier, L: intersection of noise propagation with barrier in down wind (favourable) conditions and K: intersection of view line and noise barrier[2].

$$Z_l = Z_k + \frac{R_w(R - R_w)}{26R} \tag{2.1}$$

Where;

$$Z_k = Z_B + (Z_W - Z_B) * \left(\frac{R_w}{R}\right) \tag{2.2}$$

Where;
R, R_w, Z_B, Z_W are depicted in Figure 2.6

CNOSSOS computes a radius based on the distance from source to receiver. A circle with a computed radius can than be drawn such that it intersects the source and immission point.

$$radius = max(1000, 8R) \tag{2.3}$$

Where;
Radius is the radius of the curvature.
R is the distance from source to receiver in meters.

Regarding the sources, the lowest height is leading as the ground effect will have the biggest impact and diffraction will occur more often. Also the lowest used immission (receiver) height is included to give an indication of the elevation change over distance. The minimal height is leading as the environment model should be accurate for all computations and if it is accurate enough for the lowest elevation, it will also be for higher immission sources. In the European mapping rounds (CNOSSOS) the receiver is located at 4.0m above ground. However for municipal use (RMG), receiver points are commonly placed at 1.5 m with an additional 3m per floor level (e.g. 1.5, 4.5, 7.5m). As the environment model, of which the TIN will be part of, will be used for both purposes the lowest used height, 1.5 meter for RMG and 4.0m for CNOSSOS, is used in the schematic overview in Figure 2.7.

2.2 Digital terrain modelling

As there are no standards on format or quality of the environment model, each country and their model suppliers can supply their models as they see fit. Data formats are reasonably predictable for noise
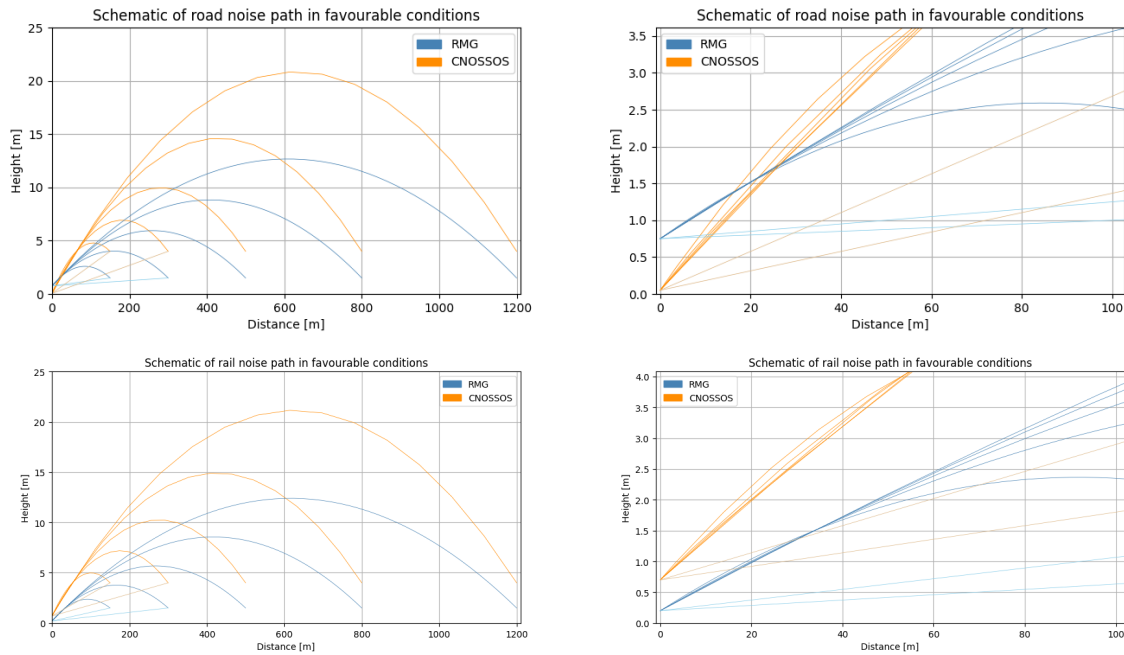
Figure 2.7: Schematic representation of a direct propagation in homogeneous and favourable conditions for both the RMG and CNOSSOS over a flat terrain for road and railway sources to the lowest used immission height. Full view on the left and a zoomed view of the first 100 meters on the right. Note that with railway noise only the lowest emission source is used as it produces a large portion of the noise and and is located closest to the ground and therefore the paths will lay closest to the ground, they are lifted 0.2m as the rail itself is not included in the terrain.

sources (road/rail center-line or point representation), ground types (a raster or 2D tessellation with irregular polygons) and noise barriers (line segments with height attribute). However, for elevation data this is not necessarily the case.

2.2.1 Overview of data structures for terrain elevation

For elevation data commonly height lines are used, a size effective data structure allowing a variable density and accuracy of height information. This section will shortly introduce other common ways of representing elevation data and how suitable they are for noise modelling.

Elevation of a terrain can be represented in different structures and formats. In geographical information system (GIS) elevation is most often represented as a raster (pixel image), iso-contours (lines of equal elevation) or as a TIN, i.e. a watertight surface mesh consisting of triangles. However, current noise modelling software in the Netherlands[34] and Europe [78] use height lines. These are lines in 3D Cartesian space representing relevant features in the terrain. When considering a format for elevation data the following conditions are sought;

1. Assuring quality of the model, i.e. no relevant heights in the terrain are omitted. The quality of the model is important, as it defines the quality of the noise output, improving certainty of the outcome.

2. Represent the terrain with the minimum necessary data, thus aiming to only store information with a significant impact in noise modelling. As noise modelling is a computer intense process

---

[7]https://www.datakustik.com/products/cadnaa/cadnaa/
[8]https://www.soundplan.eu/en/software/soundplannoise/

of which the amount of elevation data highly influences the performance, minimizing this an important objective.

3. Efficient cross section extraction; extracting the terrain below the propagation path is done for each source - receiver pair, thus the data structure should allow efficient extraction.

In table 2.4 an overview of the methods and how they meet the conditions is provided. This is further elaborated in the text below.

Table 2.4: Overview of suitability data structures for elevation for noise modelling.

Type	Quality assurance	Minimize data size	Cross section extraction
Raster	+	+/-	+
Iso-contours	+	+	- -
Height lines	-	++	- -
TIN	++	+	++

A **raster** data structure with sufficient detail where needed, will inherently provide abundant information in other areas. The quality can be assured, given a high resolution, but it exponentially decreases the performance. Extracting a cross section seems easy and straight forward, but comes with some challenges, e.g. what value should be selected if the cross section only crosses a small portion of the pixel? Does the pixel value represent the center or the average height? At last, the cross section might consist of many more or less collinear segments in flat areas, for which it might be time saving to simplify this before computing the noise level.

Using **iso-contours** allows to have a higher density of lines in steep areas and fewer in flat areas, matching with the minimal information condition. The step size provides a measure of accuracy and can provide certainty, but it does not prescribe the flow of terrain in between two lines. Finally, extracting a cross section is troublesome, as there is no information about adjacent edges, one either requires to check all edges or use a refined structure like a KD-tree. It is also common to convert it to a TIN, which allows to walk over the triangles using neighbour relationships.

Height lines allow to use logic and human input to select relevant information, rather than other structures which inherently implicate a single accuracy everywhere. The approach to place height lines provides the freedom to use other inputs, e.g. relevant man made objects, which helps to locate the relevant features of the terrain. However, height lines are either manually drawn or use an algorithm to select where to place height lines. An algorithm follows defined rules to determine where to place height lines, and where not. This approach is not fail-safe as some relevant data might be falsely judged unnecessary by the used algorithm. A large automatically generated data set is often manually checked and altered for specific areas to insert locally more detail. This requires human input and introduces human error. Extracting cross sections is troublesome due to no adjacency relationships, this is commonly solved the same as with iso-contours.

A **TIN** with a constant accuracy will, like iso-contours, provide more detail in steeper areas, and less in flat areas. The idea of a TIN is that it aims to represent a given terrain accurately, with as few points as possible, where the most relevant points from the point cloud are iteratively selected and added to the TIN. This continues until the difference between all points and the interpolated value in that position in the TIN is below a defined maximum deviation (see Section 2.2.4). Therefore it guarantees the error not only at the vertices, but also within the triangles. It can therefore provide a guarantee of quality, given the accuracy of the input data. Finally, the possibility of storing adjacency (i.e. topologic relations between neighbouring triangles) allows to "walk" over the triangle and thus extract a cross section efficiently. While this adjacency requires storing more information and increasing the data size, it can increase performance. As the TIN can be generated one time, and used many times, this could result in time saving.

2.2.2 Selection of an elevation data structure

For several years automatic generation of noise modelling input data has been a subject of research, as mentioned in Section 2.1.2. However, while the height lines structure results are sufficient, it was noted that using a TIN data structure instead has several benefits, namely;

1. A TIN can be created directly from the raw Light Detection And Ranging (LiDAR) measurements, thus allowing for only one data conversion from measurement to input for noise modelling.

2. In noise prediction software height line data is converted into a TIN, this step could be omitted.

3. Due to the nature of TIN generation a certainty of quality can be provided, omitting manual inspection.

4. A TIN data structure allows for efficient cross section extraction and thus efficient noise prediction computations.

As a TIN has a quality guarantee and additional information allowing for efficient processing, the size of such a terrain is much larger than the current height line data structures. As the size is important for decimation and processing, the data structure is not yet adopted by commercial software. However, it is worth investigating if the disadvantage can be solved by optimising a TIN such that the size is significantly reduced while the noise predictions are still accurate. To measure whether a terrain can still produce accurate noise predictions a conceptual prototype was developed. This is a proof of concept software package for cross section extraction using a TIN based elevation data structure (van Rijssel et al., 2020). The cross sections can be processed using an open implementation of CNOSSOS[9] to obtain noise values. As a result the optimisation of the TIN based terrain can now be studied. This data structure is therefore selected for this research.

2.2.3 Noise calculations using a triangular irregular network

In this research a conceptual implementation to make noise calculations using a TIN in CNOSSOS is used. There currently does not exist an implementation for RMG, in this research this is solved by converting the TIN into individual lines. These lines are then, in the modelling software, converted back into a identical triangulation. This section further elaborates the set up of the TIN for this implementation.

The implementation supports a TIN of LoD 1.3 as defined by Kumar et al. (2019). In short this is a 2.5 dimensional TIN, i.e. there are no vertical "wall" segments and each $[x, y]$ location only has a single height value associated with it. Each triangle contains semantic data to store the properties of that triangle. The terrain does not include vegetation or man made objects like buildings or noise barriers (it does include natural barriers that are part of the terrain, e.g. dykes). Each triangle contains a ground type (e.g. reflecting or absorbing) or an ID that refers to a building. The related building data set stores the height of all the buildings. In the terrain the buildings should therefore be modelled as a flat surface on ground level. During the extraction of the cross section the terrain is lifted to the roof height of the building, the cross section can therefore have vertical "wall" segments.

As each triangle can only contain a single material, the terrain is forced to include all buildings and ground type edges in the TIN. This is called a constrained triangulation.

The RMG implementation only uses the elevation model for the height and requires a separate planar polygon partition for the ground types and buildings. This terrain is therefore not required to be constrained and the shape can be purely based on the shape of the terrain itself.

---

[9]https://github.com/genell/Cnossos-EU-SWE

Figure 2.8: Terrain generation by fitting a curve

Figure 2.9: Terrain generation by honoring the points
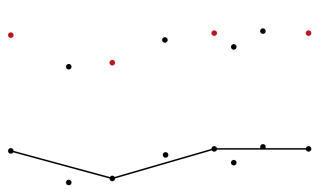
Figure 2.10: 2D Terrain generation using single-pass feature method
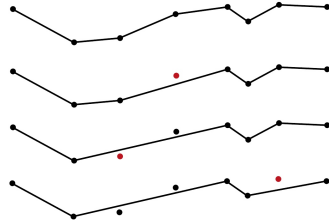
Figure 2.11: 2D Terrain generation using multi-pass decimation
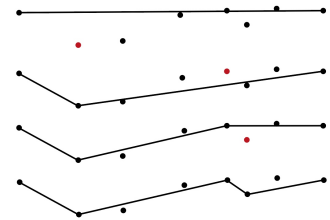
Figure 2.12: 2D Terrain generation using multi-pass refinement

2.2.4 Generating a triangulated surface mesh

During this research a terrain representation in the shape of a TIN is constructed. Therefore this section describes how such an elevation model can be constructed and which type is most suitable for this research. A good interpolation method for terrains adheres to seven properties (exact, continuous, smooth, local, adaptable, computationally efficient and automatic) (Ledoux et al., 2020, section 4.1).

An accurate model starts with accurate input data, this data is therefore as close to the original measurements as possible. For this point cloud is used, this is a (commonly large) collection of points in 3D Cartesian space (X, Y and Z distance from the origin $[0, 0, 0]$). These points are commonly retrieved using airborne LiDAR, where a point indicates the presence of a non-reflective object. The point is often provided with metadata and a classification on the type of object. Terrains are commonly generated in 2.5D. Representing the terrain in 2.5D compared to full 3D is much faster to generate and process while being sufficient for many purposes, as is the case with noise modelling.

Creating a mesh from a point cloud can be done in several ways, which can be subdivided in several categories. First of all, the method can honor the points (Figure 2.9), i.e. it will select a set of points from the input to create the mesh from. Or it can fit a function for a shape or curve (Figure 2.8), minimising the total error between the mesh and the points. While the latter produces a more smooth and continuous map, it may have difficulties with small local height differences and terrains and varying shapes (Ledoux et al., 2020). It is therefore commonly used when the accuracy of individual points is low and a higher precision can be obtained by averaging and aggregating multiple nearby points into a smooth terrain. The available point cloud in the Netherlands has a precision of 0.05m where the terrain has a highly variable shape. While time efficiency of generating the terrain is not of major importance at this stage, the approach should be scalable for large areas. Therefore honoring individual points is best suited for this research.

Then, the number of points in subset P of point cloud S should be minimal while following the terrain accurately. To determine which points in set S should be part of subset P three approaches can be used; 1) one-pass feature methods, 2) multi-pass decimation or 3) multi-pass refinement (Garland and Heckbert, 1997). One-pass feature methods (figure 2.10) use a distinctive algorithm to select important points at once and build the TIN from these points, the accuracy and performance of the tool depends on the algorithm. It does not provide a defined accuracy, but the errors can be extracted afterwards. Decimation (Figure 2.11) starts with triangulation of all the points and iteratively eliminates points from subset P. Refinement (Figure 2.12) starts with an initial triangulation and iteratively selects points to include in subset P, this continuous until the error of all the remaining points stays within a defined tolerance.
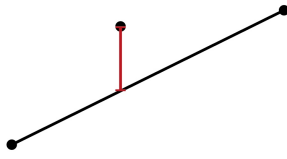
Figure 2.13: 2D point importance measurement using absolute vertical error
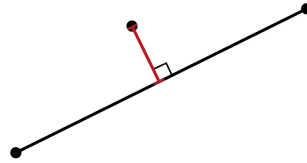
Figure 2.14: 2D point importance measurement using absolute perpendicular error
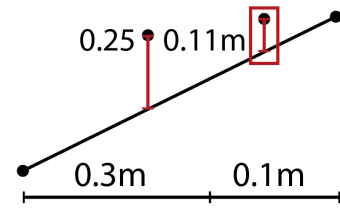
Figure 2.15: 2D point importance measurement using absolute factor of tolerance. In this case the left point has a larger absolute error, but stays within the tolerance. The right point will be added as it surpasses the tolerance.

When comparing both methods, decimation is more time intensive as inserting or removing a vertex from a TIN is less time efficient than recomputing the error between a point and a triangle. Refinement computes all errors, inserts a point and only updates the errors in the updated triangles. Both methods generate a similar result, where refinement is faster in a coarse TIN and decimation is faster when a high accuracy is maintained. Also note that decimation requires the point cloud P to be triangulated first while refinement can start with a simple initial triangulation (often a large triangle or rectangle which covers all points). As one-pass feature methods cannot assure the quality, where this is important for this study, it is not suited. As the terrain should have a varying accuracy and no initial triangulation is provided, the multi-pass refinement method is the most efficient and therefore the most suited.

To determine which point should be eliminated or selected the importance of that point is determined. This importance can be measured by the error between the point and the terrain mesh without the point, this distance can be vertical (Figure 2.13) or perpendicular (Figure 2.14), absolute or as a factor of the local tolerance (Figure 2.15). Garland and Heckbert (1997) studied the results using vertical and perpendicular error and showed the absolute vertical error provided the best overall results, which is nowadays most often used. Measuring the importance as a scalar factor of the threshold depending on the position or metadata of the point has received little attention but is very suitable for areas with varying accuracy thresholds.

As a method to select the candidate point the factor of local tolerance is favourable as it allows to have a continuous variable accuracy, allowing a variable level of detail. However, currently there is no implementation of this theory available. Implementing such a theory is out of scope as it is too large and complex to develop as a part of this project. When implementations of such software become available, this would be preferred. From the remaining options the absolute vertical error generates the best results in variable environments. To still generate variable accuracies, discrete areas can be obtained with their own accuracy values. This allows to assign regions with higher or lower accuracy values, but it does constrain the model on the edges of the regions. When the discrete areas are large, the constraints on the model are minimal while benefit of different accuracy values remains. It is therefore preferable to have discrete regions with set accuracies.

2.2.5 Analysing the effect of terrain accuracy when generating a TIN

In order to understand the effect of the accuracy of the TIN a 2D visualisation is provided in Figure 2.16. In this figure a 2D version of the Garland and Heckbert algorithm is visualised to illustrate how it works. The algorithm iteratively adds the vertex with the highest vertical error until all remaining vertices fall within the error threshold. Because the vertices are added starting with the largest error,
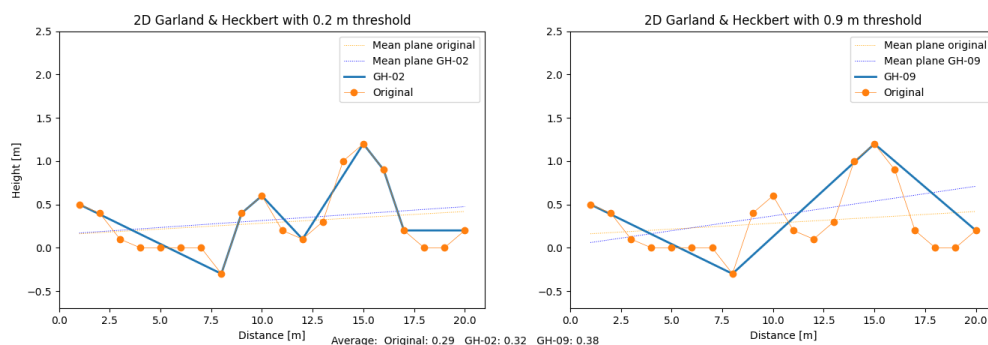
Figure 2.16: Line simplification using 2D version of the Garland and Heckbert algorithm with a 0.2 and 0.9 m error threshold.

large formations, like the hill on the right side, will be added first, as they cause the largest error in the line. This approach is suited to detect formations that are taller then the error threshold. In noise modelling the height information is used mainly for two purposes as described above; blocking the line-of-sight and a mean height level or mean height plane. The accuracy is therefore dependent on the height of the noise propagating above the local surface, so diffraction can be noticed with certainty.

2.2.6 Overview of available triangulation software

Generating an elevation model in itself is a complex process. To achieve a high quality and reliable elevation model, the input data should be accurate as well. Different techniques of filtration and interpolation can be used to obtain an elevation model in raster or vector format (of which vector is most commonly a TIN for elevation data). Other formats, like iso-contours or height lines are derived from the TIN or raster format.

To obtain a TIN, different algorithms can be used. It is common to use the Delaunay Triangulation (DT) criteria for a TIN. This is an approach on how to create the triangulation given a set of points. Given the same set of points, multiple triangulations are possible. A DT states that for each triangle the circumcircle of the three vertices does not contain any other vertex of the terrain. This results in generally evenly spaced triangles that approximate 60° angles in each corner of the triangle. as it ensures evenly spaced triangles and prevent sliver triangles (Delaunay et al., 1934). A triangulation can be made by using all vertices from the point cloud in the TIN, however, this generally results in many (small) triangles. In digital elevation modelling it is therefore common to use an algorithm which iteratively add the most suitable vertex. An example is the fast triangular approximation algorithm (Garland and Heckbert, 1997). This algorithm starts with an rough initial triangulation and per triangle iteratively adds the vertex causing the highest error until the error is below a defined threshold.

Algorithms to create such elevation maps are complex as they must be both precise and efficient to process large amounts of data within a reasonable time. Several commercial (e.g. Safe FME[10], Autodesk Recap[11], 3DReshaper[12]) and open source solutions (e.g. Cloud Compare[13], StarTIN[14] and 3Dfier[15]) are available to produce a raster or mesh from a point cloud.

A unique feature of 3Dfier is that it allows to create a constrained TIN based on input polygons and define different types of triangulation for different types of terrain(Ledoux et al., 2021). For example, building polygons can be modelled with or without roof and/or walls at a specified percentile height. There are two types of vegetation that can be modelled with a different accuracy. Water can be modelled

---

[10] https://www.safe.com/fme/

[11] https://www.autodesk.com/products/recap/

[12] https://www.3dreshaper.com/en/

[13] https://cloudcompare.org/

[14] https://github.com/hugoledoux/startin

[15] https://github.com/tudelft3d/3dfier

as a flat surface and roads as smooth surfaces. Other software include automatic removal of outliers in noisy data such that the point cloud does not require pre-processing.

2.2.7 Selection of triangulation software

This research consists of a theoretical part and a practical (implementation) part. The theoretical part is not bound by any limitation of software. However, as the theoretical model is also converted into a practical model, this practical part is bound to available software packages. As the implications of the triangulation software have a very large impact on the implementation and shape of the results, it is selected in this section.

Based upon the requirements given in Section 2.2.4 and the possible triangulation software packages provided in Section 2.2.6, 3Dfier (v1.3.0) has been selected as the most suitable software package. It has the following unique properties which makes it most suitable;

1. Possibility to triangulate different regions with a different accuracy

2. It allows to constrain the triangulation to polygons and keep semantic information, a requirement for the noise calculation in CNOSSOS as mentioned in 2.2.2.

3. It allows to model buildings as flat surfaces on ground level, a requirement in CNOSSOS as mentioned in 2.2.2.

4. The approach to the triangulation of regions is in accordance with the triangulation requests as stated in 2.2.4, e.g. an implementation of the Garland and Heckbert triangular approximation algorithm to select candidate vertices followed by a constrained Delaunay Triangulation (cDT) to insert the selected vertices into the triangles(Garland and Heckbert, 1997).

2.3 Scope of the project

In order to maintain a focus on the research goals this section describes what research related topics are explicitly left out of scope, This helps to keep a focus on the goal and communicate the expectations of the results. Therefore the following items are not covered in the research;

1. As this research focuses on the terrain elevation data, the ground type and building data sets are taken as is.

2. The output data file format is based upon the requirements for TIN based Noise modelling software as developed during the 2020 Synthesis project "3D noise modelling", also an output file format is made for GeoMilieu software for comparison.

3. Developing triangulation software itself is not considered part of the research.

4. Part of the research is limited to the limitations of the provided noise modelling software for European noise calculations (van Rijssel et al., 2020) (if possible it is not limited in the Dutch calculations), which are;

   a) Bridges and tunnels are not included.

   b) Only road and railway sources are recognized as a source (Industry and aircraft noise are excluded).

   c) Within a noise study each source emits the same level of noise, as it is hard coded in the software.

   d) A source can only emit from a single emission height (as is the case for roads, but not for rail).

   e) Noise barriers are only supported when included in the TIN, i.e. they are natural barriers.

3 Methodology

In order to obtain a model to create a TIN that is optimised for noise modelling purposes in this section a methodology is proposed. An optimised TIN has a minimal amount of triangles to describe the terrain, while preserving detail where the terrain height has a large influence on noise propagating over this terrain. Identifying where this detail is and is not required is the core of this research. Due to the nature of the selected triangulation type the detail is provided in terms of an accuracy (or in other words a tolerance between the model and the real terrain (a point cloud) as measured using airborne LiDAR).

Based on the analysis of the noise methods a set of parameters is derived upon which a model can be constructed. This model consists of a set of 'rules' that define an accuracy to use for the triangulation for a given location in the terrain. This model is purely theoretical and can be implemented in any combination of applications and or programming languages.

The model generally consists of creating an "accuracy map", a 2D map that provides an accuracy for each $[x, y]$ location. This accuracy map can then be used together with a point cloud to create the triangulated terrain.

To verify whether the model behaves as expected, it is implemented and tested. The goal of the implementation is to verify whether the (sub-)steps provide the requested results. The implementation is therefore made using Quantum GIS[1]. While this software cannot be fully automated and does not offer all the freedom of a programming language, it is quick and allows to visually inspect all intermediate steps. This is preferred as quality and verification of the output is of higher priority then automation and speed of the model.

The implementation is then used to make noise calculations in several different scenario's. These empirical tests do not provide the guarantee that the model will work in all environments at any time but should give a clear indication of what is possible when optimising the elevation model. They should also help to tune the model, i.e. determine settings of the parameters that provide the most optimised TIN while providing enough accuracy for noise calculations.

---

[1] https://www.qgis.org/en/site/

4 An environment based approach for the generation of terrain elevation data optimised for noise modelling

In this chapter a theoretical model, i.e. a set of rules upon which an accuracy can be determined for a location given its environment. These 'rules' are based upon a set of parameters (e.g. distance to a road) that might influence the required local level of detail. Each parameter has settings (e.g. accuracy, distance), these can be varied in an implementation to determine the balance between sufficient quality and a small terrain size. This balance is sought in chapter 6.

4.1 Selecting accuracy parameters for the approach

The parameters are subdivided in three categories; surface type, distance to objects and the topology of the terrain. A parameter will be selected if, through analysis, it is expected to have a distinctive impact if the terrain would have an adjusted accuracy in this region, i.e. if the terrain requires more (or less) detail in a region due to this parameter. This impact should be sufficient as additional line constraints can also introduce more triangles. Per parameter a range of the expected level of detail is provided. This range is determined based on a theoretical analysis and empirical testing.

As different parameters might indicate a different level of accuracy for the same area, some logic is also included in 4.1.4 to determine which accuracy should be picked.

Note that immission (receiver) points are not included as their placement depends on the purpose of the noise calculation. Also industry noise sources are not included as the noise emission height is commonly not close to the ground. Diffraction on smaller objects is therefore not applicable and as such detail is not required. At the moment of writing, there is also no public data set with industry noise sources available.

4.1.1 Surface types

Different types of surfaces (as provided in the Basisregistratie Grootschalige Topografie (basic registration large scale topography) (BGT) [1] have different characteristics. Roads are generally flat and have a smooth gradient without sudden height jumps. Rivers are almost flat with a very small angle where lakes and seas are flat. Creeks and waterfalls can have sudden jumps in height and are generally narrow. As they are very rare in the Netherlands they are omitted in this research. Vegetation can be flat, like grasslands, or rough in nature and mountainous areas and therefore has a variable variance.

In noise modelling the terrain is subdivided in acoustically reflective and absorbing areas by aggregating common terrain types from the Digitaal Topografisch Bestand (Digital Topographic Data) (DTB) (Peters et al., 2018). As mentioned in Section 2.3 the conceptual implementation of CNOSSOS the TIN requires to store semantic information regarding the acoustic property in the triangle. For CNOSSOS calculations the TIN is therefore constrained to this planar polygon partition, limiting the possible size reduction of the model. Because infrastructure like roads and parking lots are generally flat with, if present, vertical height jumps along ridges, staircases and walls, a higher or lower accuracy will not cause a big difference in the TIN because, as long as the tolerance is lower then the ridges.

---

[1] https://www.pdok.nl/introductie/-/article/basisregistratie-grootschalige-topografie-bgt-

While acoustically absorbing ground reduces the noise level, where reflective ground increases the noise level, they are only used to determine which portion of the path is reflective in the noise prediction methods. Therefore there is no need to require a different height accuracy based on the acoustic property of the terrain.

Water areas are difficult for triangulation software as water is reflective and the point density and precision are generally lower. This may lead to an unrealistic terrain. It is beneficial if water can be modelled as a flat surface as this will lead to more realistic models. To minimize the amount of triangles due to constraints, the amount of line segments and the density of lines should be kept to a minimum. Therefore, it might be beneficial to simplify the polygons which are inserted as constraints. However, this is out of scope as it can be optimised separately from this research. As different surface types, except waters, do not clearly require a difference in accuracy and a distinction will only cause more constraints to the TIN they are not included as a parameter.

To conclude, three types of terrain are included for CNOSSOS computations; acoustically absorbing terrain and acoustically reflective terrain, where water and other reflective terrain are separated and elevated differently. This distinction of water is considered worth looking into as water can be modelled flat in 3Dfier and this will result in a more accurate representation. Note that this planar partition does not yet contain an accuracy value, but the polygons hold the acoustic property values.

4.1.2 Distance to objects

This category analyses which objects influence the required elevation accuracy in the vicinity of this object. The objects that are included are roads, railways, noise barriers and buildings. Formations of the ground, e.g. dykes, are not characterised as objects as they are pat of the elevation topology and discussed in that section.

Roads

For road traffic the emission height is 0.75m above the road surface in the RMG method[2] and 0.05 m in the CNOSSOS method (European parliament and European Union, 2015, section 2.2). As the CNOSSOS height is lower, the noise will propagate lower and diffraction will occur sooner. It is therefore the limiting factor. Because the emission source is so close to the ground, the terrain elevation should be accurate close to the road to provide sufficient detail to correctly model the occurring diffraction. In Table 2.7 the right figures show that for favourable conditions the noise propagation height quickly rise. At 20 meters they are already about 1.5m above the road elevation while the homogeneous paths remain at 0.3m. Using this analysis the model would be accurate if the accuracy of the terrain is based upon the distance to the noise source and uses the lowest noise height according to Table 2.7. The model should therefore use an accuracy based on the distance to a road using Equation 4.1. This is only valid for short distances as a baseline accuracy will be used for remote areas, this is further elaborated in Section 4.1.4. This area in the vicinity of roads can be referred to as a road buffer.

$$\text{Accuracy}_{road}(d) = \begin{cases} \frac{3.95}{300}d + 0.05, & \text{if } 0 \leq d \leq \text{d}_{max} \\ \text{acc}_{max}, & \text{otherwise} \end{cases} \tag{4.1}$$

Where;
d is the distance to the nearest road.
d_{max} is the distance at which the noise propagation height will go above the baseline accuracy.
acc_{max} is the baseline accuracy further elaborated in Section 4.1.4.

With regard to the implementation of such an approach; currently no triangulation software is available that support a distance dependent accuracy. A practical alternative is provided in chapter 5.

Railroad

For rail roads the emission height in RMG is 0.0, 0.5, 2.0, 4.0 and 5.0 meter above the rail, where the rail is commonly placed 0.2 meter above the local ground. A significant part of the noise is produced by the wheels on rail height, therefore the 0.2 meter height source (0.0 above the rails) is the most relevant for the elevation accuracy of the ground around the rails. In CNOSSOS the noise sources are placed 0.5 and 4.0 meter above the rail.

Similar to the parameter distance to roads, the accuracy should be dependent on the distance to the nearest railway and follow the lowest noise propagation height of Table 2.7. This can be translated into Equation 4.2. This area in the vicinity of rails can be referred to as a rail buffer.

$$\text{Accuracy}_{rail}(d) = \begin{cases} \frac{1.3}{300}d + 0.2, & \text{if } 0 \leq d \leq \text{d}_{max} \\ \text{acc}_{max}, & \text{otherwise} \end{cases} \tag{4.2}$$

Where;
d is the distance to the nearest rail.
d_{max} is the distance at which the noise propagation height will go above the baseline accuracy.
acc_{max} is the baseline accuracy further elaborated in Section 4.1.4.

With regard to the implementation of such an approach; currently no triangulation software is available that support a distance dependent accuracy. A practical alternative is provided in chapter 5.

Noise barriers

Where noise barriers are deliberately placed near noise sources to block noise, it will have a significant impact on the noise propagation and as such, the requirements for the terrain around it. However, as it functions similar to a natural barrier in the terrain it is discussed in Section 4.1.3.

Buildings

In most cases a building will cause diffraction for most paths running close to buildings, therefore a low accuracy would suffice. On the other hand the RMG method will, in many cases, place the receiver points nearby buildings. Here an accurate height is preferred as the receiver is placed a set distance above the local ground and will therefore have the same elevation error as the ground. However, almost all buildings are placed in the vicinity of a road and will therefore already have an increased accuracy. Given the arguments, there is no clear advantage of applying a parameter to increase the accuracy around buildings. It is therefore not considered.

4.1.3 Elevation topology

The analysis made in 4.1.2 is based upon a flat terrain and non-elevated source and receiver points. It might be interesting to consider whether the road is elevated above the terrain, or lays on an elevation, like roads running on dykes or up to bridges, in which the surrounding terrain will be lower and the noise will therefore propagate higher above the terrain. In other cases the road may be sunken into the terrain, in which the road is lowered to reduce noise pollution, or towards the entrance of a tunnel. At last a natural noise barrier, much like a dyke, is commonly placed in between a road and neighbourhood.

It these situations, diffraction will either play a small role (in the case of elevated roads) or occur in all situations, in the case of lowered roads. In both these situations, as well as natural noise barriers, there are significant height changes. A higher accuracy is not required when the road is not visible, i.e. if the noise has to diffract to reach a location. Using the baseline accuracy in this case will not significantly
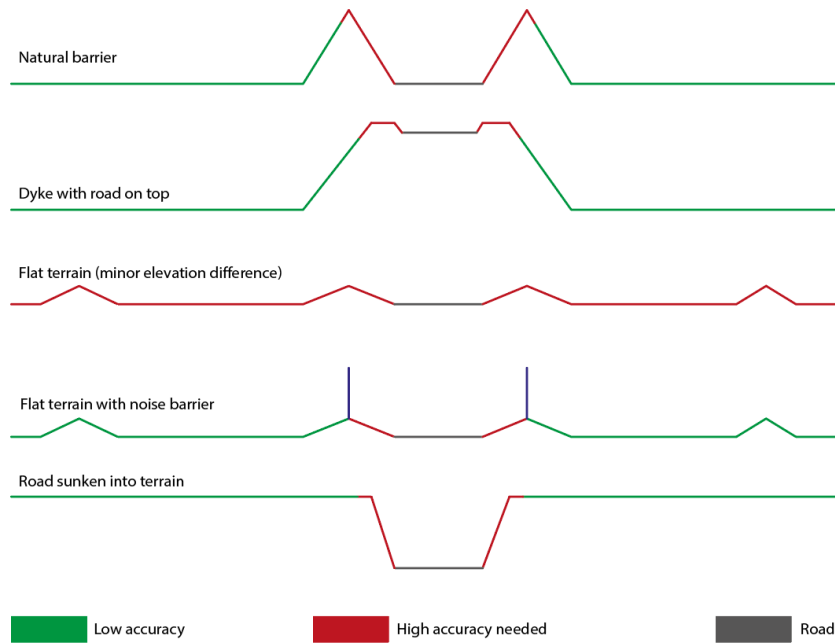
Figure 4.1: Schematic representation of several different elevation topologies around noise sources

influence the mean height and the height plane as used by the calculation methods. This is depicted in Figure 4.1.

While this approach is valid for natural barrier, that are part of the elevated terrain, as for noise barriers that are not included in the terrain. Noise barriers are separately added in noise modelling software, this feature is not yet supported for the current CNOSSOS implementation. The noise barriers will not be influenced by the accuracy of the terrain, while natural barriers are part of the terrain elevation and therefore will be part of the elevation model.

4.1.4 Summary of parameters

During the analysis of the different parameters the following conclusions are drawn; Terrain in the vicinity of noise sources require an increased accuracy, but this vicinity is (partially) decreased when a (natural) noise barrier is present. This will keep the discrete accuracy polygons as simple as possible while reducing the accuracy in these regions. Areas further from road or railways should maintain a maximum tolerance (accuracy) as immission points also require a certain accuracy. Therefore creating a map using the minimal value of all distance parameters (e.g.

$accuracy(x, y) = min(baseline(x, y), \text{Accuracy}_{road}(x, y), \text{Accuracy}_{rail}(x, y)))$ and then applying the topology parameter will provide the required accuracy for each location. The baseline accuracy will be in the range of 0.5 to 1.0m, tests using different settings should indicate what accuracy is required.

In the TIN that is created from the accuracy map, all the information from the environmental model is included for CNOSSOS calculations, i.e. ground types, buildings and ground elevation. This aggregation was decided upon during a student project which researched the possibility and benefits of a TIN based structure. It allows to retrieve the crossed buildings, ground types and elevation with the use of only one efficient cross section analysis (van Rijssel et al., 2020).

5 Theoretical and practical implementation of the approach for empirical testing

To verify and tune the parameters of the model proposed in the previous chapter, noise values will be computed using a terrain generated according to the mentioned parameters. To obtain noise predictions from such terrains several consecutive steps are taken; 1) A map is created stating what accuracy is required in which regions. 2) Using this map a terrain is generated. 3) Noise levels are predicted using this terrain. For each step the options to achieve this step are analysed and reviewed.

The noise levels in step three are predicted according to both the Dutch RMG and the European CNOSSOS. This is summarized in Figure 5.1.

The information (i.e. data sets) that are required to execute all the functions for an area are included in table general data flowchart (see Figure 5.2).

Table 5.1: Overview of used data sets

Name	Purpose	Data structure	Source	Link
AHN 3	Elevation data	5m raster	Rijkswaterstaat	PDOK
3D geluid	Building data	polygons	TU Delft and Kadaster	Kadaster
3D geluid	Groundtype data	polygons	TU Delft and Kadaster	Kadaster
BGT	water areas	polygons	Kadaster	PDOK
NWB	Noise source	linestring	Rijkswaterstaat	PDOK
Railways	Noise source	linestring	Prorail	PDOK
Soundproofing facilities	noise barriers	linestring	Rijkswaterstaat	Government

5.1 Creating an accuracy map

This step is implemented using QGIS 3.18 as is has a broad availability of functions and allows for easy interpretation of the results. To produce a fully tessellated and valid (i.e. no gaps in between polygons, and the incident vertices of two adjacent polygons are identical) set of polygons covering an area, many steps are involved. Possible limitations of the available functions in QGIS are explicitly noted in separate paragraphs. First the implementation of the distance to objects (e.g. roads and railways) parameter is executed, producing a map with polygons for high and low accuracy regions. Independently the elevation topology function is executed which results in polygons where a high quality is not required. These maps are combined and the result is used to clip with the ground types data set. At last the buildings and water bodies are cut out of the polygons such that the data is valid for 3Dfier.

For each parameter first the model is explained, independent of any implementation. Then, the implementation in QGIS is discussed where possible limitations are described.

5.1.1 Distance to objects

Ideally the accuracy value is a function of the distance to the nearest road, however no software package exists that can produce a triangulation with a continuous variable accuracy. Therefore this section explains the approach for a discrete area. Subdividing an area in a polygon where the distance to a road or rail (line segment) is less than a given threshold, and an area where it is more, can be obtained by setting
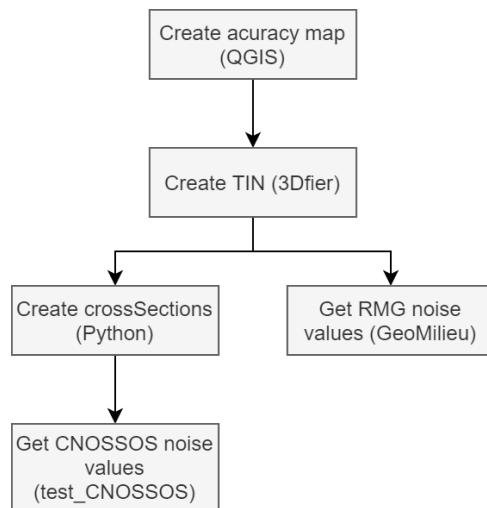
Figure 5.1: Flowchart of the workflow in general
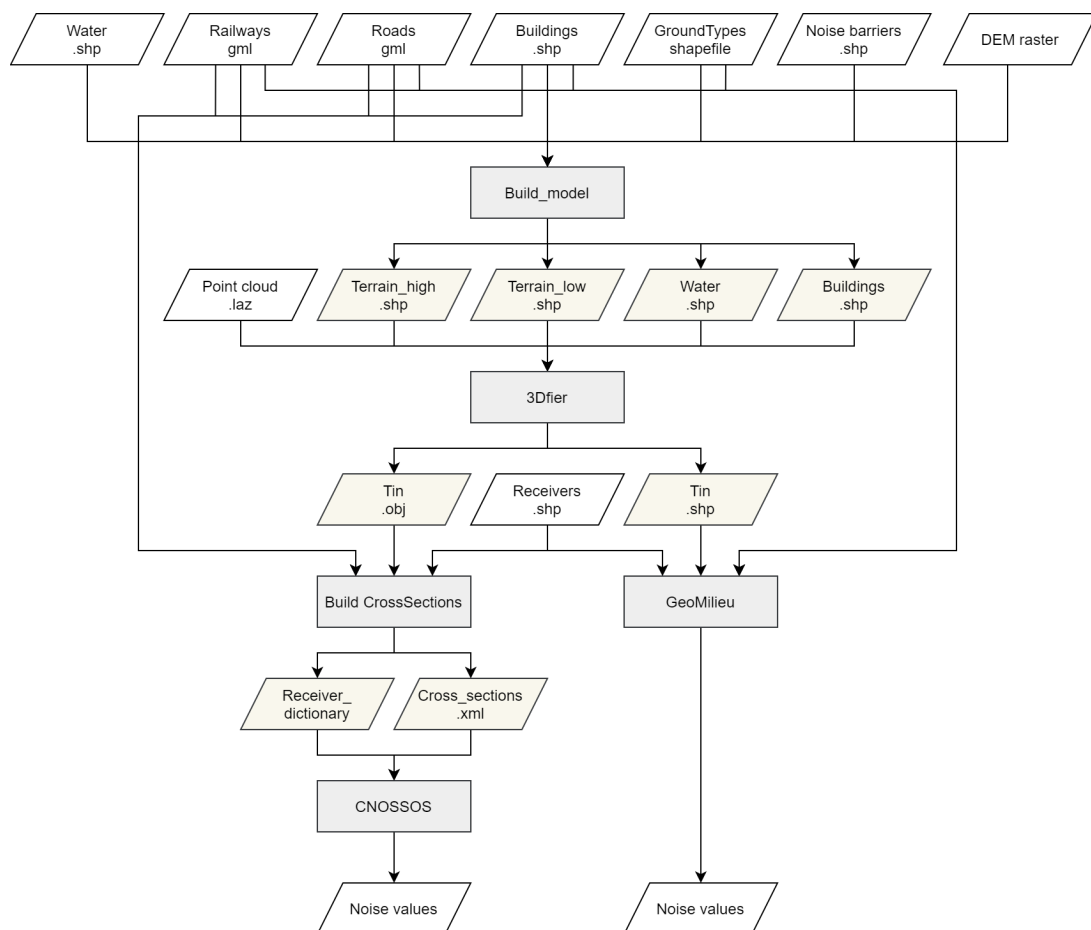
Figure 5.2: General data flowchart; a flowchart showing the general processes and where data sets are used when.
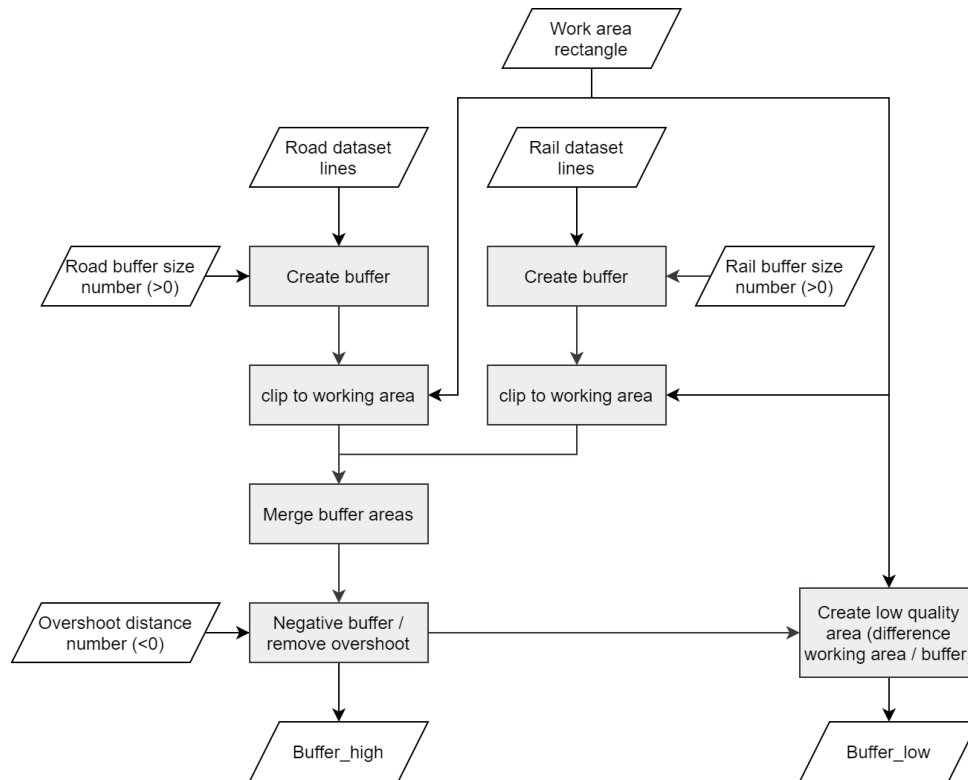
Figure 5.3: Flowchart for distance to roads and railways

a buffer around a set of lines. This provides two areas, one for higher accuracy near roads, and one for lower accuracy areas. The "low" accuracy area is obtained by removing the high accuracy area from a polygon covering the whole area (i.e. taking the inverse of the high accuracy). This buffer is different for road and rail data, also, in case two parallel roads are 45m apart, and they buffer distance is 20m, then a slim 5m 'low' accuracy region emerges in the middle, as this will only cause more and not less triangles the roads are first buffered including an overshoot, which is later again removed by a negative buffer. In the case of corners and end points the buffer curvature is simplified to two line segments for a 90 degree angle. This process is depicted in Figure 5.3.

5.1.2 Elevation topology

An algorithm that recognizes areas that are do not have a line of sight is commonly known as a view shed analysis. This is an algorithm that uses an elevation map and one or more viewpoints. For each location (commonly in a grid) it will look at all elevations in between nearby viewpoints and itself to retrieve whether there is a line of sight. As this algorithm is commonly applied to large areas, the elevation data is commonly provided in a relative low file size. Raster data sets are very suitable due to its smaller size and efficient computation. In the Netherlands this data is available in 0.5m and 5m grid sizes as both a digital elevation model (DEM) and digital surface model (DSM) where the DSM includes human made objects and vegetation. The pixel value it based upon an Inverse Distance Weighting (IDW) of points classified as "maaiveld" (ground level) from the raw measured point cloud[1]. The IDW assigns a weight to each point based on the exponential distance to the center of the pixel, as such points closer to the pixel center have a exponentially larger influence on the value.

For the purpose in this research the view shed analysis is used to locate areas occluded by a (natural) barrier close to a noise source. These areas are generally larger patches and the natural barriers are of significant size. The AHN DEM 5m raster data set is selected as it includes the natural barriers and

---

[1] https://www.pdok.nl/introductie/-/article/actueel-hoogtebestand-nederland-ahn3-

27
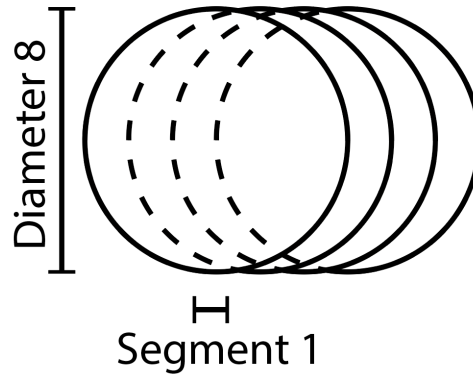
Figure 5.4: line source segmentation to extract viewpoints using a diameter to viewpoint ratio of 1:8

produces a more global result with less noise and is much faster to compute than the 0.5m version. In such algorithms, there can also be a viewing distance, a maximum distance that a viewpoint can reach. This reduces the computations by only covering the areas close to a noise source. As the view shed is used to locate areas where the high accuracy is not required, thus a low accuracy is sufficient, only the high accuracy regions require the analysis. The viewing distance is therefore set to the buffer distance for road / railways + 10m. This is twice the pixel size and thus the occluded areas will extend by at least one pixel beyond the high accuracy boundary. ensures the patches extend beyond the buffer and cutting these areas from the high accuracy regions does not leave artefacts.

To implement such an algorithm in QGIS the following approach is used; The viewpoints can be obtained by extracting the vertices of the line sources. As some line segments can be long and straight, those segments are split in to segments of 10m before extracting the vertices. Using a maximum segment length of 1/8 of the viewing distance diameter (see Figure 5.4) provides minimal gaps in the reach and provides redundant overlap of a pixel, i.e. one pixel is checked with up to 7 viewpoints. Viewer and receiver heights are set to 0.75m (from RMG as it is higher) and 4.0m (from CNOSSOS as this is higher) respectively to mimic the noise emission and immission heights in worst case, so it is certain the pixel is not visible from a source point in both RMG and CNOSSOS methods.

This algorithm only considers the terrain elevation, so no vegetation if included. However, neither does it contain buildings or noise barrier objects. These barriers are included by increasing the height of the DEM raster by 5m where a noise barrier is present, as the height of an individual noise barrier is not available in the available data sets a default value is used. To increase the dem height in presence of a barrier, the barrier should be converted to a 4-connected raster. 4-connectivity ensures the continuation of the line in the raster as all pixels are connected to at least one of the four adjacent pixels. As QGIS tools allow to convert points, but not lines, into pixels the barrier line segments are split up in 4m parts, such that the distance between points is always less then a pixel (5m). The grow and shrink algorithm is used to ensure the 4-connectivity of the pixels.

The algorithm produces a binary raster with some larger patches of connected pixels with 'blurry' edges, i.e. the edge has several spikes and cavities, and many floating, unconnected pixels, as can be seen in image 5.5

Constraining the TIN to individual 5x5m squares where a low accuracy can be used, will only add more triangles to the TIN instead of removing them. Therefore the raster image should be processed to locate and extract larger patches of connected pixels. These grouped pixels will then be translated into a polygon, as is required for further processing. The polygons covering these patches should follow the patch accurately.

To overcome these difficulties several algorithms are available; firstly the binary raster can be simplified and generalised, secondly the method to convert the raster to a polygon can be optimised to produce a reasonably simple polygon.

An overview of several raster simplification tools;
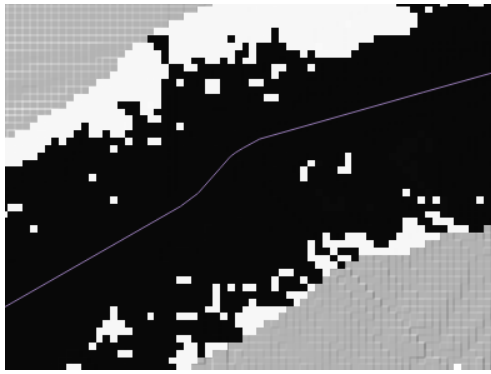
Figure 5.5: Result of view shed analysis, before post processing, purple line represents the road on which the viewpoints are placed, black pixels are visible, white pixels are occluded
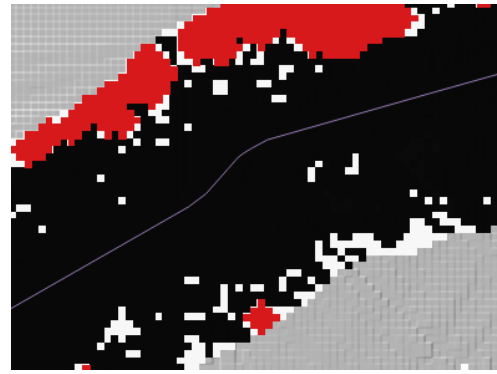
Figure 5.6: Result (red) after shrink and grow algorithm (grow size: 2, shape: circle) based on input (black and white)
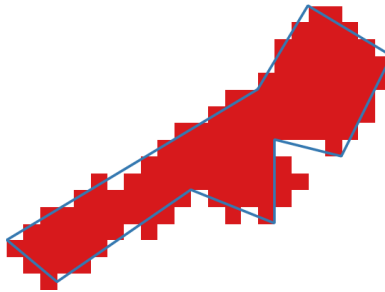
Figure 5.7: Result after simplifying initial vectorisation of raster by means of the algorithm from Douglas and Peucker (1973)
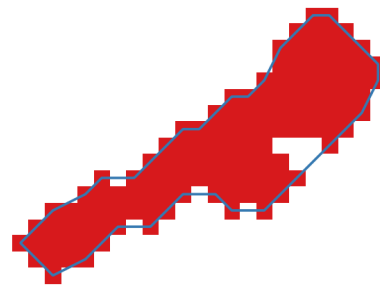
Figure 5.8: Result simplifying the raster data and vectorising the raster by means of a k-nearest neighbour concave hull approach

1. **Majority filter**; for each pixel it will count the number of occluded pixels within a set distance (commonly the 8 pixels adjacent to the pixel) and set the to pixel "occluded" or "visible" depending on the majority of the surrounding pixels. In this case it is applied on raster data with "occluded" and empty cells, this way also "majority" of n pixels can be used to locate new pixels or remove outliers.

2. **Shrink and grow**; all occluded pixels will first grow, i.e. neighbouring pixels will also become "occluded" and then shrink, i.e. the inverse of growing, this can also be done in the opposite order and one or more times, it will generally remove noise and generalize the shape of patches of pixels

3. **Connectivity filter**; used to locate groups of connected pixels, will not create more "occluded" pixels but select those that are connected to at least n other pixels.

After applying the algorithms with different settings the shrink and grow with a range of two pixels (circular shape) provided the best results (see Figure 5.6).

Then, to vectorise the generalised raster into polygons several options are available. The raster can be vectorised by following the pixel edges, leading to a blocky polygon looking much like the raster image. This can than be simplified according to a line simplification algorithm. Several have been tested, but the results where insufficient The shapes are pointy, do not follow the raster accurately and concave areas remain, see Figure 5.7.

In order to generalize the the shapes and remove remaining 'holes' is to use a concave hull algorithm based on the center points of each pixel. As described in (Ledoux et al., 2020, ch. 9) several type of
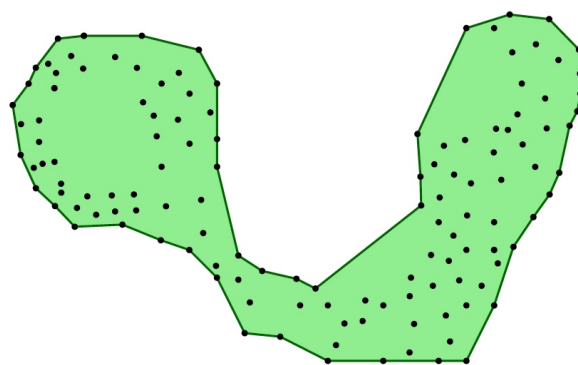
Figure 5.9: Example of the *x*-shape of a set of points((Ledoux et al., 2020, p.90)).

concave hull algorithms are available. After an analysis of the methods the *x*-shape (Figure 5.9) behaved the most appropriate. With one parameter (a maximum edge length) it allows to separate patches and create cavities where needed. However, the time complexity is not optimal (the DT is created and deleted after the polygon is extracted).

Applying this on a large data set quickly becomes computationally intense. First a complete triangulation is made, while the 'islands' of pixels can be quickly clustered prior to the *x*-shape. The islands are identified using a 8-connectivity filter to group the vertices.

In QGIS the functions to retrieve concave hulls using clustered pixels are limited. The only found option is the concaveHull plugin[2]. It uses the K-Nearest Neighbour (KNN) approach. This approach is similar to the moving arm algorithm, but only uses a k amount of nearest points in each decision. It does not guarantee a valid (not self-intersecting) polygon in the case of outliers (as mentioned in (Ledoux et al., 2020, ch. 9)). However, the points are already filtered on connectivity and are pre-processed. There are no outliers present anymore and after testing large areas, the resulting polygons are valid for this implementation. The polygons are similar to those otherwise obtained using the *x*-shape (see Figure 5.8) and the time saving of clustering is very high.

A complete overview of the workflow is provided in the flowchart in Figure 5.10

5.1.3 Aggregate maps

After the regions for high and low accuracy have been generated and polygons of the occluded areas are available, they are combined with the ground types, water and building data sets to obtain the input files for 3Dfier. At last each object in each layer is given a unique id so all objects are included in the produced TIN. This process is visualised in the flowchart in Figure 5.11.

While this process is not complex, the 3Dfier files need to be valid in order to obtain a watertight TIN. If the terrain is not watertight, the conceptual cross section software used with CNOSSOS will cause errors as it cannot locate the next triangle in the cross section. There were several challenges to overcome when implementing this model in QGIS that should be verified in all implementations;

1. As water is reflective and grasslands are acoustically absorbing, the ground types data set often has a boundary on the shoreline. However, these are, unfortunately, similar, but not exactly the same as the water bodies from the BGT, though they originate from the same data set, but a slightly different version. This caused very small and slim sliver triangles around the water areas, leading to invalid TIN geometries. While this should, in theory, not lead to holes in the TIN, 3Dfier seems to have difficulties when vertices are very close together (sub-centimeter), especially when the boundary surface only has three vertices, i.e. it is a triangle. This problem was solved by providing the water bodies with a very small buffer of 5cm. Applying the difference tool to remove the water

---

[2]https://github.com/detlevn/QGIS-ConcaveHull-Plugin
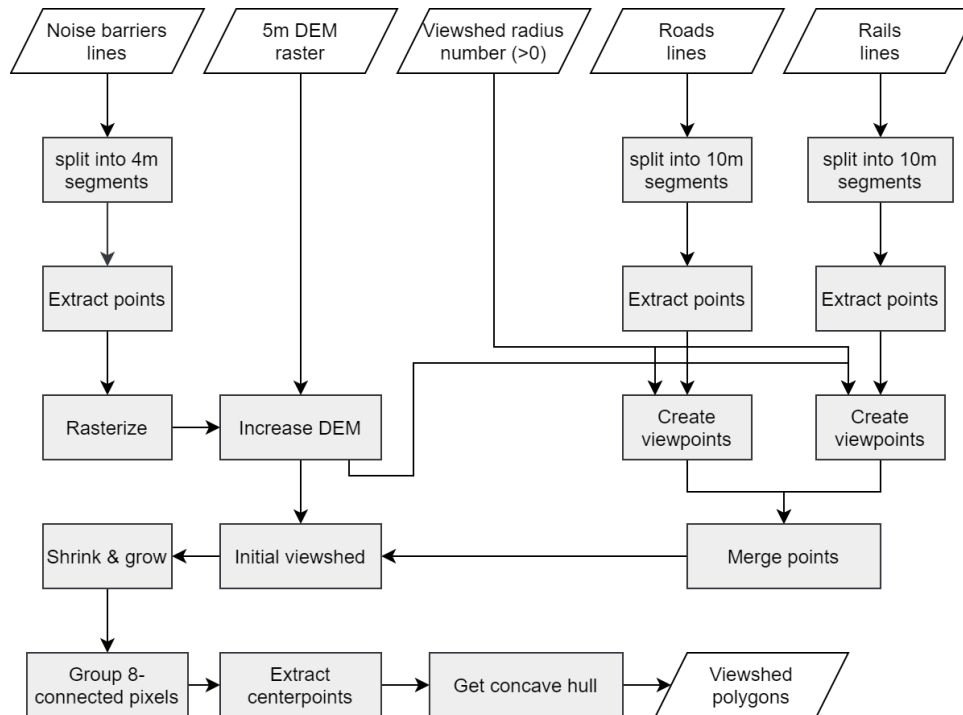
Figure 5.10: Flowchart of the view shed analysis

from the ground type data and then removing faces with an area less then 0.01 m². Inverting this areas results in the water bodies.

2. Clipping the buildings from the ground type data sets in some cases failed, this occurred when buildings are present on the edges of the area, resulting in invalid (overlapping) geometries.

3. Clipping adjacent buildings would sometimes cause the terrain to still have a line in between the buildings, which also caused overlapping triangles in the TIN, while the TIN is still water tight, duplicate triangles with different materials caused infinite loops when extracting the cross sections for CNOSSOS.

4. At last, when the ground underneath a building has a break line, be it from a high to low accuracy region or reflective to absorbing, the polygon vertices along the ground are not identical to the vertices in the building data set. This leads to holes in the TIN (see Figure 5.12). After several tries to unify the vertices on both sides of the polygon (add the breakpoints to the building polygon) no solution was sufficient. The problem is currently solved by manually inserting vertices in the building polygon.

5.2 Generate the triangular irregular network

To run 3Dfier it requires a configure file and an output file with a selected format. The configure file contains the paths to the input files (terrain_high, terrain_low, water, buildings) and the settings of how each polygon should be lifted. This consists of first setting a material for each input layer and then define the settings for each material. The settings used during this project are stated in Table 5.2. The used LAS classes refer to the classification of a point in the point cloud. Only the classes 2 (ground) and 9 (water) are used as no man made objects are included and the building (classification 6) height is already available in the building data set.

To create a fully triangulated terrain and connect all the layers 3Dfier uses the following work flow;

1. All the polygons are triangulated by splitting up the polygon in triangles.
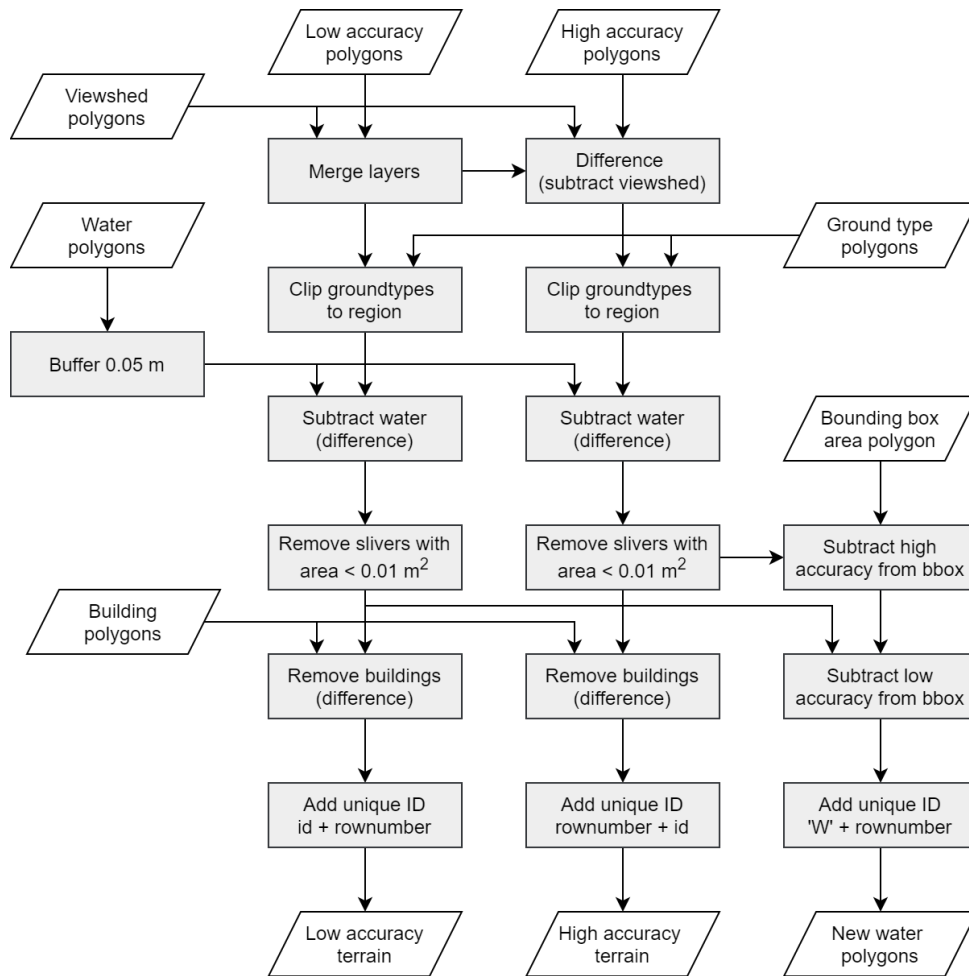
Figure 5.11: Flowchart of aggregating all parameter with the terrain to produce the high and low accuracy terrains and water areas for 3Dfier.
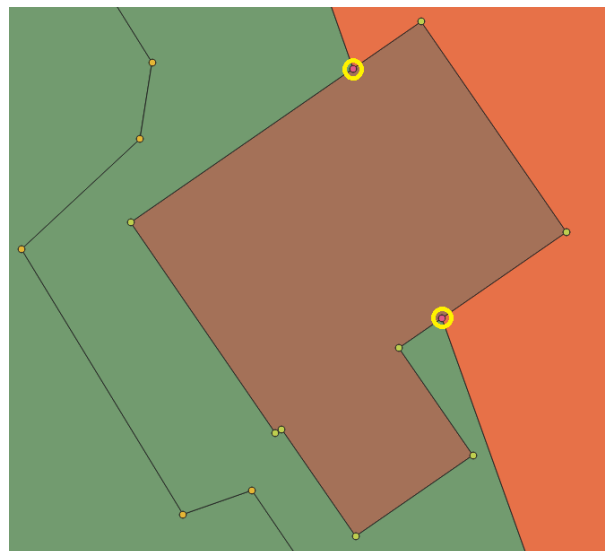
Figure 5.12: Terrain with building, the vertices of the polygons have been extracted to visualise the discrepancy between the terrain vertices and the building vertices on the yellow circles.

General	
radius_vertex_elevation	1.0
threshold_jump_edges	3.0

Terrain (terrain_high)	
simplification	0
simplification_tinsimp	*High accuracy value*
innerbuffer	0.2

Forest (terrain_low)	
simplification	0
simplification_tinsimp	*Low accuracy value*
innerbuffer	0.2

Water (and buildings)	
height	percentile-05

Input_elevation (point cloud)	
omit_LAS_classes	0,1,3,4,5,6,7,8 (use 2 and 9)
thinning	0

Table 5.2: Settings of 3Dfier, defined in the .yml configure file

2. All the points within a radius of 1.0m around each vertex in the polygons are selected to determine the initial height of the terrain.

3. For water polygons a percentile (0.05) of all points close to the polygon vertices is used as the elevation as water is modelled flat.

4. The vertices along the edges of water and ground use the water height and all other vertices use the mean of all points within the 1.0m radius.

5. The Garland & Heckbert algorithm is applied to select candidate points to be added to the constrained Delaunay Triangulation (cDT).

The file format defines which format is used for the output_file, which defines the name and where the output file is written. This and more is documented on the 3Dfier website[3].

Although it is possible to lift buildings to the ground level of the building and only include the floor level, building parts are in this case lifted to different heights and not connected with a wall, leading to holes in the terrain. Lifting buildings as water does level the building parts to the same height and creates a watertight TIN. Using the metadata that is stored in the model (depending on the output file format) the buildings can later be separated from the water.

The .obj format was selected to visualise the output for manual verification. However it stores only one identifier for each object making it less use full for further processing. The .json (CityJSON; Java Script Object Notation) is used for the CNOSSOS approach as this is currently the only supported file format and it stores all available metadata. However, if two objects in the TIN have the same identifier, the second one is simply skipped without warning. The .shp (ShapeFile) format is selected for use in the RMG method, it is simple to visualise in GIS software and is supported by GeoMilieu.

5.3 Generate noise maps

Using the generated terrains noise values can now be calculated. This section will describe how this process is performed. It is separately performed with a conceptual implementation of CNOSSOS and

---

[3]https://tudelft3d.github.io/3dfier/index.html
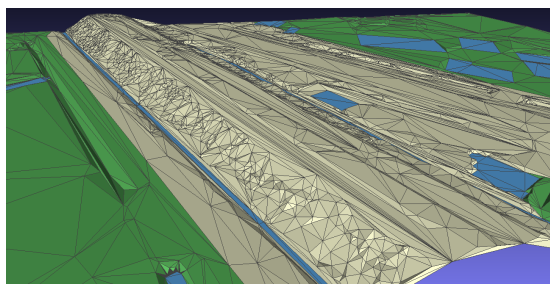
Figure 5.13: Close up of tin from scene 2 with 15 cm accuracy: a dyke upon which the rails lays.
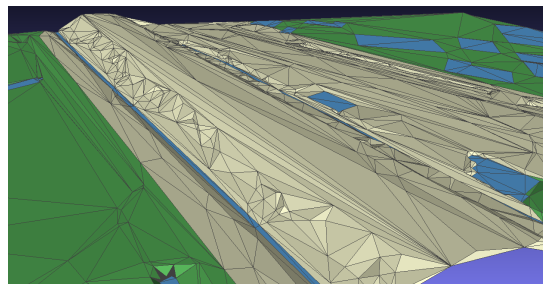
Figure 5.14: Close up of tin from scene 2 with 30 cm accuracy: a dyke upon which the rails lays.

with GeoMilieu according to the RMG method. Both methods use the identical terrain in the different settings, be it in a different format, and the same noise sources and receiver points.

5.3.1 GeoMilieu

GeoMilieu does not support a TIN as data structure. However, it allows height information in the shape of height lines, therefore the TIN Shapefile is converted to individual lines. This maintains the same heights in the terrain and is therefore identical to the .json output as used for the CNOSSOS calculations. The sources emissions are set to the type of the source, i.e. the rail sources have rail noise emissions and road sources have road emissions.

The results have been generated for 1.5, 4.5 and 7.5 m altitude for each individual source and the sources combined. As GeoMilieu does not support road and railway point sources, they have been added as 1 meter long line segments on location of the point source. The intensity of the sources have been increased to produce a dB range similar as to the source had the original line and length. In the computation only direct, vertically diffracted and single order reflective (one reflection) -paths have been used.

5.3.2 CNOSSOS

In order to compute noise levels according to CNOSSOS guidelines an open implementation[4] is used. As this implementation only does the noise calculation for a given path from source to receiver, the path itself is generated using conceptual software developed as a proof of concept by van Rijssel et al. (2020). The source code of this implementation is available on github [5]. This concept software uses an intermediate file format which stores adjacency of the connected triangles as well as ground type / building id in each triangle. The TIN is first converted to this format. Then the cross sections are extracted and the noise calculations can be made.

Semantically enriched TIN

This is stored in an unofficial data structure (.objp or obj plus) which is created for each data set. The implementation contains a python program that converts a .json into a .objp (optionally it can also write the .obj without the semantics, which can be visualised for manual inspection). Here the absorption index of ground and water is added as "G1" or "G0" for absorbing and reflective ground respectively. Buildings are added with a 'B' + the building id. Figures 5.13 and 5.14 depict the generated TIN for the dyke on which the train rail lays.

---

[4]https://github.com/genell/Cnossos-EU-SWE
[5]https://github.com/Constantijn-Dinklo/3D_Noise_Modelling
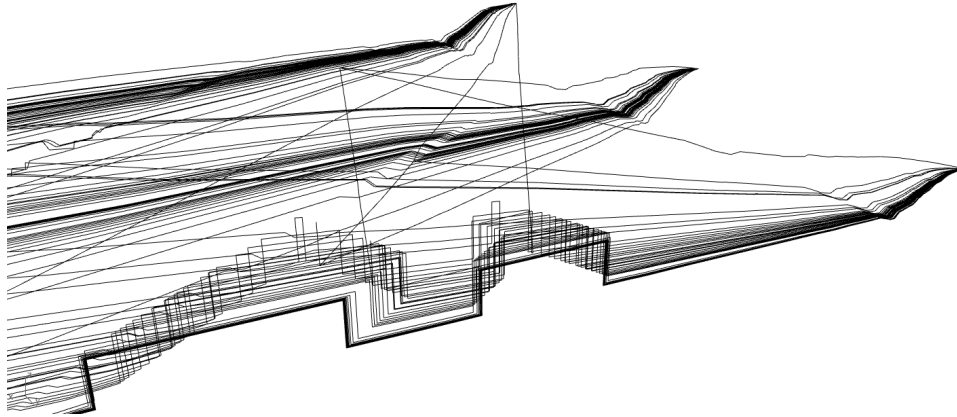
Figure 5.15: Close up of cross section paths produced using the conceptual implementation for CNOSSOS for the scene shown in Figure 5.13 with the noise sources on the right top

Extracting propogation paths

The implementation is in python with a shellscript to connect the CNOSSOS implementation to the python code. As it is a proof of concept not all functionalities are available. Source- and receiver- heights and source emission values are hard coded (i.e. it is constant for one area, which means there can only be one source type in the area) and there is no support for horizontal and multi-order reflection paths.

The emitted noise is provided as a default value for 1m length of road noise. Rail noise is not implemented. To provide an accurate prediction of the noise level they are provided as points with a road length of 30m per source, as the distance between sources is approximately this length. The implementation did not support point sources so this has been added.

The resulting cross sections are written as .xml files for CNOSSOS, all the cross sections are also written as 3D objects and have been visualised for manual inspection (see Figure 5.15).

Retrieve noise levels

The cross sections are read by the CNOSSOS implementation and the noise value is computed. For each receiver the noise levels (L_{den}) are energetically added and written to a Shapefile. The results can then be visualised as preferred.

6 Verification of the approach

In this chapter the approach proposed in chapter 4 is verified and tested using the implementation of chapter 5. This is done by generating (intermediate) results for several areas. These areas are described in Section 6.1. The intermediate and final results are presented in various ways. In chronological order the accuracy maps from which the TIN is produced are presented, followed by the TIN itself. At last calculated noise values for different parameter settings are presented. These values are compared to a reference value to identify how much the values start to deviate in simplified terrains. The results are also compared with a version of the TIN according to settings used for the TIN currently available on PDOK[5].

6.1 Locating areas to test the approach in diverse environments

To test the effect of the parameters on noise modelling, noise predictions are performed with various TINs. These TINs are based on different settings of the parameters. The impact should be measured for different cases; a variety of terrains using different noise path lengths. To allow for a high variety of terrains and path lengths while keeping the workload acceptable, four strips of terrain are selected. The areas are approximately 2000 by 120 meters with a noise source located on one side for three out of four scenarios (the fourth has the sources in the middle).

It is expected that the simplified terrain will cause an increase in noise level when tall objects are modelled lower compared to a less simplified terrain and vice versa. Based on the analysis of terrain triangulation, it is expected some objects will be modelled higher while others are modelled lower. When adding the noise levels of many paths together for one source, the higher and lower noise predictions cancel out while for this study the local effects of the changes in terrain on the noise predictions are important. To focus on these differences, it is proposed to use few noise sources, such that influences don't cancel out and it can be tested in many different environments. The road or rail noise sources are therefore modelled not as a line source but as three point sources along the road / rail. This results in each receiver having three noise sources which are exactly the same for all receivers.

To measure the effect of the terrain over shorter and longer paths, receivers are placed every 100 meters perpendicular to the noise source. To account for local effects of the terrain near receiver points also 3 to 4 receivers are placed parallel to the noise source 20 to 40 meters apart. This leads to a grid of 40 to 60 receiver points (depicted in Figure 6.1). The three sources provide around 150 noise propagation paths for each scenario with each setting.

An overview of the scenario's is provided in tables 6.2 (noise related data), 6.1 (Google maps street view images)[1] and 6.3 (descriptive data) A description of each scenario is listed below;

---

[1]https://www.google.nl/maps

Figure 6.1: Schematic of source (red) and receiver points (blue) within a selected test area. Missing receiver points are removed due to buildings (currently not visible).

Table 6.1: Photos of the scenarios taken from (close to) the source using Google Maps street view

Scene 1 from road looking north
(right on overview in table 6.2)

Scene 2 with the rail (source)
behind the trees on the left side
and grasslands starting on the right.

Scene 3 rail source in flat terrain with ditches
(left) and view from near rail
towards the hill west/left(right).

Scene 4 view of the road source
with natural barrier on both sides
viewed towards north.

- **Scene 1:** A provincial road on top of the Grebbeberg in Rhenen, a smooth hill with a parking lot (reflective ground) and the Ouwehand Zoo on the left and later turns into forest, in the valley on the right it smooths out again into grasslands with several ditches.

- **Scene 2:** A railway north of Rhenen is lifted above the ground in an otherwise flat agricultural area with mostly grasslands and ditches.

- **Scene 3:** A railway next to the Utrechtse heuvelrug with mostly forest and paved paths across the hill.

- **Scene 4:** A provincial road in a neighbourhood, on both sides of the road a natural barrier is placed to reduce noise levels. Most other roads and buildings have been removed to improve the measurements and remove invalid data, note that altering the area does not have negative effects on the accuracy or precision of the predictions but the results are no longer representing the reality.

- **Scene 4b:** Same area as Scene 4, but without implementing the elevation topology, so the effect of this parameter can be separately measured.
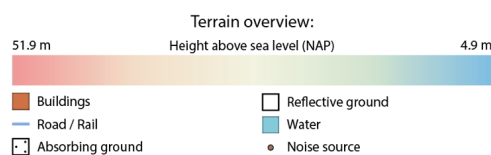
Figure 6.2: Legend of the scenario's in table 6.2

Table 6.2: Overview of the scenario's, a legend is provided in 6.2
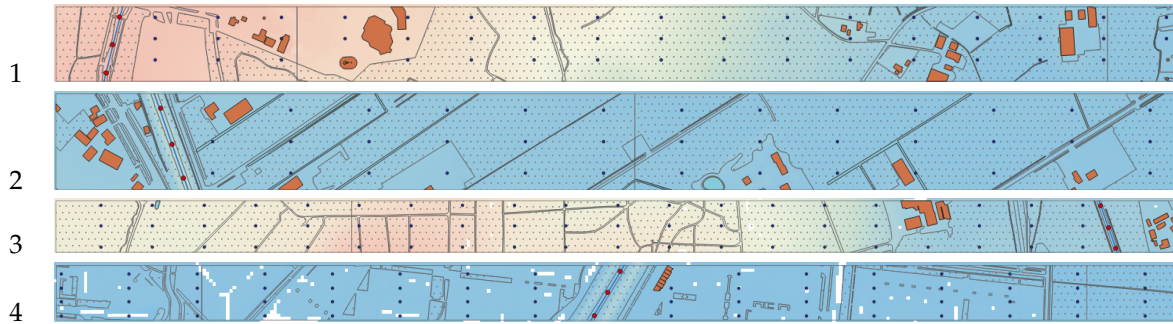
Table 6.3: Additional information of the scenario's

nr.	width [m]	height [m]	# of receivers
1	1.865	123	49
2	1.433	121	37
3	2.168	100	58
4	1.656	80	63

6.1.1 Verification of the results

In order to verify the results, they have to be compared to a ground truth, however, no such data is available. Real world measurements are not widely available and are only placed close to the noise source. A comparison with the current height information (height lines) is interesting. However, while current results are believed to provide a good prediction, given manual inspection and the physics behind the calculations. It remains unclear how accurate the results actually are. An alternative is to produce a TIN with a high accuracy, which will follow the terrain very accurate. It will therefore contain all objects in the scene, making sure nothing is omitted. Using the same data structure will produce noise results based on the same accurate LiDAR measurements. As it uses the same LiDAR measurements, all maps originate from the same data. As such there are no differences when the terrain has been altered in between measurements. All differences in noise level are due the to difference in terrain accuracy. The high accuracy terrain has 0.15m accuracy in the first 20 meters around noise sources, as these are the most critical, and 0.30m in the remaining areas. 0.15m is selected as a higher accuracy will include noise in the terrain (both from grass and small objects as well as the precision of the measurements). 0.3m is selected as it will follow the terrain accurately, the small objects that are omitted have a negligible impact on the noise predictions as the noise will propagate much higher above the ground. In this research this map will be referred to as the reference map or reference terrain.

6.1.2 Selection of parameter settings

Chapter 4 provided settings for each parameter (e.g. distance to the road and accuracy within that distance). The value of that setting is determined by empirical testing in this chapter. This section describes the settings that have been tested. The results of the noise calculations with different settings provide an indication of the optimal parameter settings. Due to the time frame not every parameter can be individually tested. Therefore a set of reasonable scenario's is selected by taking discrete steps within a range of reasonable values.

Initially 0.30m is chosen as lower limit as noise propagation paths will quickly rise above this height (see table 2.7). Road and rail sources are generally already elevated up to 0.5m above the area, as such the propagation height will quickly rise as the terrain height decreases. Finally, not only significant diffracting objects (e.g. noise barriers, dikes, ridges) but also low elevation on the roadside will not be omitted in this case.

0.60m is selected as upper limit as significant objects such as small dikes and ridges will start to get omitted. A step size of 10 cm is selected as the difference will not cause too many changes in the terrain while the amount of steps (four) is feasible. The corresponding buffer distance around the sources is based upon whether objects, given the accuracy value, will be included in the terrain or not. It is therefore based upon the figures in table 2.7.

Initially, a value of 1.0m will be used for areas beyond the buffer distances. Noise will propagate higher over this terrain and as such diffraction will not occur in generally flat areas. The mean height as used in the computation of the ground effect is not expected to be significantly influenced by the accuracy, while the 1.0m will maintain large formations in the terrain.

As will be concluded in Section 6.5.1, to better locate a balance, more tests were performed. A complete overview of all tested settings is given in table 6.4. The setting number is composed of first the low accuracy threshold in decimeter (dm), followed by the low accuracy setting (dm), separated by a dot.

Table 6.4: Parameter settings upon which terrains will be generated

Setting nr.	Accuracy high (m)	Buffer distance road (m)	Buffer distance rail (m)	Accuracy low (m)
Reference	0.15	20	20	0.30
Batch 1				
3.10	0.30	20	20	1.00
4.10	0.40	25	40	1.00
5.10	0.50	35	65	1.00
6.10	0.60	40	100	1.00
Batch 2				
2.05	0.20	20	20	0.50
2.07	0.20	20	20	0.70
2.10	0.20	20	20	1.00
3.05	0.30	20	20	0.50
3.07	0.30	20	20	0.70
4.05	0.40	20	20	0.50
4.07	0.40	20	20	0.70
4.10	0.40	20	20	1.00
Current	-	0	0	0.30

6.2 Accuracy maps

In table 6.5 an overview is provided of the scenes with their accuracy maps. As there is a lot of duplicate information in the low accuracy area across the different settings a close up is provided of the area around the barriers. Note that the accuracy value is defined as material characteristic in the configure file of 3Dfier and therefore only the size of the high accuracy area changes. For each scene all the high accuracy regions are placed on top of each other, allowing to see all the distances in a single overview. Here the darkest color shows the higher accuracy buffers where the lighter color represent the lower accuracy buffers. Note that scene 2 and 3 have larger buffer distances as these contain rail sources.

6.3 The generated triangular irregular networks

For each scene fourteen TINs have been produced, of which one reference terrain. Initially four parameter settings have been applied to obtain a general idea of the influence of the high accuracy near noise sources and the distance around the source that this accuracy is used. This provided several insights upon which a new batch of nine terrains using different parameter settings have been generated. These settings are further explained at the end of Section 6.5.1.

Table 6.5: Overview of the produced accuracy maps per scene (numbered on the left) integrated in one image where the high accuracy regions overlay each other from the less accurate, large buffer distance to the more accurate smaller buffers. Note that these accuracy layers are presented on top of each other, but processed per setting.
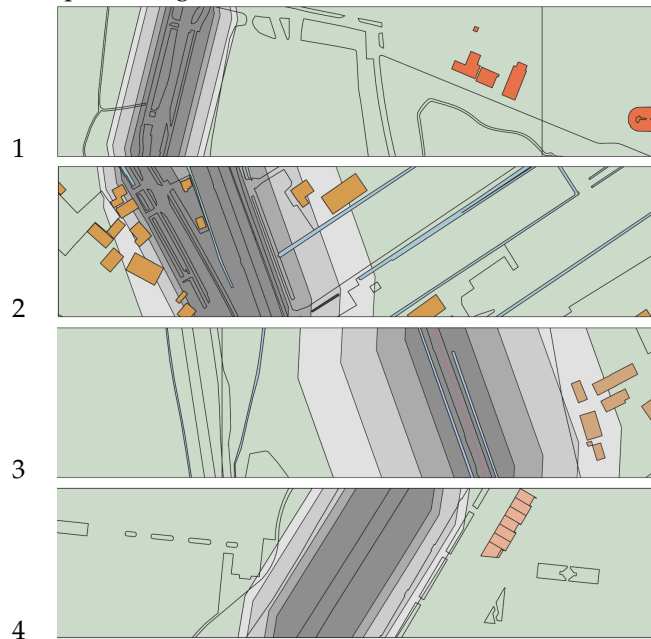
One very accurate and thirteen with the different accuracy settings. A visual overview of the terrains is given in table 6.6. In all terrains the high accuracy area only covers a portion of the terrain. In a real world situation this would be similar in rural areas. But in urban areas high accuracy regions will be mostly present.

Because the accuracy value for low accuracy terrain is the same for all settings, the generated triangles are identical with an exception close to the transition to high accuracy, as this boundary moves with each setting. Most of the triangles in the low accuracy terrain are caused by constraints, which therefore prescribe where vertices are initially added and highly influence the shape of the terrain instead of leaving this to the triangulation algorithm.

Upon visual inspection of the terrains a few characteristics were noted;

1. The water and ground type polygons in the input data sets describe relatively simple shapes with an extraordinary large amount of vertices and lines, leading to locally many constraints and a high density of triangles as can be seen in Figure 6.3.

2. The TIN is constrained to the input polygons, i.e. the TIN will initiate a triangulation with these lines and they cannot be removed or split into segments. This causes the TIN to have long and thin (sliver) triangles. If the terrain height along the long edges has height jumps in it, the used algorithm will insert vertices close to the line constraint because the error threshold is passed. This makes the area with a error above the threshold small, but it cannot fully eliminate the error, as it is not allowed to alter the constrained line (see Figure 6.4 and 6.5). While this effect leads to inaccurate representations of the terrain and may lead to inaccurate predictions when the receiver is located close on such an artefact, it is very rare and only affects a small area.

6.3.1 Size comparison of the generated terrains

The reason to simplify the TIN in the first place, is to reduce the size of the TIN, these sizes are presented in tables 6.7, 6.8 and 6.9. The terrain file (.json) in table 6.9 is the TIN as produced by 3Dfier, without any

Table 6.6: Overview of all generated terrains, the first number refers to the scene where the second part refers to the accuracy setting further elaborated in table 6.4

1:ref

1:3.10

1:4.10

1:5.10

1:6.10

2:ref

2:3.10

2:4.10

2:5.10

2:6.10

3:ref

3:3.10

3:4.10

3:5.10

3:6.10

4:ref

4:3.10

4:4.10

4:5.10

4:6.10

4b:ref

4b:3.10

4b:4.10

4b:5.10

4b:6.10
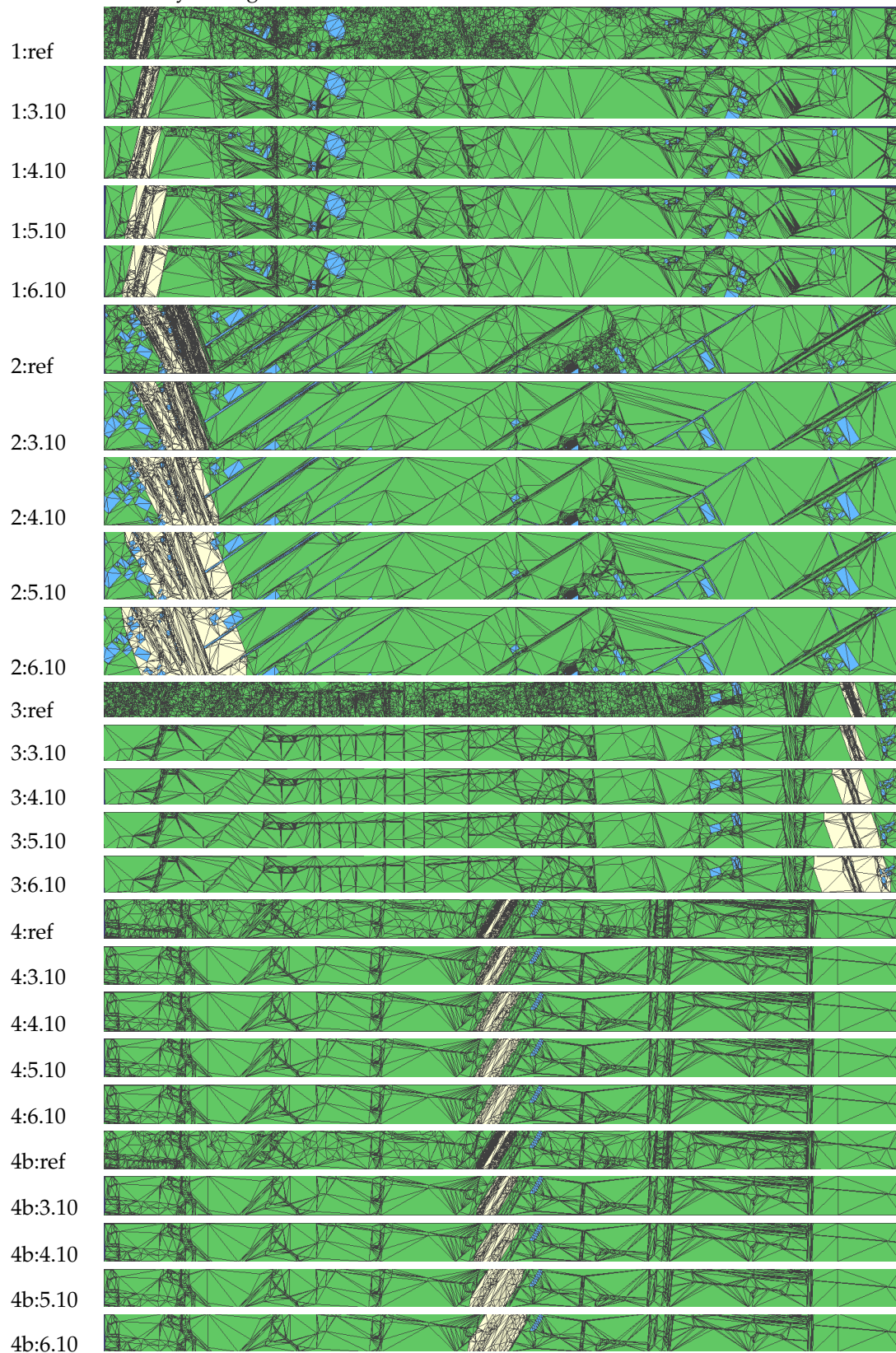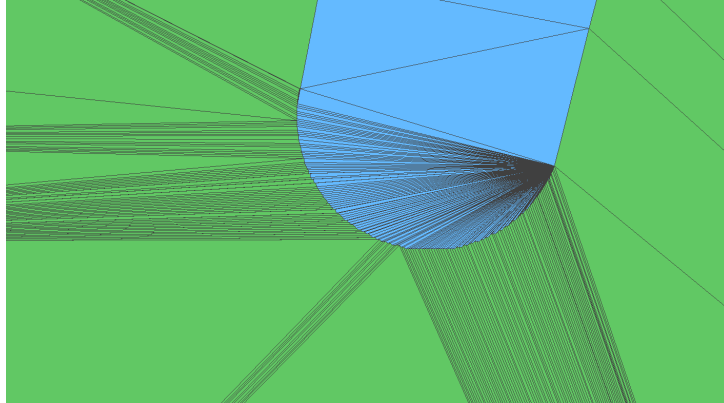
Figure 6.3: Close up of a triangulated terrain with water showing the result of constraints to complex polygons
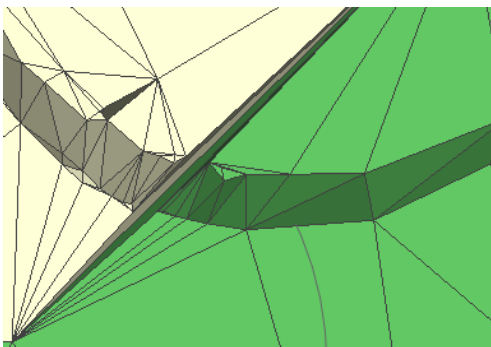
Figure 6.4: Artefact of constraining the tin (topview)
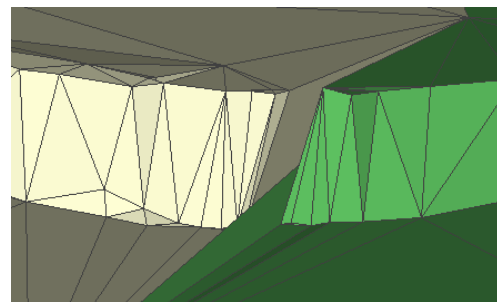
Figure 6.5: Artefact of constraining the tin (sideview)

Table 6.7: Amount of triangles per scene (rows) and per accuracy (columns)

Scene	Reference	3.10_NC	3.10	4.10	5.10	6.10
1	20513	1874	9138	9005	8949	8951
2	16204	2114	10042	9700	9462	9374
3	15153	896	3076	3032	3006	3030
4	7314	932	2383	2256	2186	2146
4b	7437	932	2598	2199	2154	2148
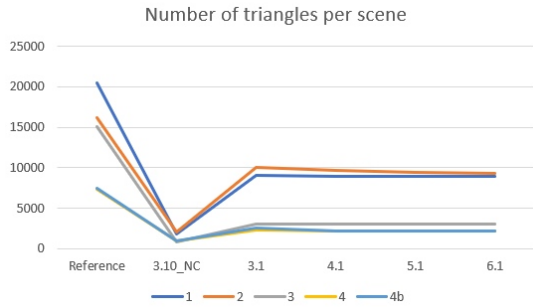
Figure 6.6: Line plot of the number of triangles for each setting in each scene
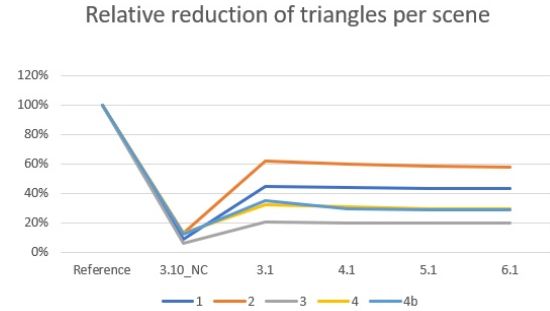
Figure 6.7: Line plot of the relative reduction of triangles for each setting in each scene

modifications. It contains all metadata that was available in the 3Dfier input files, including the ground type and building data, therefore this one file combines all information of the complete environmental model into a single file.

As many of the triangles are due to constraints to the ground types, buildings and water bodies, also accuracy setting 3.10 (see table 6.4) is triangulated without any constraints from water, ground type or buildings. This comparison allows to measure the 'cost' of the constraints in terms of size. This terrain can be used as height information in GeoMilieu (RMG) but not with the implementation of CNOSSOS. This implementation requires the semantic data about buildings and ground types to be stored inside the triangle. The file size is provided in column "3.10_NC" (not constrained) of the tables. It is not included in table 6.9 as these files do not contain the metadata, thus that comparison is not fair.

Over the accuracy different settings (3.10 - 6.10) the high accuracy value decreases, generating less triangles, while the buffer distance increases, increasing the number of triangles. Even though the high accuracy region enlarges, it remains a small part of the total terrain and therefore has a small influence. The terrain sizes therefore remain similar across the settings. Compared to the reference TIN with the most accurate model there is about 50 to 70% reduction in size, in which the low accuracy value will cause the most effect as it affects the biggest area. The terrain without constraints (3.10_NC) shows a reduction of 85 to 90%.

Table 6.8: Amount of vertices per scene (rows) and per accuracy (columns)

Scene	Reference	3.10_NC	3.10	4.10	5.10	6.10
1	10337	942	4622	4554	4526	4527
2	8176	1063	5096	4923	4805	4766
3	7643	453	1607	1585	1572	1584
4	3721	471	1256	1192	1157	1137
4b	3784	471	1363	1165	1141	1138
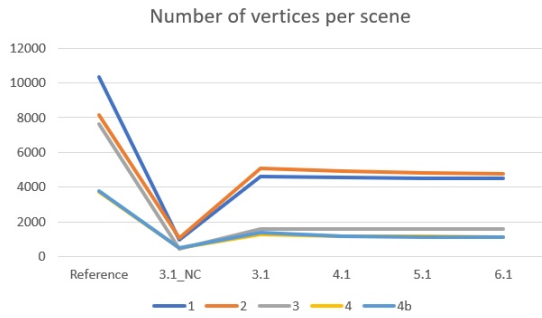
Figure 6.8: Line plot of the number of vertices for each setting in each scene
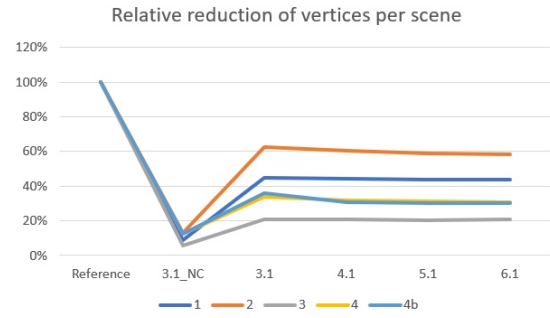
Figure 6.9: Line plot of the relative reduction of vertices for each setting in each scene

Table 6.9: Size of tin in .json file format (kB) per scene (rows) and per accuracy (columns)

Scene	Reference	3.10	4.10	5.10	6.10
1	713	227	330	328	329
2	568	364	353	286	283
3	520	120	119	118	119
4	267	107	103	101	99
4b	267	105	100	101	101
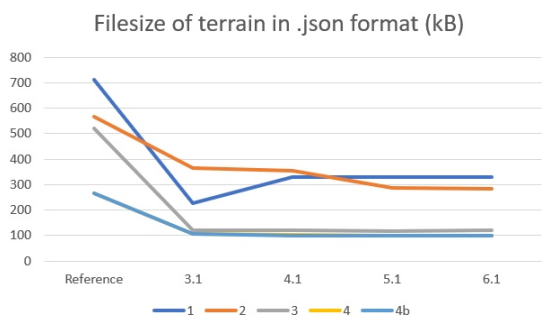
Figure 6.10: Line plot of the file size for each setting in each scene
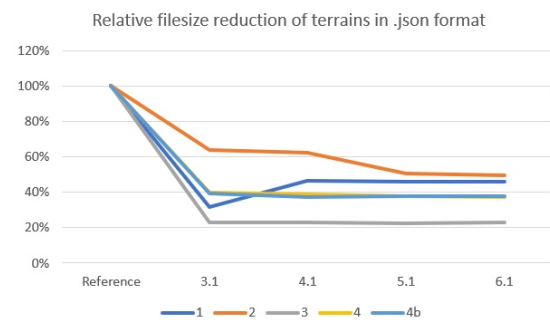
Figure 6.11: Line plot of the relative reduction of file size for each setting in each scene

Table 6.10: Run time (seconds) to compute cross sections per scene (rows) and per accuracy (columns), single core, same conditions. *The reference of scene 4b is the same as 4, as the impact of the view shed only affects the higher buffer distances.

Scene	Reference	3.10	4.10	5.10	6.10
1	18.38	7.47	8.78	7.24	9.32
2	8.98	5.89	4.79	4.45	4.93
3	33.76	5.87	4.96	5.59	4.73
4	10.98	4.33	6.97	6.11	5.92
4b	10.98*	7.22	6.65	6.03	6.11
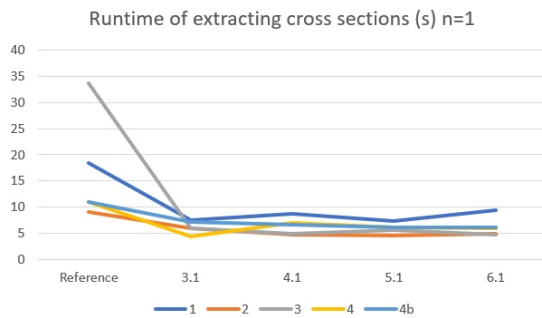
Figure 6.12: Line plot of the run time of cross sections extraction for each setting in each scene
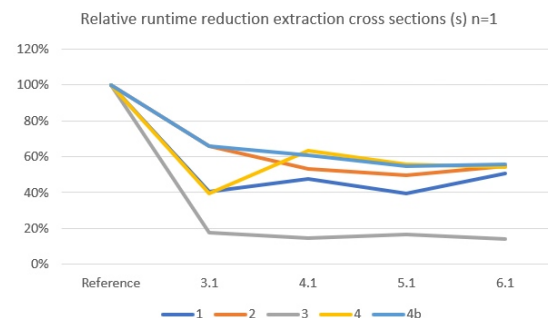
Figure 6.13: Line plot of the relative reduction of run time for cross section extraction for each setting in each scene

6.4 Produced cross-sections

The cross sections produced with the conceptual implementation for CNOSSOS were also exported as .obj files for manual inspection, shown in Figure 5.15 in the previous chapter. The cross sections did not show any abnormalities and behaved as expected. Table 6.10 shows the computation time for the different settings and scenes. These where computed on a consumer laptop where all commands where executed consecutively under the same circumstances. As can be seen, there was a large reduction of computation times (50-80%), as was expected due to the lower amount of triangles. This computation consists of reading in all files, extracting direct path cross sections, locating reflection paths, extracting reflective path cross sections and writing the cross sections to an .obj file and individual .xml files.

6.5 Noise accuracy assessment

In this section the noise prediction results are presented and compared. For each scene 36 noise maps have been produced, 23 according to the RMG and 13 according to CNOSSOS of which one reference map and 22 or 12 accuracy settings respectively. Initially four maps and a reference map were produced using each method. Using the insights from these results the rest of the maps were produced (see Section 6.5.2).

A "noise map" is a visual representation of the predicted noise levels (L_{den}) on the receiver points. These are linearly interpolated to provide a visually pleasing representation. However, as the distances between the receiver points is between 20 and 100 meters, the interpolation of noise values does not represent a realistic view of the local noise values in between receivers. The RMG receivers are placed at 1.5, 4.0 and 7.5m (the visualisations are using the 1.5m receivers only) above ground with the source at 0.75m for road and 0.0, 0.5, 2.0, 4.0 and 5.0m (excluding 0.2m rail height) for rail, in accordance with the regulation. The CNOSSOS receivers are placed at 4.0m with sources at 0.05m for road and 0.5m for rail.

The noise emission levels (dB), as hard coded in the conceptual software, remain those from road noise and can only be at a single height. Therefore the lowest height of the regulation is used.

Visually, a noise map is a pleasing presentation. It can highlight outliers and help determine their origin. However, statistical values provide better insight in the accuracy and precision of the results. A set of relevant statistical values is presented in a box plot format. The box plot has filtered outliers from the data set and presents the minimum, maximum and the 25th, 50th (median) and 75th percentile. Given the data contains outliers and the distribution is not necessarily balanced, the median provides a better representation than the mean. The statistical values are also presented in a table format in appendix A.

The accuracy settings change the height of the terrain, this does not only affect the path in between the source and receiver, but also the height of the source and receiver. As this may cause additional effects, the correlation is determined for each scene. The correlation is plotted using a joint scatter and histogram plot. This scatter plot shows the difference in height of the terrain below the receiver, compared with the difference in predicted noise value. It also shows Pearson's correlation coefficient. The scatter plots are based on the data from GeoMilieu, as that software is more advanced and includes the receiver height. The effect of the height difference of the source is not known. However, the error will be less, as the accuracy of the terrain is higher and the road / rail is in a flat area. This is manually checked by inspecting the TIN.

The aim of this research and this accuracy analysis is to provide insight on the effect of the accuracy settings and determine which accuracy settings are best to provide reliable results while reducing the complexity of the terrain. To visualise the effect of the accuracy settings, each result is compared to the reference map.

6.5.1 Analysis of initial noise calculations

In this section the results from the initial parameter settings are presented and summarised. First a visual overview of all scenario's in both methods is presented, followed by a statistical overview. Several conclusions are drawn upon which a updated set of parameter settings is determined.

Visual overview and analysis of the results

For each scene a table is used to present the results. On the top an overview and reference noise map are displayed followed by maps showing the difference between the accuracy setting and the reference map. A positive (green) difference shows that the accuracy setting provided a higher noise level, where a negative (red) difference shows the accuracy setting predicted a lower noise level. As most errors fall within a small range, that range is visualised. Values that extend beyond this range are colored in a more saturated color to clearly display outliers (see Figure 6.14). Although the CNOSSOS maps cause larger errors, the used range is the same for both maps so the differences can be compared between the methods. In table 6.4 an overview of the used settings for each figure is provided. As a guide the maps are coded used the applied settings. This is coded according to the following setup: [high_accuracy(dm)].[low_accuracy(dm).[method; R:RMG, C:CNOSSOS].

Scene 1 holds the largest differences between the reference map and the noise settings in the CNOSSOS method.

As the terrain in this scene is located on a hill with the road on the top, most receivers will not have a line of sight with the source. Also the terrain is high compared to the source and receiver, therefore the ground effect will play a larger part in the noise reduction compared to other types of noise reduction. The road side does have a small height elevation increase, but there is no clear height difference in the different accuracy settings compared to the reference terrain.

The outliers in the results using RMG are the same in each accuracy setting and show no indicative pattern. This indicates this variance is not caused by the terrain close to the road, but is due to the receiver height. This is confirmed in a correlation(ρ) of 0.54 as well as the scatter plot that shows there is
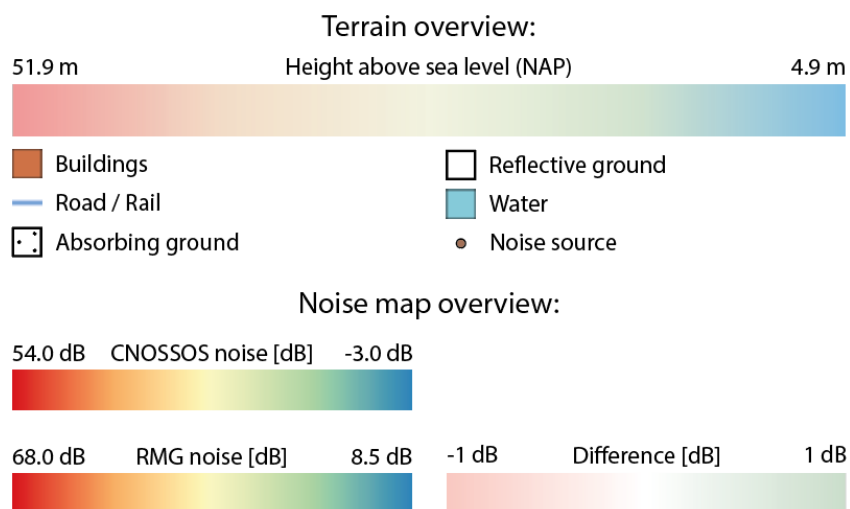
Figure 6.14: Legend for noise maps (same for all cases)

Table 6.11: Terrain overview (M) of scene 1, noise maps according to RMG (O1) and CNOSSOS (O2) and difference in noise level of the different settings from table 6.4 with the corresponding reference noise map (RMG and CNOSSOS)
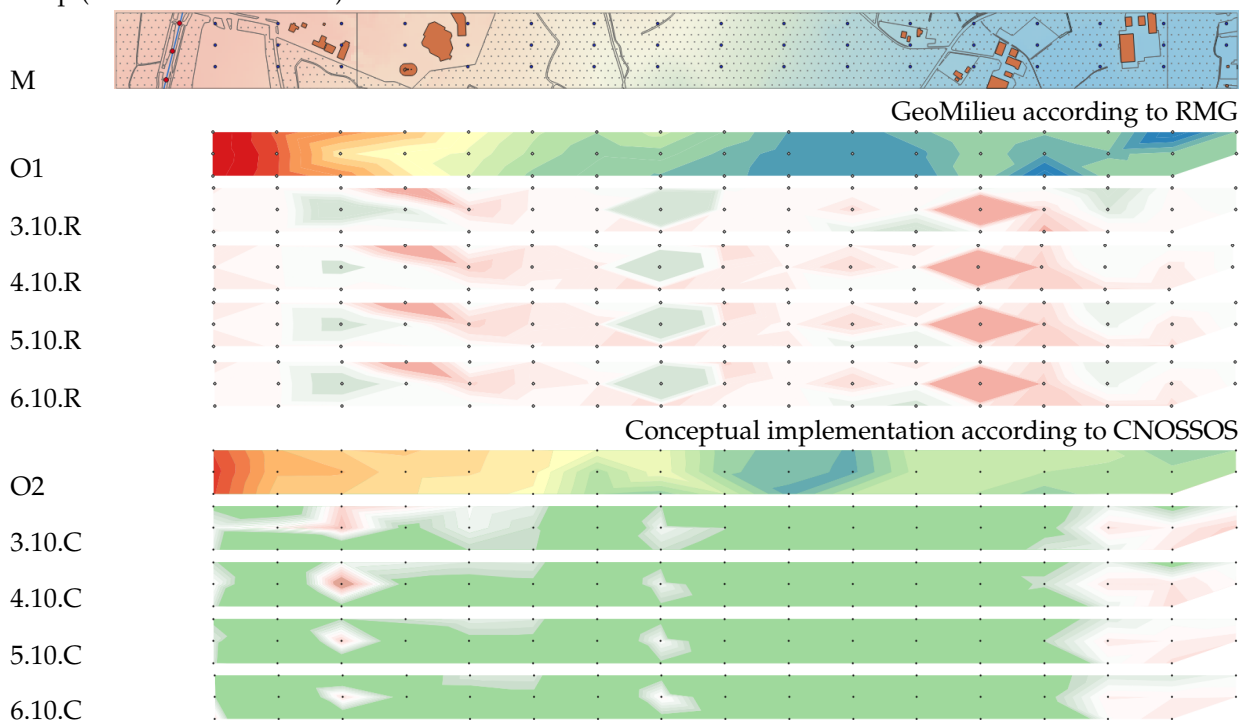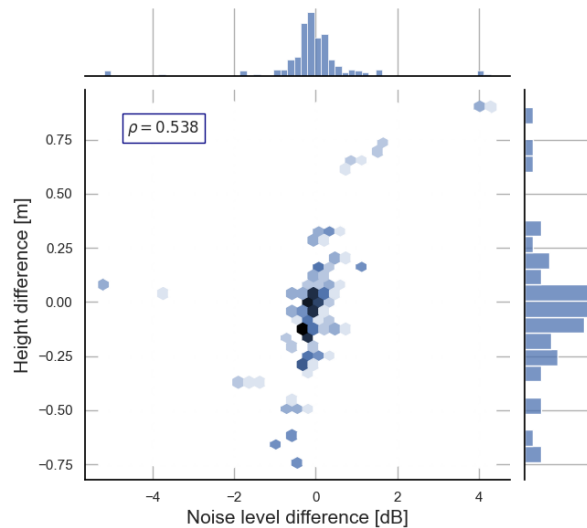
Figure 6.15: Scatter plot of the correlation between noise level difference and receiver height difference for scene 1 using the constrained TIN in RMG

a strong correlation between the receiver height and the noise difference. Especially the positive outliers have a big influence.

While the ground heights are not available with CNOSSOS, they are based upon the same terrain, and should therefore be the same. However, the CNOSSOS noise maps show a different pattern. As the receiver height is 4.0m the effect of the local elevation difference at the receiver is not noticeable.

This scene is the only scene with road sources where there are no barriers present (scene 2 and 3 are rail sources). The large green area in the CNOSSOS map is most likely related to a difference in terrain height in the low accuracy region as CNOSSOS uses the complete height profile in between the source and receiver. As the terrain is sloped, line of sight is not applicable. Thus diffraction occurs for homogeneous conditions and favourable conditions are dominant. This does have a lower impact near the right side of the terrain, where the terrain is flat again and the noise is less diffracted.

Scene 2 shows low noise differences in both methods. The terrain consists of flat grasslands with several ditches, which are lower than the surrounding grasslands. The break lines from the ground type data are also placed close to the water. The height assigned to the initial terrain and forest vertices is the mean height of the points within a 1.0m radius (for water it is the 0.05 percentile of all points within the radius of the vertices). The reference terrain shows several vertices were inserted to lift the terrain closer to the measurements (Table 6.6). These are not present in the other terrains, i.e. the height difference was less than 1.0m and the terrain is therefore not lifted the same as with the reference map.

There is a strong correlation (0.61) in the RMG map as the noise values are also generally on the negative side. This is confirmed when interpreting the scatter plot in figure 6.17. This correlation is not present with CNOSSOS as the receiver is placed much higher. CNOSSOS creates a linear interpolation of the terrain in the cross section using all the terrain. The further away the receiver gets from the source, a larger portion of the terrain is estimated lower. The effect of a lower receiver (in absolute position) is therefore also lower. This is not the case with RMG as it uses the first and last 70m and as such the effect does not fade with a longer distance between source and receiver.

Scene 3 shows very promising results for the 0.30m and 0.40m accuracy settings of RMG, the differences are subtle while the size reduction of the terrain is the highest of all data sets. As most of the terrain covers a forest with natural elevation difference the reference model picked up a lot of local elevation changes which turn out to have a negligible impact of the noise predictions using RMG. This may be partly explained as the terrain is generally lower than the line of sight between source and receiver. The ground effect will therefore have a lower impact and other noise decimation types are more dominant.

Table 6.12: Terrain overview (M) of scene 2 noise maps according to RMG (O1) and CNOSSOS (O2) and difference in noise level of the different settings from table 6.4 with the corresponding reference noise map (RMG and CNOSSOS)

M

GeoMilieu according to RMG

O1

3.10.R

4.10.R

5.10.R

6.10.R

Conceptual implementation according to CNOSSOS

O2

3.10.C

4.10.C

5.10.C

6.10.C
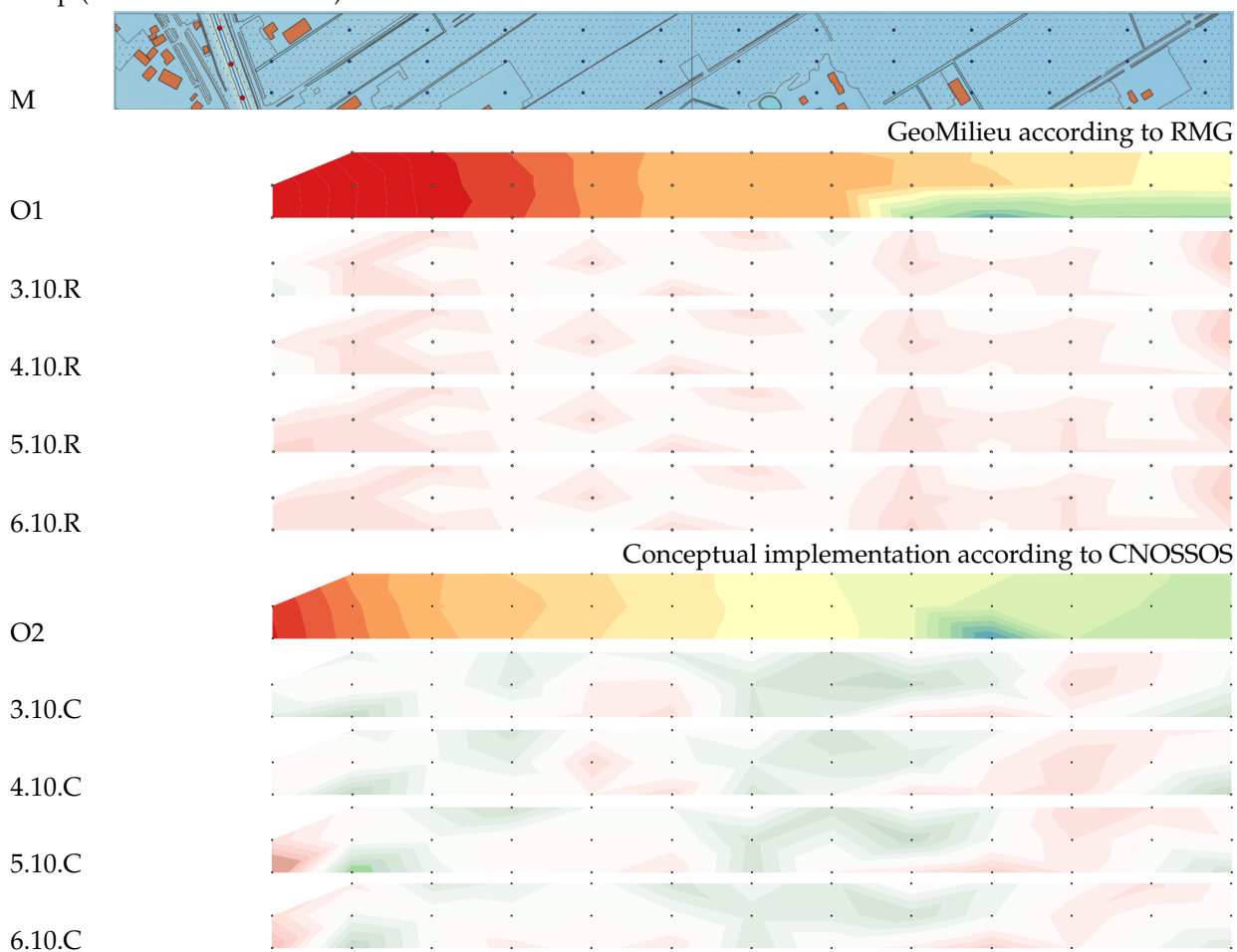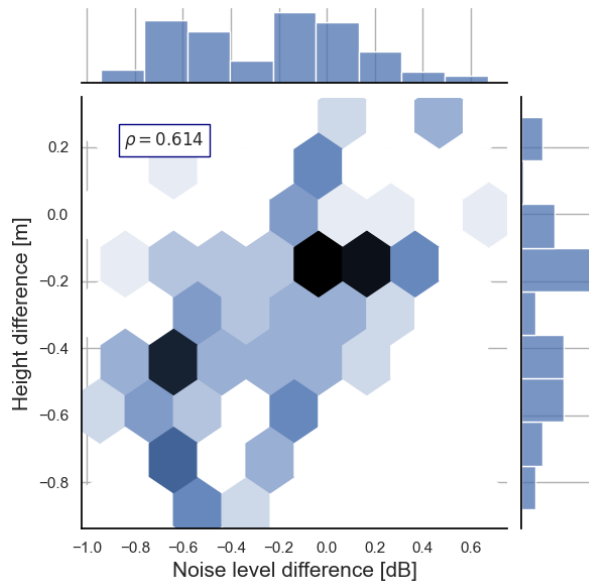
Figure 6.16: Scatter plot of the correlation between noise level difference and receiver height difference for all settings in scene 2 using the constrained TIN in RMG

Table 6.13: Terrain overview (M) of scene 3, noise maps according to RMG (O1) and CNOSSOS (O2) and difference in noise level of the different settings from table 6.4 with the corresponding reference noise map (RMG and CNOSSOS)
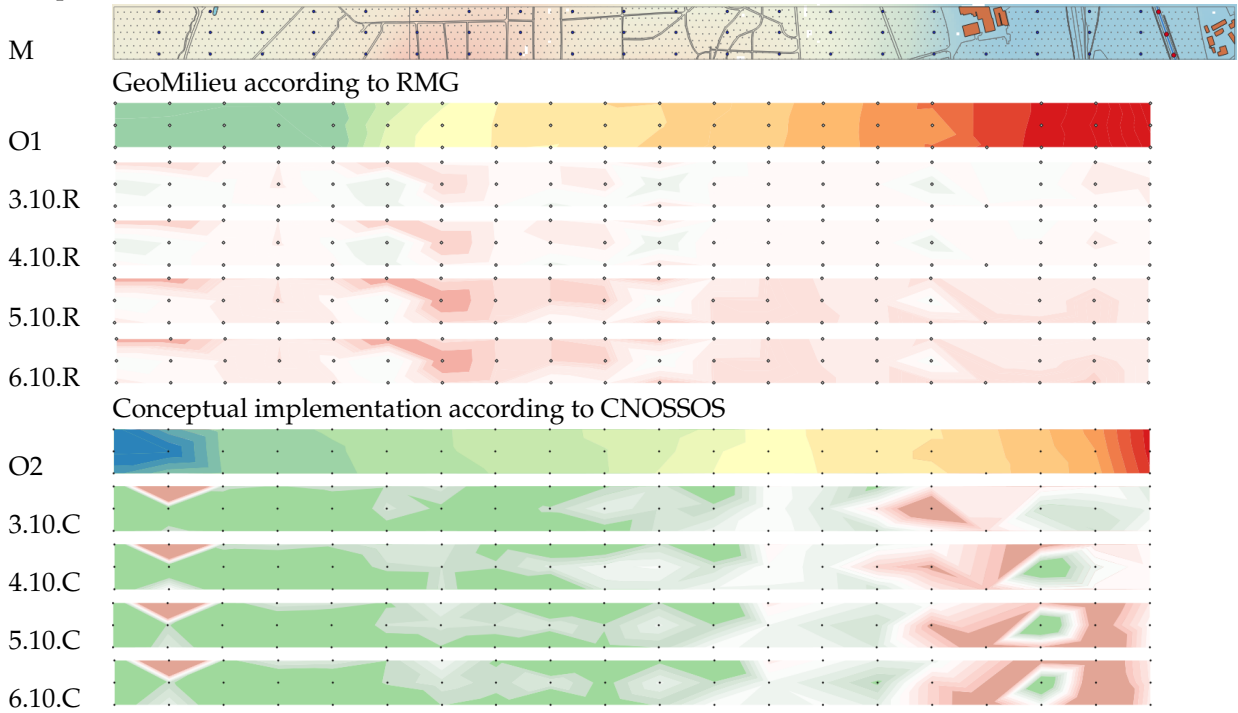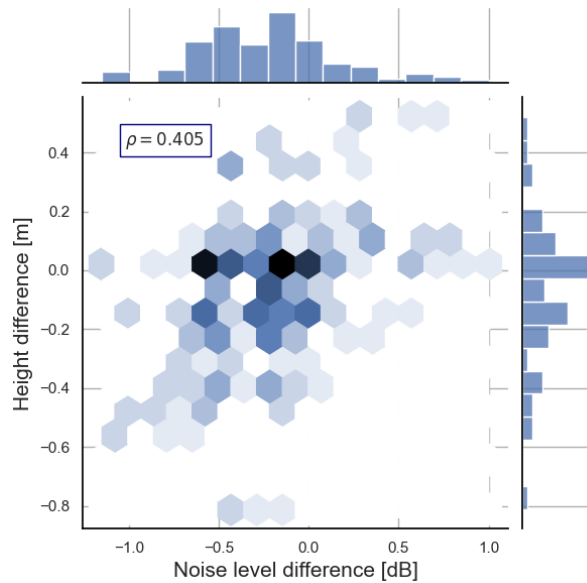
Figure 6.17: Scatter plot of the correlation between noise level difference and receiver height difference for all settings in scene 3 using the constrained TIN in RMG

Inspection of the TIN shows the reference terrain has several smaller ridges included in the terrain which are not present on the other terrains as they are less then 1.0m high. This is the logical explanation for the increasing differences as the distance to the receivers gets larger. The mean plane of the terrain is lower, causing less noise reduction due to less diffraction and a reduced ground effect in CNOSSOS.

The railway lays slightly elevated above the terrain surrounded by two ditches. This elevation, and the track itself is included accurately in the reference model, but less as the high accuracy region gets a lower accuracy. Therefore the noise sources are placed lower and cause a higher ground effect, causing a generally lower noise prediction in the lower accuracy settings (5.10.R and 6.10.R). This is also visible especially in figure 5.10.C and 6.10.C where the lower source height leads to unpredictable results close to the source.

The correlation with height difference is present (0.41), but it is not very strong. This indicates other parameters, like described above, have a larger impact.

Scene 4 shows a large impact of the natural barriers over an otherwise flat terrain. The generally lower noise level in the accuracy settings can be partially explained due the generally lower ground elevation, but this relation is very weak. By inspecting the terrain, especially the natural barriers are represented with much fewer vertices, but the height differences on the top are minimal. As the vertices from the point cloud with the highest error are first added, the top of the barrier is estimated slightly higher in less accurate settings. In the accurate models the overshoot of the barrier top is reduced. This effect is slightly noticed in the maps using RMG. However, it is not noticeable in the maps according to the CNOSSOS method. Here the differences have the biggest offset close to the sources (up to 1.9 dB). As the barrier is about 5 meters high, it will cause diffraction for all paths, also for CNOSSOS which has a 4.0m high receiver.

While the differences in the RMG maps only increase slightly, there are significant changes when the accuracy drops to 0.50m and lower for the CNOSSOS maps. The effect of the less accurate maps is clearly more noticeable for the CNOSSOS method, this is as expected as the receivers are placed higher, therefore small differences in the buffer height have an increased effect in the diffraction.

The effect of decreasing the high accuracy region using the view shed analysis has, as expected, a negligible effect on the noise level. At the same time it reduces the high accuracy surfaces area in presence of a (natural) noise barrier.

Table 6.14: Terrain overview (M) of scene 4, noise maps according to RMG (O1) and CNOSSOS (O2) and difference in noise level of the different settings from table 6.4 with the corresponding reference noise map (RMG and CNOSSOS)

M	
	GeoMilieu according to RMG
O1	
3.10.R	
4.10.R	
5.10.R	
6.10.R	
	GeoMilieu according to RMG, diffraction terrain simplification disabled
3.10.R2	
4.10.R2	
5.10.R2	
6.10.R2	
	Conceptual implementation according to CNOSSOS
O2	
3.10.C	
4.10.C	
5.10.C	
6.10.C	
	Conceptual implementation according to CNOSSOS, diffraction terrain simplification disabled
3.10.C2	
4.10.C2	
5.10.C2	
6.10.C2	
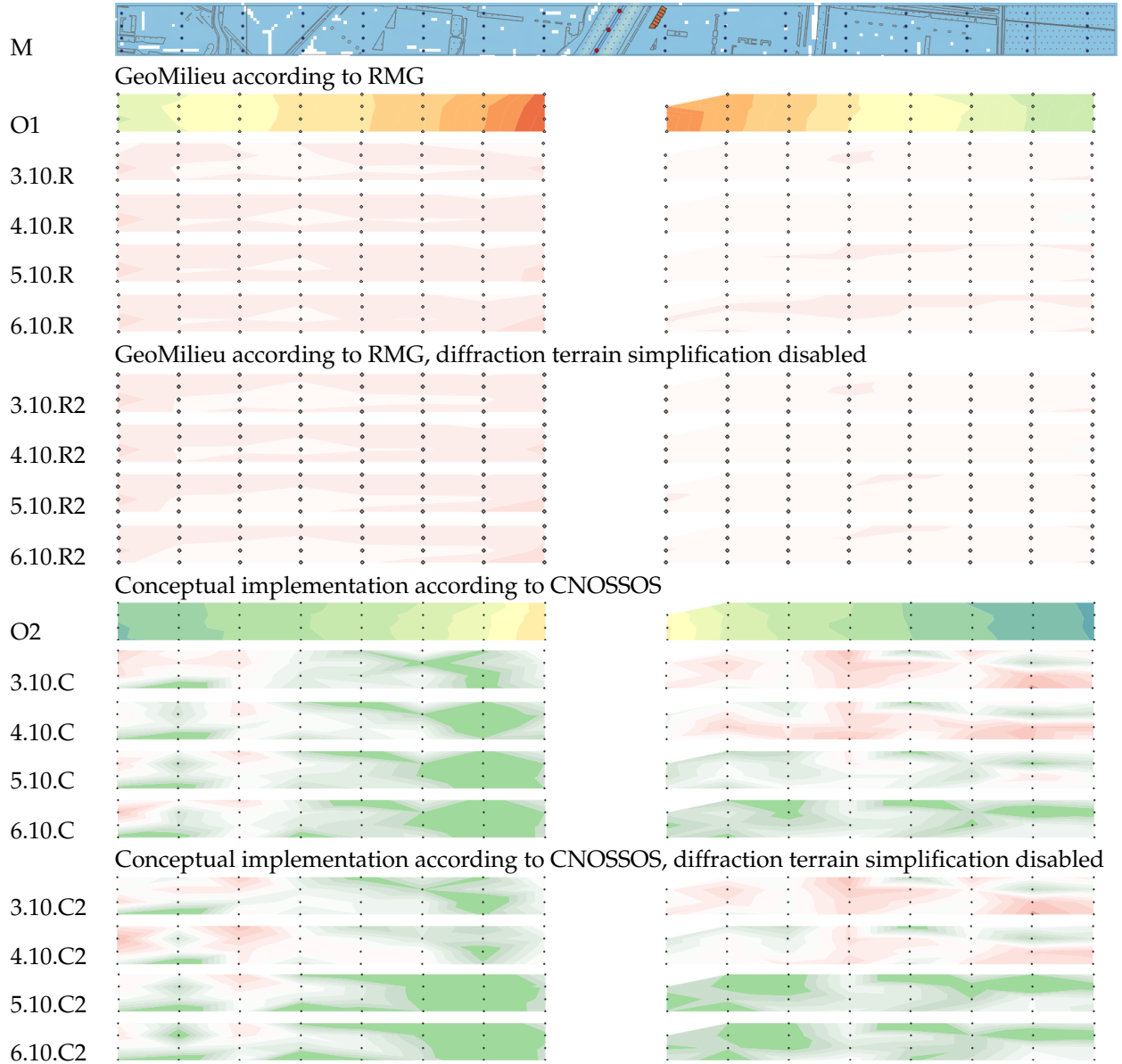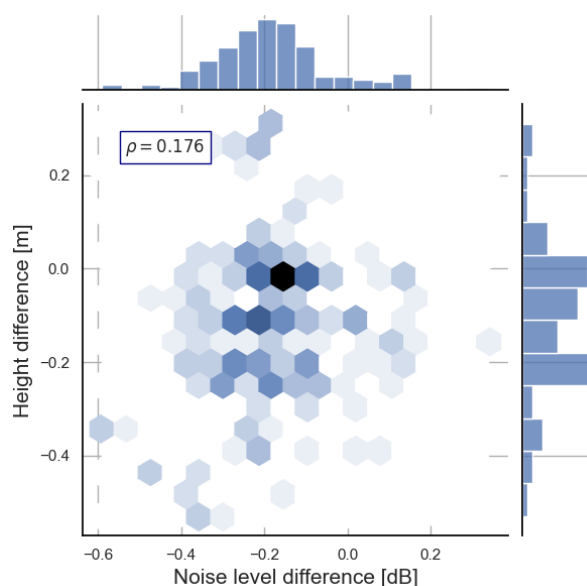
Figure 6.18: Scatter plot of the correlation between noise level difference and receiver height difference for all settings in scene 4 using the constrained TIN in RMG

Statistical overview

The box plots allow to easily compare the overall accuracy across the scenario's and the settings. As both noise methods have shown to react differently on changing terrains, they are individually assessed.

The **RMG** calculations show different results across the scenario's (Figure 6.19). The median deviates over scenario 1, but the variance is very similar. Only scenario 3 shows a clear increase in variance, which was the expected result. In general the median diverges further from zero as the accuracy decreases, confirming a higher accuracy leads to more accurate results. Scene 4 shows a slightly increasing offset with a low variance for the 0.3m accuracy settings, yet the variance is the same for the other settings, except for 0.4m.

The varying results are not very conclusive, but in general it can be said that the results for the RMG are promising as the medians are generally close to zero and just about all predictions stay within a 1.0 dB range (note that outliers have been removed in the box plot).

The **CNOSSOS** calculations are generally not much influenced by the decreasing high_accuracy (Figure 6.20). Only scenario 2 is affected, but opposite to what one would expect, the median gets closer to zero and the variance decreases as the high_accuracy decreases. No clear reason can be determined other than that the dyke upon which the rail source is placed is, by accident, represented more like the reference map in the lower accuracy settings. The other scenario's show the CNOSSOS calculations are not much influenced by the high_accuracy, but rather by the low_accuracy value. Both the medians and the variances do not decrease with a more accurate high_accuracy.

Overall it can be said that CNOSSOS is sensitive to changes in the terrain, of which the low_accuracy plays a large role. The differences are larger in areas with height difference (scene 1 and 3) and tend to be rather larger than smaller in less accurate areas.

Summary

When comparing the results from the different scenarios it can be said that the differences increase as the accuracy close to the road decreases. It can also be said that the predicted noise values among the different accuracy settings are similar in comparison to the reference map. The correlation with the

Error distribution Lden with reference Lden using a constrained terrain
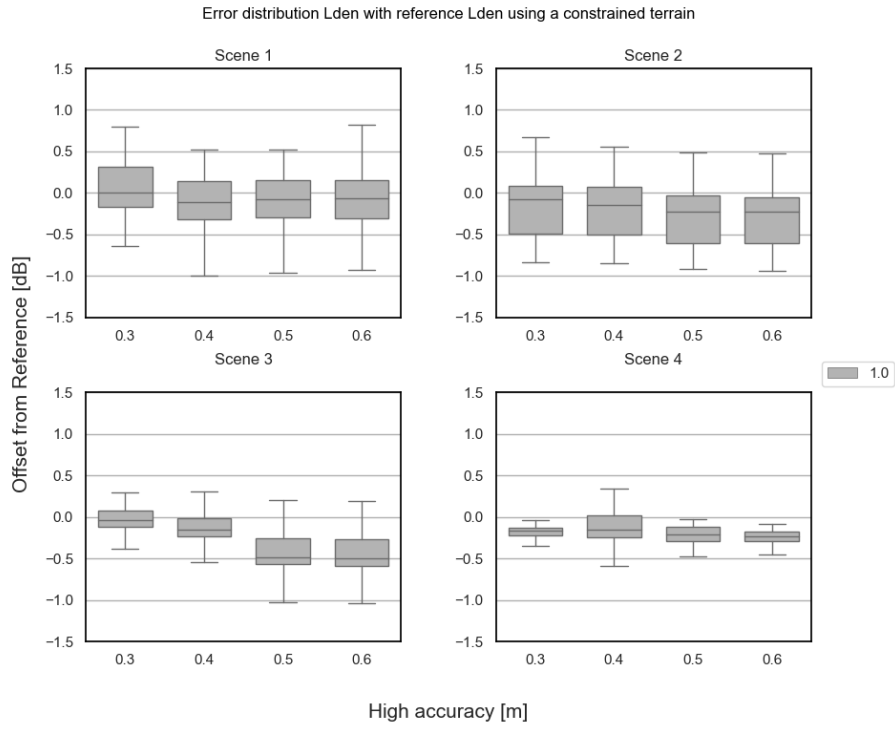
Figure 6.19: Box plots of the four settings applied to each scenario using RMG

Error distribution Lden with reference Lden using a constrained TIN and variable receiver heights in CNOSSOS
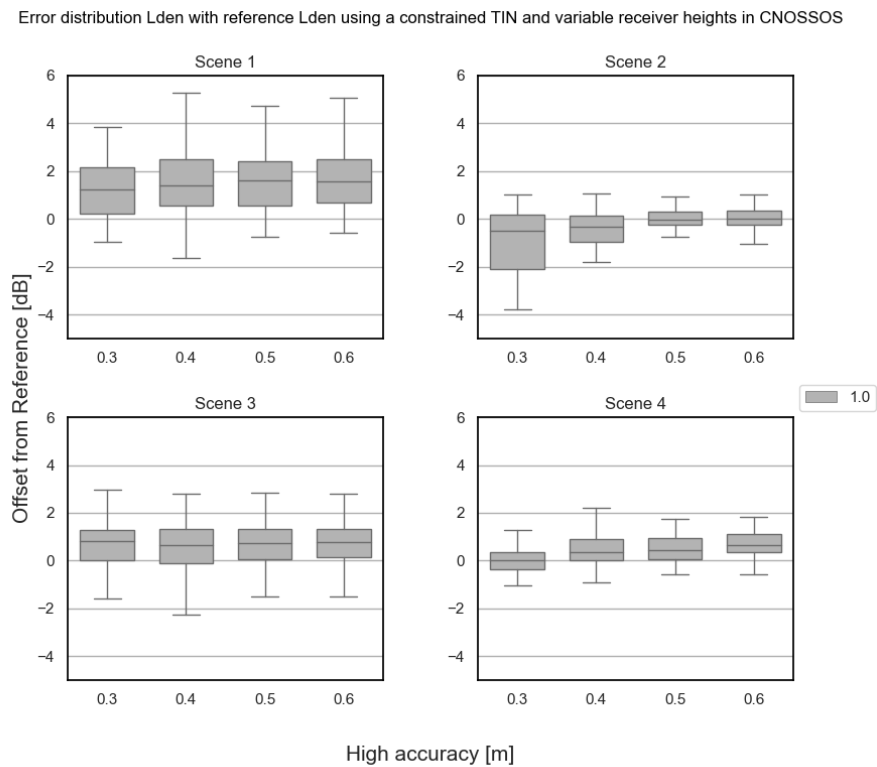
Figure 6.20: Box plots of the four settings applied to each scenario using CNOSSOS

difference in terrain height at the receivers show that the low accuracy value may cause this difference, not only in changing the absolute height of the receiver, but also in a more varying mean height which caused more variation in the noise predictions. These variations are generally negative with RMG and positive with CNOSSOS, while the used terrains are identical. This is most likely due to the low source height and high receiver height of CNOSSOS compared to a relatively high source height and a lower emission height of RMG.

The CNOSSOS maps show the method is generally more sensitive to changes in the terrain elevation, especially when the noise is diffracted, the variance in this case is about three to four times larger (see Appendix A). The outliers that are present in the differences are generally present in all accuracy settings, the most significant difference between the reference map and the results from the different settings is the accuracy value for low accuracy terrain. This can, in several cases be related to the difference in the local height of the terrain underneath the receiver. In other cases this is due to differences in the terrain in between the source and the receiver, as that is the only other difference in the cross section. This effect occurs more often and it causes larger outliers in the CNOSSOS noise predictions.

The CNOSSOS method simplifies the terrain into a straight line (explained in Figure 2.4). This line is extracted by minimizing the root mean square error (RMSE) over the total cross section. As most of the terrain has a low accuracy, especially for the longer paths, this terrain has a large influence on the noise level.

The RMG uses the mean value of the first 70 meters from both source and receiver. Therefore a much larger part of the height information used has a high accuracy. This can explain why both the differences can be very different between both methods as well as why the difference is generally larger with the European method.

The size reduction of the terrain is mostly due to the reduced low accuracy value as the reduction is similar for the different accuracy settings. Also the ground type constraints are, in both the high and low accuracy regions, responsible for 40% of the triangles.

Extending the accuracy parameter settings

Based on the initial calculations a balance between accurate noise predictions and a small file size could not yet be obtained. Based on the results the following conclusions for a new set of parameter settings are drawn;

1. The increasing buffer distance did not provide a noticeable advantage. Therefore they are set to 20m for both road and rail, according to the lowest setting.

2. The low accuracy affects the receiver height, leading to artefacts in RMG and influences the ground effect in CNOSSOS; testing this parameter should confirm this

3. The RMG results show a clear correlation with the receiver height for multiple scenario's, to test the high accuracy parameter this impact should be removed. This is possible in the noise modelling software GeoMilieu.

4. The height errors across the terrain are influenced by the constraints in the terrain. This leads to terrains where a whole area is modelled lower then reality. Modelling the terrain without such constraints should be tested to correct this effect. This is not possible in the used CNOSSOS implementation, but GeoMilieu does allow for it.

5. Whether the origin of the errors in the 0.30m high accuracy setting are in the high accuracy, or in the low accuracy should be determined by applying a extending the high accuracy range to 0.20m.

6. In order obtain a better understanding of what error is acceptable or 'better' than the current also a parameter setting is applied where the current TIN setting as available on PDOK is calculated.

7. The impact of the elevation topology parameter which reduced the high accuracy area in scenario 4 was negligible compared to not constraining the TIN. It can be concluded that this parameter performs well and no further testing is required at this stage of the research.

8. While the noise maps depict patterns and may help determine the origin of a single artefact, they are time consuming to generate. The statistical representation provides a better insight of the effect across a whole terrain and allows for quick and easy comparison across settings. Therefore the calculations using updated parameter settings will be presented using statistical values only.

Based upon these conclusions a second batch of noise calculations is performed where the terrains are no longer constraint in the RMG calculations. Also the RMG calculations are performed twice, where the receiver heights are taken from the reference model for all parameter settings in one calculation and left variable in the other. The low accuracy value will be tested with 0.50 and 0.70m additionally. Also the high accuracy range is extended to 0.2m while the 0.5 and 0.6m settings are removed. Using these adjustments the following parameter settings are used;

Table 6.15: Parameter settings upon which terrains will be generated

Setting nr.	Accuracy high (m)	Buffer distance road (m)	Buffer distance rail (m)	Accuracy low (m)
2.05	0.20	20	20	0.50
2.07	0.20	20	20	0.70
2.10	0.20	20	20	1.00
3.05	0.30	20	20	0.50
3.07	0.30	20	20	0.70
4.05	0.40	20	20	0.50
4.07	0.40	20	20	0.70
4.10	0.40	20	20	1.00
Current	-	0	0	0.30

6.5.2 Analysis of noise calculations from updated parameter settings

This section presents the results of the noise calculations using the updated parameter settings. First the sizes of the updated settings are provided to provide insight on the size reduction. Then the results of the extended high accuracy and varying low accuracy are discussed. Thirdly, the effects of removing the receiver height error are presented. At last the effect of having no constraints on the TIN is evaluated.

Analysis of size reduction using the updated accuracy parameters

The sizes of the currently available and generated terrains according to the updated parameter settings are shown in Figures 6.21 to 6.24. Figure 6.21 and 6.22 use the constrained terrain, similar to the initial terrains. Figure 6.23 and 6.24 use the non-constrained terrain as used in the RMG calculations.

The constrained terrains can provide up to 40 or 80% reduction depending on the scenario. This is comparable to the reduction of the initial settings, however the influence of the low accuracy shows a more gradual reduction.

The non-constrained terrains provide much higher size reductions up 90% reduction. Also here a more gradual reduction is observed as the accuracy reduces. The relation however, is not linear. As the accuracy reduces the number of triangles reduces exponentially. From 0.30m to 0.50m low accuracy generates up to 60% size reduction.

The reduction is mainly caused by the low accuracy setting. The high accuracy setting causes a slight reduction as it only influences a small part of the terrain. Note that in regular circumstances the amount of high accuracy terrain would be larger as only one road in the scenarios is used.
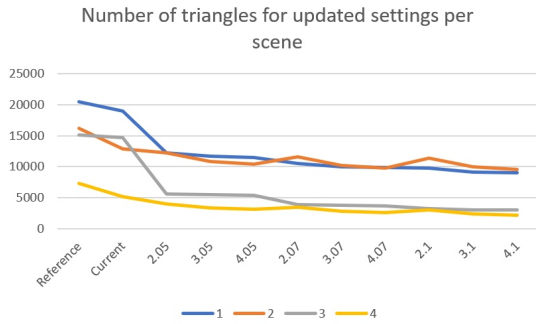
Figure 6.21: Size reduction of constrained terrains using the updated settings and the terrain currently available on PDOK.
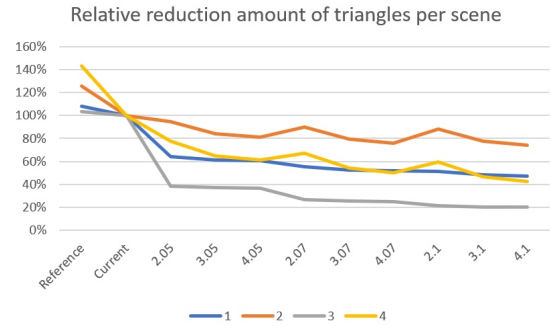
Figure 6.22: Relative size reduction of constrained terrains using the updated settings and the terrain currently available on PDOK.
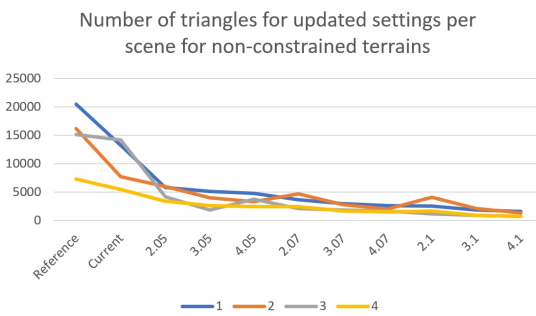
Figure 6.23: Size reduction of non-constrained terrains using the updated settings and the terrain currently available on PDOK.
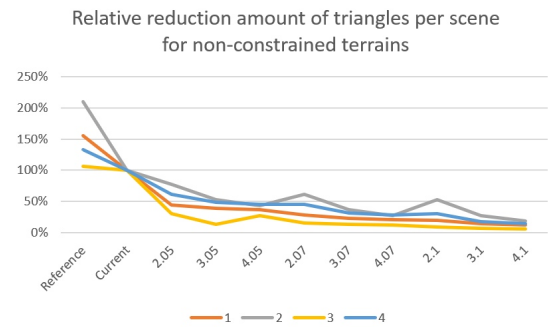
Figure 6.24: Relative size reduction of non-constrained terrains using the updated settings and the terrain currently available on PDOK.
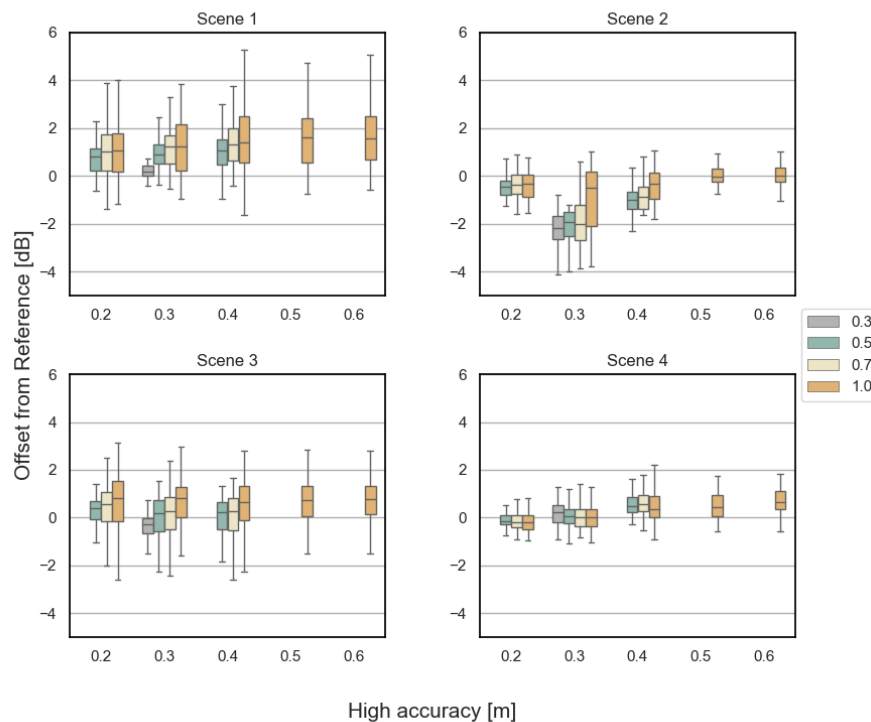
Figure 6.25: Box plot of all parameter settings (batch 1 and 2) using CNOSSOS, the color defines the lower accuracy setting where the x axis defines the high accuracy.

Analysis of the range extension of the high and low accuracy parameters

In CNOSSOS the low accuracy settings show a large impact on both the median and the variance of calculations, of which the variance is the most persistent (see Figure 6.25). Extending the high accuracy to 0.2m does reduce the variance, but the median is not noticeably influenced. The high accuracy has a negligible impact on the prediction. Except for scene 2 where the high accuracy area causes diffraction and the 0.3m high accuracy has a larger error with the reference terrain then the other settings.

The results using RMG generally show a decrease in variance and median for the more accurate low accuracy setting (see Figure 6.26). This setting has a larger impact than the high accuracy impact, indicating the high accuracy is less important. However, the high accuracy value of only applied in a small part of the terrain, therefore the increase in accuracy is 'cheap' in terms of file size. The results for setting 3.05.R (RMG) for scenario 3 were invalid and are left out.

Comparison of calculations with the currently available terrain on PDOK

The current model as available on PDOK[2] has a constant accuracy of 0.3m without any constraints. In this comparison the TIN is generated with constraints to allow for CNOSSOS calculations. For RMG the terrain is not constraint. When interpreting the calculations using the current model in CNOSSOS, note that the only difference with the reference terrain is in the high accuracy area close to the source. Low accuracy is the same as with the reference model and therefore most of the terrain will be identical, leading to the exact same heights for most receivers.

The calculations using the current model provide less accurate prediction in CNOSSOS in scenario's 2 and 4. In scenario 3 it shows a negative median with a lower variance caused by the low accuracy terrain.

---

[2]https://3d.kadaster.nl/3d-geluid/
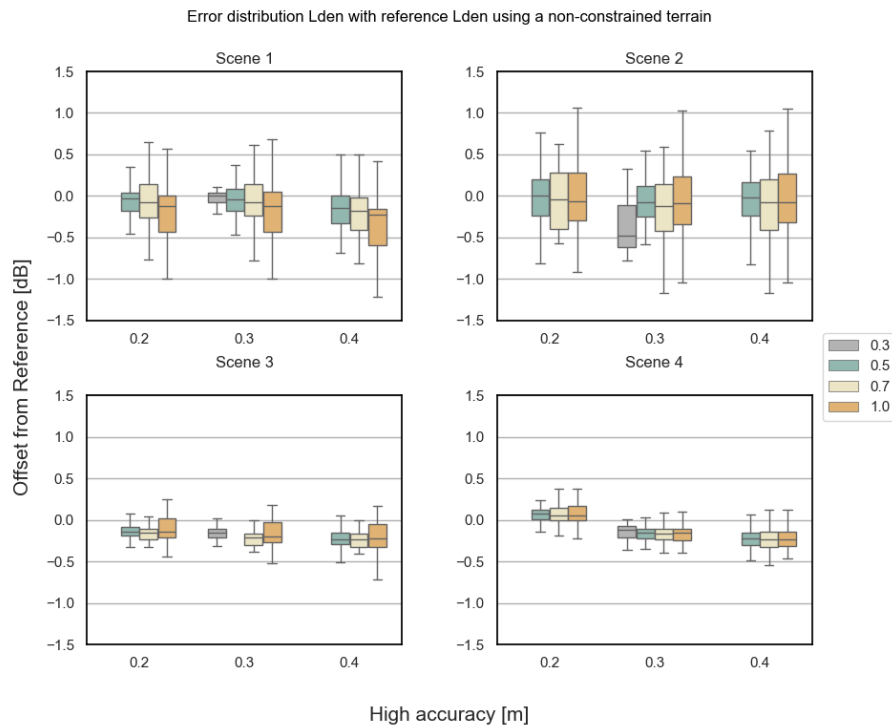
Figure 6.26: Box plot of the updated parameter settings using RMG without water, building or ground type constraints in the terrain. The color defines the lower accuracy setting where the x axis defines the high accuracy.

Only in scenario 1 does the current model out perform the other settings, this is also the scenario where the low accuracy area has the largest impact on the predictions as the terrain is higher than the line of sight for most of the receivers.

Analysis of the influence of receiver height on noise calculation

Figure 6.27 shows the results of setting the receiver height as a constant, i.e. it is not computed by interpolating on the used terrain, but it is taken from the reference model to eliminate possible effects of this change in height. The results in scenario 1 and 2 have been highly improved, of which scenario 1 the strongest. These are also the scenario's where the correlation between noise value and receiver height difference was the strongest. The ranges for scenario 1 have decreased from +/-0.5 to +/-0.2 on average. The median values have not been influenced much. This was expected as the difference in receiver height has a stronger effect on the outliers.

Analysis of the influence of not constraining the terrain

Figure 6.28 shows the non-constrained results using a constant receiver height. Figure 6.29 shows the difference in calculated noise value for the initial settings compared to the 1.0m low accuracy settings of the updated settings. It is shown that in most cases the constrained TIN shows a equal or lower variance. The median is also closer to zero for 3 in 4 scenario's. Note that the reference terrain remains constrained and as such artefacts present in the reference model have a negative impact on the non-constrained TIN.

The box plots confirm there is a larger range of height errors leading to an increase in variance of the results. Yet, these heights are compared to a constrained reference terrain. This terrain may also be

Error distribution Lden with reference Lden using a constrained terrain and constant receiver heights
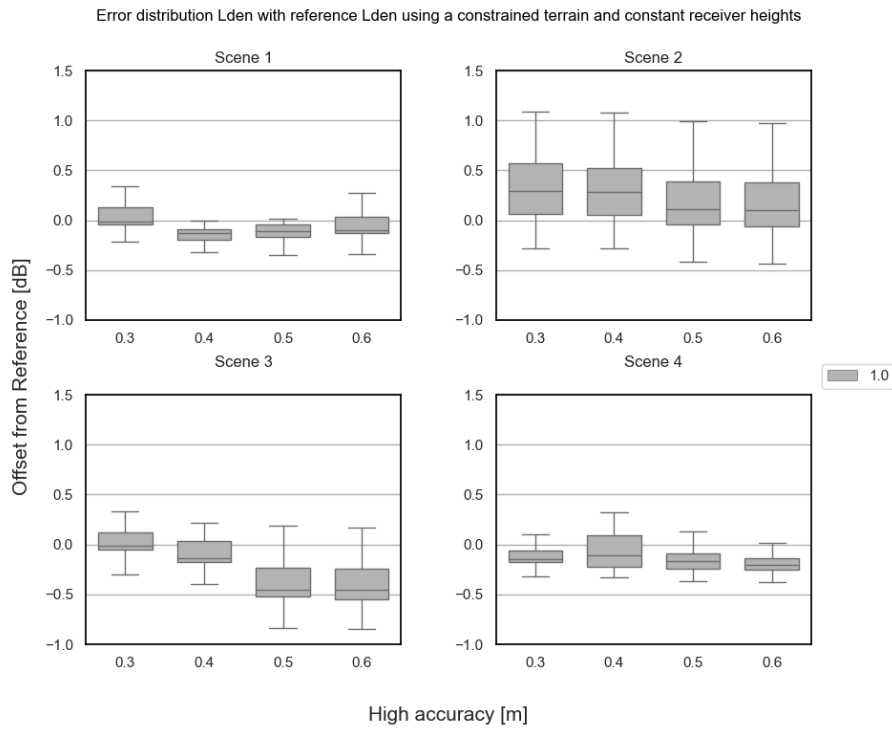
Figure 6.27: Box plot of the updated parameter settings using RMG using a constrained TIN. Here the receiver height from the reference terrain is applied to all settings.

Error distribution Lden with reference Lden using a non-constrained terrain and constant receiver heights
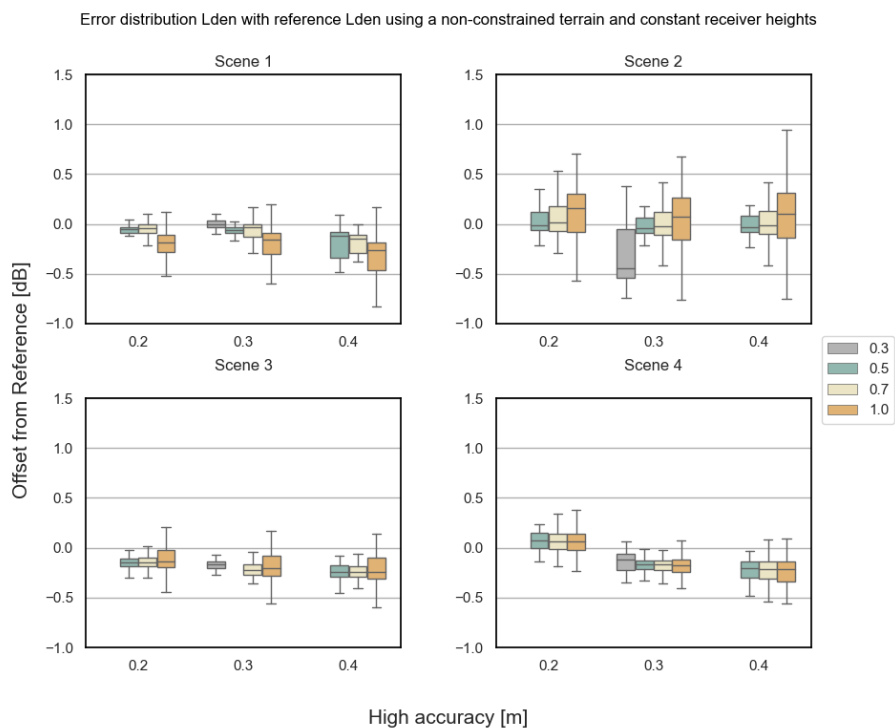
Figure 6.28: Box plot of the updated parameter settings using RMG without water, building or ground type constraints in the terrain. Here the receiver height from the reference terrain is applied to all settings. The color defines the lower accuracy setting where the x axis defines the high accuracy.
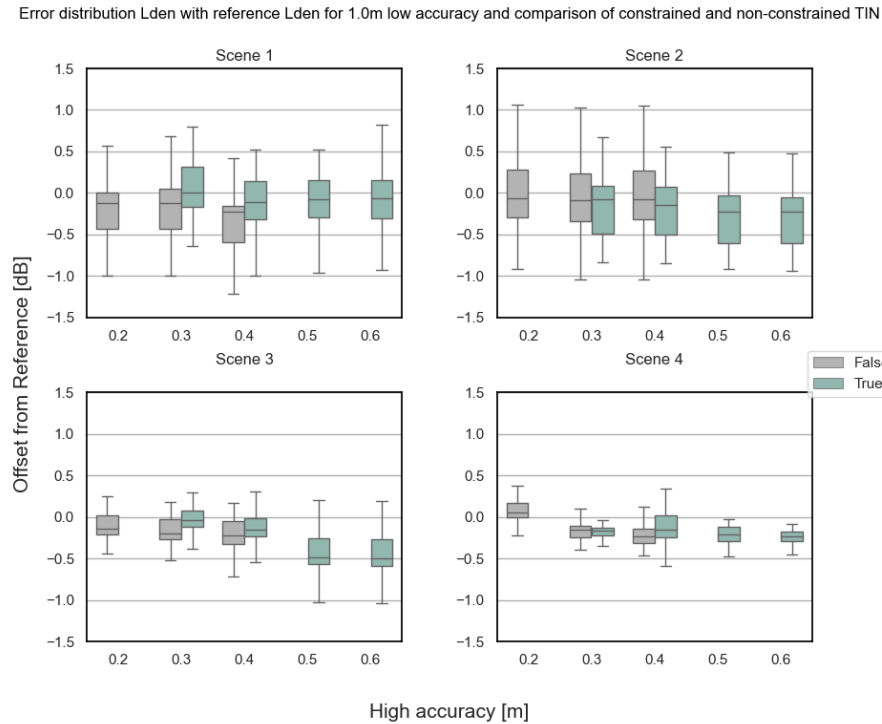
Figure 6.29: Box plot of the updated parameter settings using RMG where the constrained and non-constrained TIN are compared. True is constrained while False is not constrained.

different when not constrained. The effect of a terrain that is modelled lower then the reference model due to the constraints is solved by not constraining the terrain. While the variance increases, the distribution becomes more predictable and the mean and median are now zero. While this empirical test indicates constraining the TIN rather has a positive impact then a negative, future studies should use a non-constrained reference model to verify this effect.

6.5.3 Conclusions

When comparing all the results of different parameter and triangulation settings it can be stated that the low accuracy does have a significant impact on the noise calculations. This effect is present in both CNOSSOS and RMG. With RMG it is less visible when the receiver determines it's absolute height based on it's own terrain. This can be explained as when the terrain is modelled lower, so is the receiver. These effects partially cancel each other out while the constant receiver height only has a differently modelled terrain.

When comparing the box plots with the terrain size graphs it shows more accurate setting provide more accurate results. A logical result, as the terrain become more and more similar to the reference terrain. In CNOSSOS the high accuracy plays a small role and is even negligible in flat areas. In hilly areas (scene 1 and 3) it shows much larger errors that are mainly solved by increasing the low accuracy value. In RMG the results show a much smaller impact of the terrain accuracy. Even low accuracies provide accurate predictions. It is however, more sensitive to the receiver height. Constraining the TIN impacts the overall accuracy of the terrain, leading to a bias in the results.

The current model shows accurate results for most scenario's, but it comes at the cost of a large file size. In RMG the current model does not necessarily perform better then less accurate settings. In CNOSSOS however, it shows significantly more accurate predictions, this is mainly due to the impact of the low accuracy, which has shown to have a large impact on CNOSSOS calculations.
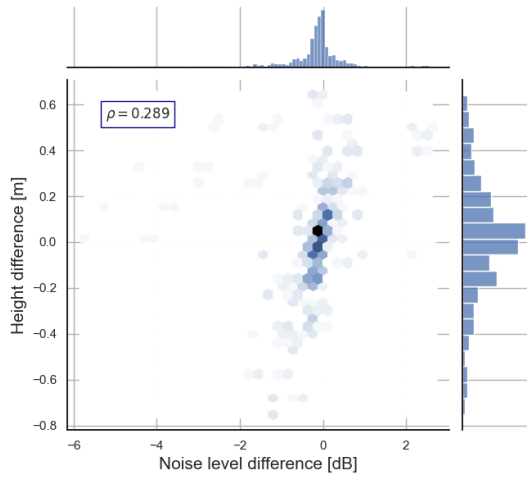
Figure 6.30: Scatter plot of correlation noise level difference and receiver height difference for all settings in scene 1 using the non-constrained TIN
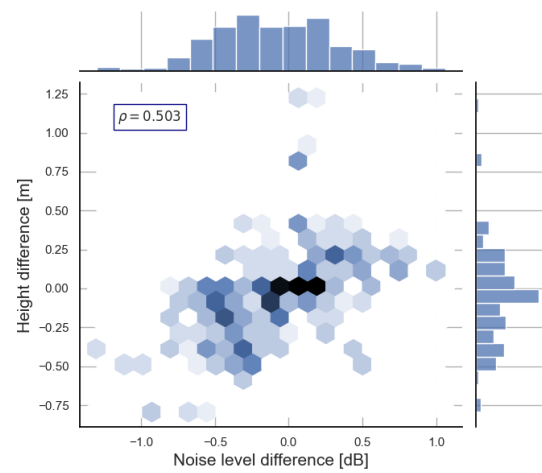
Figure 6.31: Scatter plot of correlation noise level difference and receiver height difference for all settings in scene 2 using the non-constrained TIN
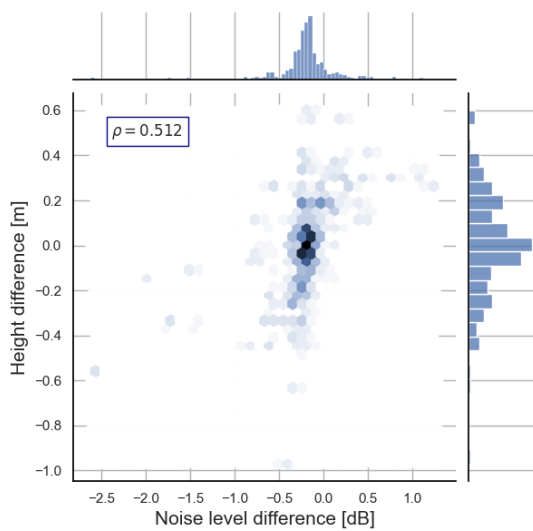
Figure 6.32: Scatter plot of correlation noise level difference and receiver height difference for all settings in scene 3 using the non-constrained TIN
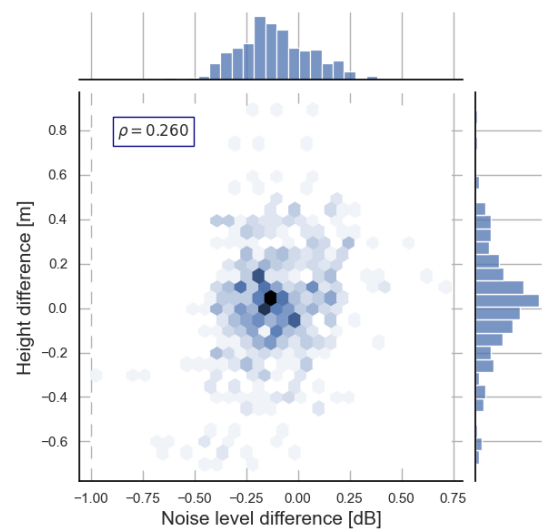
Figure 6.33: Scatter plot of correlation noise level difference and receiver height difference for all settings in scene 4 using the non-constrained TIN

7 Discussion

In the previous chapter all results are presented and explained. This chapter explains how these results are to be interpreted, what is the value of the result in the larger context of this research and noise modelling in general.

The aim of the research is to find a balance between maintaining accurate noise prediction while reducing the size and number of triangles in the TIN. In the analysis, all modelled results are compared to a reference terrain with a maximum error of 0.15m within 20m of a road and 0.30m further away from a noise source. This accuracy is not feasible on a large scale due to the large size of the terrain. The currently used height lines may provide a similar accuracy for the lines, but the terrain height is interpolated in between the lines, which may lead to higher errors and especially less certainty on these errors.

In these tests only three sources relative close together were used. Due to the narrow and long scenarios, the three paths each receiver has mostly cross similar terrain, the same ditches and dykes and therefore similar terrain differences are included in each path. This was applied on purpose to increase the effect of changes in the terrain on the noise prediction. In regular cases a receiver would have sources from multiple directions, which are expected to highly reduce the differences and outliers. Therefore having lower errors than in the test scenarios from this study. It is therefore important to state that while the differences can locally be very significant, using existing height lines in regular cases the differences may also be significant compared to the reference terrain.

The results show that the low accuracy settings have the largest impact. The differences generally increase slightly with lower accuracy settings close to the source (0.50 and 0.60m), leading to an increase in the number of receivers with more than 1.0 dB difference. The buffer distance around the noise sources showed no noticeable impact indicating the area from 20m to 100m did, in many cases, not cause diffraction or other noticeable impacts. Scene 4 has shown the differences between 4 and 4b are negligible. A high accuracy beyond the diffraction point does not provide more accurate results compared to reducing the high accuracy region to just past the diffraction point.

The updated parameter settings provided many insights into the effects of the low accuracy, the influence of constraining the TIN. The influence of the receiver height showed to have a large impact on the computed noise value. Further research onto how this receiver height could be alternatively determined in the noise methods could be valuable considering current noise data do not necessarily provide a high accuracy close to the receiver.

In general it was noticed that the height assigned to the constraint vertices in the triangulation, especially those of terrain and forest class have a large influence on the shape of the terrain, given not many vertices were added due to the low accuracy value. In flat areas, especially when ditches are present, such that the constraint vertices are placed on low areas in the terrain, cause the terrain to be modelled lower. Where the constraints of the ground types have also shown to add a significant portion of the triangles, it may be considered to separate the ground types from the TIN.

If assuming the currently available model (0.3m everywhere) provides sufficient quality, the error it shows can be observed as an acceptable error. When comparing this error with the other settings, the following conclusions can be drawn (the size reductions are compared to the current model using the same constraints);

- In CNOSSOS overall an accuracy setting of 4.05 suffices for variable terrains, providing 20 to 60% size reduction. In flat areas even an accuracy of 6.10 (50-75% reduction) is sufficient as the errors remain small. The theoretical analysis in this research focused on flat areas as that represents the Dutch landscape the best. A separate study focusing on areas with more height differences might

be interesting to investigate whether a terrain in these areas can be modelled such that it will have similar prediction errors as flat areas.

- RMG predictions using a constrained TIN can be represented using setting 6.10 for flat areas, leading to 50 to 75% reduction. However, the prediction accuracy in more hilly areas does not show a clear pattern, the 3.10 setting (20 to 80% reduction) provided accurate results for scene 1 and 3, but the 6.10 setting was also sufficient for scene 1.

- RMG predictions using a non-constrained TIN using setting 3.05 provided better results then the current model for flat areas but shows more variance in the hilly areas. This provides 50 to 90% size reduction. In this research there was no non-constrained reference model. The predictions using non-constrained terrains may therefore look less accurate then they are in reality.

- The RMG predictions are sensitive to the receiver height. When this effect is canceled out by using a constant receiver height for all predictions, it shows the low accuracy has a much higher impact on the variance and the median. Compared to the current model a setting of 3.07 provides similar results with a 64 to 87% reduction.

Concluding, the parameter settings in table 7.1 are advised for variable terrain types and will provide results similar to the currently available model while reducing the size with

Table 7.1: Overview of advised parameter values to be used for efficient and accurate noise predictions.

Parameter	setting
Constrained terrain	20 to 60% reduction
Buffer distance road	20.0m
Buffer distance rail	20.0m
High accuracy value	0.40m
Low accuracy value	0.50m
Non-constrained terrain	50 to 90% reduction
Buffer distance road	20.0m
Buffer distance rail	20.0m
High accuracy value	0.30m
Low accuracy value	0.50m

8 Conclusion & future work

This research aims to provide a model to determine the optimal shape of the elevation model for noise modelling. To answer this question first a theoretical analysis has been executed from which several parameters were identified. A model has been made in QGIS in which these parameters have been implemented. To 1) verify if the parameters are useful to create a fruitful TIN for noise modelling purposes and 2) to determine which settings of the parameters provide the balance between sufficiently accurate noise predictions and good performance, noise predictions have been calculated for different settings of the parameters.

In this chapter the intermediate and final results of this study are used to determine to which degree the research questions can be answered. Next to these conclusions several recommendations are given. These origin from several identified limitations of used data sets and tools as well as from features related to the work which may improve the results. At last related research topics are mentioned which might be interesting for further development of TIN based noise modelling on a country wide scale.

8.1 Conclusion

In this section the research is concluded by describing to which degree each research question is answered.

Which parameters influence the required elevation accuracy of the environment model?

The research question is answered by analysing the noise prediction methods to understand how elevation data is used to predict noise levels. This knowledge is used to assess all possible parameters categorised in three categories. Based on this analysis two parameters where identified;

1. Distance to road and railways consisting of a distance and an accuracy to maintain within this distance from these noise sources.

2. Elevation topology to determine regions where noise will need to diffract over an object to reach the area and as such the higher quality is not required.

In addition to these parameters the terrain has a base accuracy which will be used when a high accuracy is not required.

How can a triangular irregular network (TIN) be generated according to the local accuracy based on the parameters?

As the research question implicates, it consists of first determining a local accuracy on every location within a region, i.e. an accuracy map, followed by translating this map into a TIN. In chapter 5 the parameters have been translated into a model, i.e a consecutive list of algorithms that provides an accuracy map, this accuracy map can be used to generate a TIN. To answer the third research question and verify if the model works and the parameters provide the requested results, an implementation of this model is created in QGIS. As this research is more of a theoretical nature, the implementation is rather a tool than an aim in the research, optimising the implementation on performance and fully automating the process is therefore not a priority. Where possible the limitations were kept to a minimal to keep the results mostly in line with the model. The model is kept independent from restrictions in the implementation by explicitly mentioning the limitations caused by the used software packages. Therefore the model can also be implemented using other tools without implicitly adding limitations.

Which parameter settings provide a balance between quality of the output and performance?

To answer this question noise predictions have been made using both the Dutch RMG and the European CNOSSOS method. Using 209 receiver points and 12 sources divided over 4 areas, each generated in 13 (CNOSSOS and 23 (RMG) accuracy settings, all computed using two noise methods, resulted in 22.572 propagation paths. These results have been visualised and analysed in chapter 6 to analyse the effect of each parameter. In chapter 7 conclusions are drawn from the results. In order to test and balance every parameter individually, many different settings should be tested in several source - receiver configurations. These configurations should be tested in different regions of which the results need to be analysed which is, all combined, a very time intensive task. To provide a proper analysis within the graduation time frame, 22 configurations of the accuracy settings have been applied to four regions and compared to an accurate reference model. Based on these results the parameter settings mentioned in table 7.1 from the previous chapter are advised. Using these settings, a reduction of 20% in the worst case up to 60% in the best case can be realised for a constrained terrain. In non-constrained terrains the reduction is 50 to 90% in the best case.

8.2 Recommendations and future work

Based upon experiences with tools and data sets several recommendations can be made;

1. The buildings in the LoD 1.3 building data set sometimes have unrealistic shapes for the inner building parts, or consist of many short line segments, for noise prediction purposes the algorithm used to create these building parts should simplify the building.

2. While the used software 3Dfier allows many options for triangulation, there is also room for improvement; 1) An additional class could be created to allow for more than two accuracies in the triangulation. 2) While the surfaces are not invalid, some small (in area and in # of vertices) polygons are triangulated wrong, the z is placed tens of meters below the ground and it contains holes. 3) If the vertices of two adjacent polygons are not identical, e.g. a straight line has an abundant vertex on this line on one side only, the triangulation contains a hole. This could be fixed by inserting vertices in the polygon in 3Dfier. 4) Constraining line segments are always a single line, even though this sometimes causes vertical errors exceeding the threshold. Identifying such artefacts and splitting up the segment (making it a confined triangulation) might solve this issue.

3. Using a triangulation not by discrete thresholds values and areas but allowing for normalised error measurements based on a function or area allows to not constrain the TIN when this is not needed (if the metadata in the triangle is not required). This prevents artefacts as mentioned above and allows for a more accurate, continuous and simpler triangulation. It can still allow for constraints or a confined triangulation, but this is optional.

4. The ground type and water data sets sometimes use an extraordinary amount of vertices to store a simply shape. By representing the line with fewer vertices using a simplification algorithm or simplifying the generation of such lines the constrained triangulation can be largely reduced in size.

During this project also the following ideas for additional features and future work have come up;

1. In this study the generated terrains are analysed by means of several parameters, they are however not compared to the reference terrain in terms of height difference. It could be interesting to produce a map presenting the differences in height between an accuracy setting and the reference terrain. This allows for a deeper analysis of why noise predictions are higher or lower. Currently this is done with the receiver height, which provides valuable information, but does not provide enough insight into the the terrain in between the source and the receivers. For relevant areas, e.g. top of a barrier or ridge, this is done using visual inspection of the terrains.

2. The used reference model is not analysed whether it is an accurate representation of the terrain. While the accuracy will certainly force the terrain to follow the point cloud, the constraints may cause errors. It might be worthwhile to develop a reference models without constraints.

3. To obtain a better understanding of how accurate current elevation models are, converting height line models to TINs and compare them to the reference model as well may provide valuable insight into what error is acceptable.

4. It was shown that RMG predictions are sensitive to the local receiver height. When the terrain below the receiver is not accurate, it has a large impact on the calculated noise level. Further studies using current commercial elevation models may provide insight onto how the receiver height may be determined more accurate.

5. To further automate the process the model could be implemented in other programs, which can reduce the limitations, increases performance and ease of use.

6. In this state of noise modelling using a TIN only "simple" features in the terrain are tested. Buildings are LoD 1.3 at most and bridges or tunnels are not supported. It might be interesting to study how a TIN with adjacency included can be used in a 3-manifold, i.e. an edge can have more the two adjacent triangles.

A Statistical information of noise level predictions

Table A.1: Statistical values scenario 1

figure	Median	Variance (σ^2)	sigma (σ)	Min	Max	$\rho_{\text{height, dB}}$
3.10.R	0.000	0.929	0.964	-3.710	4.280	0.61
4.10.R	-0.110	1.149	1.072	-5.160	4.050	0.52
5.10.R	-0.080	1.150	1.072	-5.150	4.070	0.52
6.10.R	-0.060	1.151	1.073	-5.180	4.050	0.52
Not constrained:						
2.5.R	-0.030	0.309	0.556	-3.020	0.560	0.06
2.7.R	-0.070	0.722	0.850	-4.290	2.510	0.39
2.10.R	-0.120	0.806	0.898	-3.760	2.450	0.39
3.3.R	0.000	0.197	0.444	-1.540	2.050	0.18
3.5.R	-0.040	0.279	0.528	-2.860	0.560	0.09
3.7.R	-0.070	0.685	0.828	-4.050	2.520	0.42
3.10.R	-0.120	0.761	0.872	-3.570	2.390	0.39
4.5.R	-0.140	0.610	0.781	-4.390	0.500	-0.08
4.7.R	-0.180	1.067	1.033	-5.730	2.630	0.27
4.10.R	-0.230	1.133	1.065	-5.280	2.320	0.31
3.10.C	1.226	2.880	1.697	-0.957	8.502	
4.10.C	1.403	3.101	1.761	-1.614	8.787	
5.10.C	1.594	3.281	1.811	-0.767	8.634	
6.10.C	1.563	3.504	1.872	-0.578	8.571	
2.5.C	0.804	1.497	1.224	-1.523	6.991	
2.7.C	1.027	2.384	1.544	-1.385	8.101	
2.10.C	1.046	2.683	1.638	-1.155	8.489	
3.3.C	0.196	0.344	0.586	-1.233	2.644	
3.5.C	0.896	1.871	1.368	-0.945	8.246	
3.7.C	1.214	2.548	1.596	-1.323	8.193	
4.5.C	1.071	2.437	1.561	-0.959	8.701	
4.7.C	1.320	2.973	1.724	-1.463	7.909	

Table A.2: Statistical values scene 2

figure	Median	Variance (σ^2)	sigma (σ)	Min	Max	$\rho_{\text{height, dB}}$
3.10.R	-0.070	0.136	0.369	-0.840	0.670	0.68
4.10.R	-0.140	0.122	0.349	-0.850	0.560	0.68
5.10.R	-0.220	0.126	0.354	-0.920	0.490	0.57
6.10.R	-0.220	0.121	0.348	-0.940	0.480	0.56
Not constrained:						
2.5.R	0.000	0.134	0.365	-0.810	0.760	0.69
2.7.R	-0.040	0.137	0.371	-0.570	0.630	0.63
2.10.R	-0.060	0.209	0.457	-0.920	1.060	0.45
3.3.R	-0.480	0.100	0.317	-0.780	0.330	0.40
3.5.R	-0.070	0.136	0.368	-1.300	0.540	0.65
3.7.R	-0.120	0.142	0.376	-1.170	0.590	0.61
3.10.R	-0.090	0.238	0.488	-1.040	1.030	0.44
4.5.R	-0.020	0.155	0.394	-1.300	0.800	0.63
4.7.R	-0.070	0.162	0.403	-1.170	0.790	0.60
4.10.R	-0.080	0.247	0.497	-1.040	1.050	0.45
3.10.C	-0.490	1.702	1.305	-3.794	1.004	
4.10.C	-0.330	0.728	0.853	-3.606	1.074	
5.10.C	-0.034	0.294	0.542	-1.602	1.262	
6.10.C	0.012	0.196	0.442	-1.042	1.014	
2.5.C	-0.450	0.568	0.754	-3.409	0.709	
2.7.C	-0.351	0.551	0.743	-3.409	0.905	
2.10.C	-0.338	0.584	0.764	-3.432	0.759	
3.3.C	-2.182	0.882	0.939	-4.108	0.527	
3.5.C	-1.918	0.823	0.907	-4.012	0.527	
3.7.C	-2.011	0.937	0.968	-3.850	0.604	
4.5.C	-1.001	0.561	0.749	-3.679	0.357	
4.7.C	-0.862	0.639	0.799	-3.687	0.814	

Table A.3: Statistical values scenario 3

figure	Median	Variance (σ^2)	sigma (σ)	Min	Max	$\rho_{\text{height, dB}}$
3.10.R	-0.045	0.111	0.333	-0.680	1.000	0.49
4.10.R	-0.160	0.109	0.330	-0.800	0.870	0.49
5.10.R	-0.490	0.113	0.336	-1.140	0.540	0.47
6.10.R	-0.500	0.113	0.336	-1.150	0.530	0.46
Not constrained:						
2.5.R	-0.140	0.114	0.338	-1.950	0.290	0.48
2.7.R	-0.150	0.135	0.367	-1.710	1.140	0.59
2.10.R	-0.145	0.232	0.482	-2.550	1.290	0.47
3.3.R	-0.160	0.022	0.148	-0.590	0.260	0.70
3.7.R	-0.210	0.134	0.366	-1.760	1.080	0.59
3.10.R	-0.205	0.230	0.479	-2.590	1.210	0.47
4.5.R	-0.240	0.112	0.334	-1.990	0.200	0.48
4.7.R	-0.240	0.133	0.365	-1.780	1.030	0.59
4.10.R	-0.225	0.231	0.481	-2.620	1.180	0.46
3.10.C	0.802	2.111	1.453	-6.801	2.954	
4.10.C	0.634	2.328	1.526	-7.050	2.781	
5.10.C	0.751	1.936	1.391	-5.961	2.857	
6.10.C	0.784	1.959	1.400	-5.990	2.798	
2.5.C	0.408	2.190	1.480	-7.748	2.333	
2.7.C	0.559	2.524	1.589	-6.833	2.489	
2.10.C	0.817	2.997	1.731	-6.794	3.128	
3.3.C	-0.260	2.115	1.454	-8.135	2.575	
3.5.C	0.180	2.244	1.498	-7.761	1.547	
3.7.C	0.280	2.248	1.499	-6.671	2.363	
4.5.C	0.225	2.348	1.532	-7.622	1.318	
4.7.C	0.280	2.861	1.691	-7.181	1.659	

Table A.4: statistical values scenario 4

figure	Median	Variance (σ^2)	sigma (σ)	Min	Max	$\rho_{height, dB}$
3.10.R	-0.170	0.012	0.110	-0.540	0.110	0.28
4.10.R	-0.150	0.032	0.180	-0.590	0.340	0.02
5.10.R	-0.210	0.014	0.119	-0.590	0.150	0.25
6.10.R	-0.230	0.011	0.105	-0.590	0.100	0.32
Not constrained:						
2.5.R	0.070	0.009	0.095	-0.140	0.340	0.23
2.7.R	0.050	0.025	0.158	-0.420	0.710	0.48
2.10.R	0.050	0.031	0.175	-0.730	0.650	0.36
3.3.R	-0.120	0.011	0.107	-0.360	0.200	0.29
3.5.R	-0.160	0.010	0.102	-0.420	0.090	0.31
3.7.R	-0.170	0.026	0.162	-0.620	0.410	0.48
3.10.R	-0.160	0.025	0.159	-0.800	0.350	0.35
4.5.R	-0.220	0.014	0.118	-0.490	0.120	0.20
4.7.R	-0.240	0.030	0.172	-0.680	0.440	0.42
4.10.R	-0.230	0.032	0.179	-0.970	0.380	0.27
3.10.R2	-0.192	0.011	0.107	-0.600	0.110	0.04
4.10.R2	-0.146	0.028	0.167	-0.550	0.290	0.3
5.10.R2	-0.195	0.018	0.133	-0.540	0.200	0.05
6.10.R2	-0.186	0.016	0.127	-0.480	0.190	0.06
3.10.C	0.015	0.382	0.618	-1.055	1.978	
4.10.C	0.348	0.403	0.635	-0.898	2.213	
5.10.C	0.450	0.293	0.541	-0.553	1.740	
6.10.C	0.639	0.292	0.541	-0.933	1.818	
2.5.C	-0.146	0.229	0.479	-0.722	2.389	
2.7.C	-0.195	0.261	0.510	-0.899	2.018	
2.10.C	-0.203	0.228	0.477	-0.936	1.024	
3.3.C	0.228	0.318	0.564	-1.384	1.274	
3.5.C	0.076	0.250	0.500	-1.059	1.394	
3.7.C	0.002	0.296	0.544	-0.824	1.783	
3.10.C	0.015	0.382	0.618	-1.055	1.978	
4.5.C	0.475	0.280	0.530	-0.266	2.312	
4.7.C	0.563	0.230	0.479	-0.529	1.801	

B Data sizes of terrains using the updated parameter settings

Number of triangles per parameter setting per scene for the updated parameter settings using an constrained TIN

Scene	Reference	Current	2.05	3.05	4.05	2.07	3.07	4.07	2.1	3.1	4.1
1	20513	18985	12205	11647	11497	10551	9993	9843	9723	9165	9015
2	16204	12874	12208	10814	10418	11592	10198	9802	11360	9966	9570
3	15153	14671	5611	1842	5399	3917	3757	3705	3183	3023	2971
4	7314	5112	3978	3324	3120	3422	2768	2564	3036	2382	2178

Number of triangles per parameter setting per scene for the updated parameter settings using an non-constrained TIN

Scene	Reference	Current	2.05	3.05	4.05	2.07	3.07	4.07	2.1	3.1	4.1
1	20513	13240	5834	5112	4826	3686	2964	2678	2596	1874	1588
2	16204	7710	5988	4024	3310	4760	2796	2082	4078	2114	1400
3	15153	14210	4228	1842	3760	2160	1842	1692	1214	896	746
4	7314	5504	3396	2648	2468	2470	1722	1542	1680	932	752

Bibliography

Basner, M., Babisch, W., Davis, A., Brink, M., Clark, C., Janssen, S., and Stansfeld, S. (2014). Auditory and non-auditory effects of noise on health. *The lancet*, 383(9925):1325–1332.

Biljecki, F., Ledoux, H., and Stoter, J. (2016). An improved lod specification for 3d building models. *Computers, Environment and Urban Systems*, 59:25–37.

Delaunay, B. et al. (1934). Sur la sphere vide. *Izv. Akad. Nauk SSSR, Otdelenie Matematicheskii i Estestven-nyka Nauk*, 7(793-800):1–2.

Douglas, D. H. and Peucker, T. K. (1973). Algorithms for the reduction of the number of points required to represent a digitized line or its caricature. *Cartographica: the international journal for geographic information and geovisualization*, 10(2):112–122.

European Environmental Agency (2020). Environmental noise in europe — 2020. `https://www.eea.europa.eu/publications/environmental-noise-in-europe/`. Last accessed on 03-05-2021.

European parliament and European Union (2002). Directive 2002/49/ec of the european parliament and the council of 25 june 2002 relating to the assessment and management of environmental noise. *Official Journal of the European Communities, L*, 189(18.07):2002.

European parliament and European Union (2015). Commission directive (eu) 2015/996 of 19 may 2015 establishing common noise assessment methods according to directive 2002/49/ec of the european parliament and of the council. *Official Journal of the European Communities, L*, 168(996):823.

European parliament and European Union (2020). Commission delegated directive (eu) .../... amending, for the purposes of adapting to scientific and technical progress, annex ii to directive 2002/49/ec of the european parliament and of the council as regards common noise assessment methods.

Garland, M. and Heckbert, P. (1997). Fast triangular approximation of terrains and height fields. *Submitted for publication*.

Kephalopoulos, S., Paviotti, M., and Anfosso-Lédée, F. (2012). Common noise assessment methods in europe (cnossos-eu).

Kok, A. and van Beek, A. (2019). Amendments for cnossos-eu: Description of issues and proposed solutions.

Kumar, K., Labetski, A., Ledoux, H., and Stoter, J. (2019). An improved lod framework for the terrains in 3d city models. *ISPRS Annals of Photogrammetry, Remote Sensing and Spatial Information Sciences*, IV(4/W8):75–82. 14th 3D GeoInfo Conference 2019, 3DGeoinfo ; Conference date: 24-09-2019 Through 27-12-2019.

Ledoux, H., Arroyo Ohori, G., and Peters, R. (2020). *Computational modelling of terrains*. v0.7 edition.

Ledoux, H., Biljecki, F., Dukai, B., Kumar, K., Peters, R., Stoter, J., and Commandeur, T. (2021). 3dfier: automatic reconstruction of 3d city models. This work received funding from the National Kadaster https://www.kadaster.nl/ .

Murphy, E. and King, E. (2014). *Environmental noise pollution: Noise mapping, public health, and policy*. Newnes.

Peters, R., Dukai, B., Commandeur, T., and Stoter, J. (2018). 3d-inputgegevens voor geluidssimulaties gegenereerd uit bestaande landsdekkende datasets. *Geo-Info*, 15(6):8–12.

Bibliography

Stoter, J., Peters, R., Commandeur, T., Dukai, B., Kavisha, K., and Ledoux, H. (2020). Automated reconstruction of 3d input data for noise simulation. *Computers, Environment and Urban Systems*, 80. Green Open Access added to TU Delft Institutional Repository 'You share, we take care!' – Taverne project https://www.openaccess.nl/en/you-share-we-take-care Otherwise as indicated in the copyright section: the publisher is the copyright holder of this work and the author uses the Dutch legislation to make this work public.

van Rijssel, L., Dinklo, C., Prusti, M., Giannelli, D., and Hobeika, N. (2020). 3d noise simulation: Final report of the 2020 synthesis project.

Vergoed, T. and van Leeuwen, H. J. (2018). Evaluation and validation of the cnossos calculation method in the netherlands. In *EuroNoise*.

WHO Regional Office for Europe (2018). Environmental noise guidelines for the european region. accessed on 21-04-2021.

World Health Organization and Joint Research Committee (2017). Burden of disease from environmental noise: quantification of healthy life years lost in europe.